

**FoxO1 in the regulation of adipocyte autophagy and biology**

By

Longhua Liu

Dissertation submitted to the faculty of the Virginia Polytechnic Institute and  
State University in partial fulfillment of the requirements for the degree of

DOCTOR OF PHILOSOPHY

In

Human Nutrition, Foods, and Exercise

Zhiyong Cheng, Chair  
Fabio A. Almeida  
Benjamin A. Corl  
Dongmin Liu

November 08, 2016  
Blacksburg, Virginia

Keywords: FoxO1, AS1842856, adipogenesis, obesity, autophagy, FSP27,  
mitochondrial uncoupling protein, Tfeb, Tamoxifen, adipose tissue, ROS.

# **FoxO1 in the regulation of adipocyte autophagy and biology**

Longhua Liu

## **ABSTRACT (ACADEMIC)**

Obesity is a rapidly growing epidemic in the USA and worldwide. While the molecular and cellular mechanism of obesity is incompletely understood, studies have shown that excess adiposity may arise from increased adipogenesis (hyperplasia) and adipocyte size (hypertrophy) . Emerging evidence underscores autophagy as an important mediator of adipogenesis and adiposity. We are interested in the upstream regulator of adipocyte autophagy and how it impacts adipocyte biology.

Given that metabolic stress activates transcription factor FoxO1 in obesity, my dissertation project is designed to depict the role of FoxO1 in adipocyte autophagy and biology. We found that FoxO1 upregulation was concomitant with elevation of autophagy activity during adipogenesis. Inhibition of FoxO1 suppressed autophagy flux and almost completely prevented adipocyte differentiation. For the first time, we found that the kinetics of FoxO1 activation followed a series of sigmoid curves that showed multiple activation-inactivation transitions during adipogenesis. Our study provides critical evidence casting light on the controversy in the literature that either persistent inhibition or activation of FoxO1 suppresses adipogenesis. In addition, we identified two central pathways that FoxO1-mediated autophagy regulated adipocyte biology: (1) to control lipid droplet growth via fat specific protein 27 (FSP27) in adipocytes; and (2) to differentially regulate mitochondrial uncoupling proteins (UCP) that have been implicated in browning of white adipose tissue and redox homeostasis. Mechanistically, FoxO1 appears to induce autophagy through the transcription factor EB (Tfeb), which was

previously shown to regulate both autophagosome and lysosome. Chromatin immunoprecipitation assay demonstrated that FoxO1 directly bound to the promoter of Tfeb, and inhibition of FoxO1 attenuated the binding, which resulted in reduced Tfeb expression.

To investigate the role of FoxO1 *in vivo*, we have developed mouse models to modulate FoxO1 in adipose tissue using an inducible Cre-loxP system. Tamoxifen is widely used to activate the inducible Cre recombinase that spatiotemporally control target gene expression in animal models, but it was unclear whether tamoxifen itself may affect adiposity and confounds phenotyping. Part of my dissertation work was to address this important question. We found that tamoxifen led to reduced fat mass independent of Cre, which lasted for 4-5 weeks.

Mechanistically, Tamoxifen induced reactive oxygen species (ROS) and augmented apoptosis.

Our data reveals a critical period of recovery following tamoxifen treatment in the study of inducible knockout mice.

Together, my dissertation work demonstrates FoxO1 as a critical regulator of adipocyte autophagy via Tfeb during adipogenesis. FoxO1-mediated autophagy controls FSP27, lipid droplet growth, and mitochondrial uncoupling proteins. Further study of FoxO1-autophagy axis in obese subjects is of physiological significance, and the investigation is under way.

# **FoxO1 in the regulation of adipocyte autophagy and biology**

Longhua Liu

## **ABSTRACT (PUBLIC)**

Obesity incidence is rapidly growing in the USA and worldwide. The mechanism of obesity is incompletely understood at present. My dissertation project was designed to address the cellular aspect of obesity. The data suggest that FoxO1, a molecule that can regulate gene expression, controls fat cell formation and expansion, both of which have been shown to increase fat mass in obese individuals. My research also indicates that FoxO1 regulates the ability of fat cells to store lipids and expend energy in the form of heat. Mechanistic studies show that FoxO1 exerts the above mentioned functions by mediating autophagy, a process that plays important roles in cellular component recycling and modeling. To validate these findings in a more physiological setting, our research team and I have started to generate mouse model and study how the modulation of FoxO1 and autophagy may affect fat mass and energy expenditure. This exciting work is under way.

## ACKNOWLEDGEMENTS

As my time as a PhD student at Virginia Tech comes to an end, I cannot express how grateful I am to all of my teachers, colleagues, friends, and family members. Without the support and care from all of you, attaining my PhD in three and a half years would not have been possible. I owe much of my success to each of you and could not be more thankful for your support.

I would first like to thank my research adviser, Dr. Zhiyong Cheng. Not only did he teach me how to conduct research in a professional and effective manner, such as designing experiments, generating new ideas, and using creative thinking, he also taught me invaluable lessons on how to conduct myself as a person. He helped me to hone the skills needed for a successful future academic career. His constant reiteration of the importance of “working hard and working smart” will stay with me for the rest of my life. I truly admire his passion, critical thinking, desire to learn, and responsibility in conducting research. I look forward to the opportunity to collaborate with him in the future.

I would also like to thank Louise Zheng. She has helped me so much during my time in the lab, including teaching me oral English, demonstrating many experiments, and providing excellent cooking tips. As our lab manager, she operated our lab professionally, maintained the machines, and kept the lab organized. I really appreciate the lengths she has gone to in helping me become a successful researcher.

My special thanks to all the previous and current members of our lab, including Dr. Peng Zou, Lu Liu, Zhipeng Tao, Sarah Donnelly, Cayleen Smith, Joseph Brooke, Leah Linarelli, et al. You helped me so much during my time here, inside and outside of the lab. At times when I felt down, you helped me get through. I will always cherish our friendships and keep you in my heart.

I would also like to thank my other committee members: Dr. Fabio Almeida, Dr. Benjamin Corl, and Dr. Dongmin Liu. Their advice and suggestions, from the very beginning of my study and research, were appreciated. I sincerely appreciate the time and energy they gave to me during the entirety of my PhD education.

I also want to give my sincere thanks to Ms. Michele Lewis. I am so lucky to have had the opportunity to be a GTA for her class for five semesters! She was a kind, easy-going, and supportive mentor. Her help in building up my confidence was truly appreciated. I will always admire her passion for teaching and working with students.

I also want to thank Dr. Donald Mckeon, who taught my oral English class. Although my oral English is still constantly improving, I greatly benefitted from his profound knowledge of the English language and willingness to help me improve my own oral communication skills.

I want to give my deep thanks to all of the members of Dr. Dongmin Liu's lab, including Dr. Aihua Wang, Wei Zhen, Jing Luo, Yao Wang, Liru Chen, Na Li, William Moore, Dr. Hana Alkhalidy et al. All of you have been so kind to me and have given me your generous support on experiments and also in my personal life.

Furthermore, I would like to thank Haiyan Zhang. She has helped me a great deal on my experiments and has given me very good suggestions in my personal life.

I also want to thank Dr. Madlyn Frisard, Ms. Michelle Rockwell, Dr. Matthew Hulver, Dr. Robert Grange, Dr. Eva Schmelz, and other faculty and staff members in our department who helped me during my time as a student at Virginia Tech. Also, Ms. Pam Suroski and Mr. Charles Nwaihesie, who graciously helped to take care of our mice and allowed for our animal studies to run smoothly.

I am grateful for others who I have met during my time here, especially Suzanna Bowser and Justin Sperringer. Many other wonderful friends, including Yimeng Xie, Yichao Mao, Wei Chen, Qian Wu, Qingchun Lei, Yue Wu, Shaohua Lei, Shengjian Guo, Chaopin Xie, Bowen Shi, Xiaoning Kang, Miao Yuan et al. helped a lot during my time in Blacksburg. I really appreciate and cherish each of our friendships.

My greatest thanks are going to my whole family. My parents and sister, who have loved and supported me more than what I could have ever imagined. I love each of you. I give my sincere thanks to my other family members, including my grandparents, uncles, aunts, cousins, and nephews. I could not have accomplished this without your support.

## ATTRIBUTIONS

Each author listed in this dissertation has contributed sufficiently and practically. All authors share the responsibility for the content in the published papers.

In chapter 2, Peng Zou and Longhua Liu carried out the experiments and participated in study design, data analysis, and manuscript preparation. Zhiyong Cheng participated in study design, data analysis and manuscript preparation. Louise Zheng, Lu Liu, Rebecca E. Stoneman, Alicia Cho, Ashley Emery and Elizabeth R. Gilbert conducted experiments and/or revised the manuscript. All authors read and approved the final version of manuscript.

In chapter 3, Longhua Liu carried out the experiments and participated in study design, data analysis, and manuscript preparation. Zhiyong Cheng participated in study design, data analysis and manuscript preparation. Louise D. Zheng, Peng Zou, Joseph Brooke and Cayleen Smith conducted experiments and revised the manuscript. Yun Chau Long, Fabio A. Almeida and Dongmin Liu analyzed data and revised the manuscript. All authors read and approved the final version of manuscript.

In chapter 4, Longhua Liu carried out the experiments and participated in study design, data analysis, and manuscript preparation. Zhiyong Cheng participated in study design, data analysis and manuscript preparation. Zhipeng Tao, Louise D. Zheng, Joseph Brooke and Cayleen Smith conducted experiments. Dongmin Liu, Yun-Chau Long analyzed data and revised the manuscript. All authors read and approved the final version of manuscript.

In chapter 5, Longhua Liu carried out the experiments and participated in study design, data analysis, and manuscript preparation. Zhiyong Cheng participated in in study design, experiments, data analysis, and manuscript preparation. Peng Zou, Louise Zheng, Leah E. Linarelli, Sarah Amarell and Austin Passaro conducted experiments and data analysis. Dongmin

Liu analyzed data and revised the manuscript. All authors read and approved the final version of manuscript.

## TABLE OF CONTENTS

ABSTRACT (ACADEMIC).....	ii
ABSTRACT (PUBLIC).....	iv
ACKNOWLEDGEMENTS.....	v
ATTRIBUTIONS.....	viii
TABLE OF CONTENTS.....	x
LIST OF ABBREVIATIONS.....	xvi
CHAPTER 1 INTRODUCTION.....	1
1. THE FOXO FAMILY.....	2
2. THE ROLE OF FOXOS IN METABOLISM.....	3
2.1 <i>FoxOs in adipose tissue</i> .....	3
2.2 <i>FoxOs in liver</i> .....	8
2.3 <i>FoxOs in muscle</i> .....	10
2.4 <i>FoxOs in pancreatic <math>\beta</math> cells</i> .....	11
3. FOXOS REGULATE AUTOPHAGY.....	13
3.1 <i>Autophagy</i> .....	13
3.2 <i>FoxOs regulate autophagy in liver</i> .....	15
3.3 <i>FoxOs regulate autophagy in muscle</i> .....	16
3.4 <i>FoxOs regulate autophagy in heart</i> .....	18
3.5 <i>FoxOs regulate autophagy in cancers</i> .....	19
3.6 <i>FoxOs regulate autophagy in immunity</i> .....	21
3.7 <i>FoxOs regulate autophagy in aging</i> .....	21
3.8 <i>FoxOs regulate autophagy in neurology</i> .....	22
4. DISSERTATION PROPOSAL.....	22

ABBREVIATIONS .....	23
FIGURES .....	26
REFERENCES .....	32
CHAPTER 2 TARGETING FOXO1 WITH AS1842856 SUPPRESSES ADIPOGENESIS .....	42
ABSTRACT .....	43
KEYWORDS .....	43
INTRODUCTION .....	44
RESULTS AND DISCUSSION.....	45
<i>Persistent inhibition of FoxO1 by AS1842856 prevented adipocyte differentiation.</i> .....	45
<i>AS1842856 reduced PPAR<math>\gamma</math> protein levels.</i> .....	46
<i>AS1842856 reduced mitochondrial protein levels.</i> .....	47
<i>FoxO1 underwent sigmoid activation during adipocyte differentiation.</i> .....	47
<i>AS1842856 had stage-dependent effects on adipogenesis.</i> .....	49
CONCLUSION.....	50
MATERIALS AND METHODS .....	51
<i>Materials</i> .....	51
<i>Cell culture and differentiation induction</i> .....	51
<i>AS1842856 Treatments</i> .....	52
<i>Oil Red O staining</i> .....	52
<i>Western Blot</i> .....	53
STATISTICAL ANALYSES.....	53
FUNDING .....	53
CONFLICT OF INTEREST.....	54

ABBREVIATIONS .....	54
FIGURES .....	55
REFERENCES .....	68
<b>CHAPTER 3 FOXO1 ANTAGONIST SUPPRESSES AUTOPHAGY AND LIPID DROPLET GROWTH IN ADIPOCYTES .....</b>	<b>70</b>
ABSTRACT .....	71
KEYWORDS .....	71
INTRODUCTION .....	72
RESULTS .....	73
<i>FoxO1 antagonist suppressed autophagy during adipocyte differentiation.....</i>	<i>73</i>
<i>FoxO1 antagonist reduced LD size in adipocytes. ....</i>	<i>74</i>
<i>Targeting autophagy with BL phenocopied the effects of FoxO1 antagonist on adipogenesis and LD size. ....</i>	<i>75</i>
<i>FSP27 was regulated by the FoxO1-autophagy axis in adipocytes. ....</i>	<i>75</i>
<i>The FoxO1-autophagy-FSP27 axis functioned in SVF primary cells. ....</i>	<i>76</i>
<i>FoxO1-autophagy axis regulated FSP27 in white adipose tissue. ....</i>	<i>76</i>
DISCUSSION .....	77
MATERIALS AND METHODS .....	79
<i>Mice.....</i>	<i>79</i>
<i>SVF isolation and culture .....</i>	<i>79</i>
<i>3T3L1 cell culture and treatment.....</i>	<i>79</i>
<i>Oil red O staining .....</i>	<i>80</i>
<i>Autophagy flux assay .....</i>	<i>81</i>

<i>Western blotting</i> .....	81
STATISTICAL ANALYSES .....	82
FUNDING .....	82
CONFLICTS OF INTEREST .....	82
ABBREVIATIONS .....	82
FIGURES .....	84
REFERENCES .....	93
CHAPTER 4 FOXO1 INTERACTS WITH TRANSCRIPTION FACTOR EB AND DIFFERENTIALLY REGULATES MITOCHONDRIAL UNCOUPLING PROTEINS VIA AUTOPHAGY IN ADIPOCYTES.....	96
ABSTRACT .....	97
KEYWORDS .....	97
INTRODUCTION .....	98
RESULTS .....	100
<i>Expression patterns of UCPs during adipocyte differentiation</i> .....	100
<i>Inhibition of FoxO1 suppressed the coordinated expression of UCPs in adipocytes</i> .....	100
<i>Suppression of autophagy recapitulated the effects of silencing FoxO1 on UCPs</i> .....	101
<i>Distribution and activity of nuclear FoxO1 was upregulated in differentiating adipocytes</i> .....	102
<i>FoxO1 regulated Tfeb by directly binding to its promoter</i> .....	102
DISCUSSION .....	103
MATERIALS AND METHODS .....	105
<i>Materials</i> .....	105
<i>Cell culture and treatment</i> .....	106

<i>Measurement of lipid accumulation in adipocytes</i> .....	107
<i>RNA extraction and cDNA synthesis</i> .....	107
<i>Real time PCR</i> .....	108
<i>ChIP assay</i> .....	108
<i>Measurement of nuclear FoxO1 activity</i> .....	109
<i>Western blotting</i> .....	109
STATISTICAL ANALYSES .....	110
ACKNOWLEDGEMENTS.....	110
CONFLICTS OF INTEREST .....	110
ABBREVIATIONS: .....	110
FIGURES .....	112
REFERENCES .....	118
CHAPTER 5 TAMOXIFEN REDUCES FAT MASS BY BOOSTING REACTIVE OXYGEN SPECIES .....	121
ABSTRACT: .....	122
KEYWORDS: .....	122
INTRODUCTION .....	123
RESULTS .....	124
<i>Tam induced fat mass reduction in mice</i> .....	124
<i>Tam promoted apoptosis and autophagy in adipose tissue</i> . .....	125
<i>Tam promoted the production of reactive oxygen species (ROS)</i> .....	126
<i>Antioxidant abolished Tam-induced ROS, apoptosis and autophagy</i> .....	126
<i>Antioxidant reversed Tam-induced reduction in cell density and adipocyte population</i> ....	127

<i>Antioxidant reversed Tam-induced downregulation of Peroxisome proliferator-activated receptor gamma (PPAR<math>\gamma</math>).</i> .....	127
DISCUSSION .....	128
MATERIALS AND METHODS .....	130
<i>Materials</i> .....	130
<i>Mice</i> .....	131
<i>Cell culture and Treatment</i> .....	131
<i>ROS measurement</i> .....	132
<i>Western Blot</i> .....	133
STATISTICAL ANALYSES .....	134
ACKNOWLEDGEMENT .....	134
CONFLICT OF INTEREST .....	134
ABBREVIATIONS: .....	134
FIGURES .....	136
REFERENCES .....	144
CHAPTER 6 CONCLUSIONS AND FUTURE DIRECTION .....	148
CONCLUSIONS .....	148
FUTURE DIRECTION .....	149
REFERENCES .....	151

## LIST OF ABBREVIATIONS

### A

ACO: Acyl-CoA oxidase

AMPK: AMP-activated protein kinase

AR: adrenoceptor

AS1842856: 5-amino-7-(cyclohexylamino)-1-ethyl-6-fluoro-4-oxo-1,4-dihydroquinoline-3-carboxylic acid

ASOs: antisense oligonucleotides

Atg5: autophagy related 5

Atg7: autophagy related 7

ATP: adenosine triphosphate

### B

BAT: brown adipose tissue

BL: bafilomycin-A1 and leupeptin

BMI: basal media I

BMI: body mass index

BMII: basal media II

### C

C/EBPs: CCAAT/enhancer-binding proteins

C1: mitochondrial complex I

C3: mitochondrial complex III

Carboxy-DCFDA: 5, 6-carboxy-2', 7'-dichlorofluorescein diacetate

Cas3(c): cleaved caspase 3

CCAR1: cell cycle and apoptosis regulator 1

CD36: cluster of differentiation 36

CGRP:

ChIP: chromatin immunoprecipitation

CMV: controlled mechanical ventilation

CRC: colorectal cancer cell

CREB: cAMP response element binding protein

### D

DAF-16: Dauer Formation-16

df-Irs: Irs1/Irs2 double floxed mice

DI: differentiation induction

DMI: differentiation media I

DMII: differentiation media II

### E

EGCG: Epigallocatechin gallate

eWAT: epididymal white adipose tissue

## **F**

Fas: fatty acids  
FAT: fatty acid translocase  
FBS: fetal bovine serum  
f-FoxO1: FoxO1 floxed mice  
FGF21: fibroblast growth factor 21  
FIP200: the focal adhesion kinase family interacting protein of 200 kD  
FoxO1: factor forkhead box O1  
FSP27: fat specific protein 27

## **G**

G6Pase: Glucose-6-phosphatase  
GAPDH: glyceraldehyde 3-phosphate dehydrogenase  
GR: Glucocorticoid Receptor

## **H**

HDAC6: histone deacetylase 6  
HDACIs: Histone deacetylase inhibitors  
HFHSD: high-fat high-sucrose diet  
HIF1 $\alpha$ : hypoxia-inducible factor 1 $\alpha$   
HO1: heme oxygenase 1

## **I**

I.P.: intra-peritoneal  
IGF-1: insulin-like growth factor-1  
iNK: immature NK  
Irs: insulin receptor substrate

## **J**

JNK: c-Jun N-terminal kinase

## **K**

KAA: ketogenic amino acid  
KLFs: Krupel-like factors

## **L**

LC3: light chain 3  
LC3: microtubule-associated protein 1A/1B-light chain 3-phosphatidylethanolamine conjugate  
LD: lipid droplet  
LDHA: Lactate dehydrogenase A  
LPL: lipoprotein lipase

## **M**

mb: mushroom body

MEFs: Mouse embryo fibroblasts  
MI: myocardial infarction  
MST1: Mammalian Sterile 20-like kinase 1  
mTORC1: mammalian target of rapamycin complex 1  
MTP: microsomal tryglyceride transfer protein  
MuRF-1: muscle RING finger enzyme-1

## **N**

NAC: N-acetyl cysteine  
NCoR: nuclear receptor corepressor  
NK: natural killer

## **O**

OA: osteoarthritis

## **P**

p62: sequestosome 1 (SQSTM1)  
PDK4: pyruvate dehydrogenase kinase 4  
Pdx1: pancreas/duodenum homeobox gene-1  
PEPCK: phosphoenolpyruvate carboxykinase  
PGC-1 $\alpha$ : peroxisome proliferator-activated receptor- $\gamma$  coactivator-1 $\alpha$   
PI3P: Phosphatidylinositol 3-phosphate  
PKA: protein kinase A  
PKM2: Pyruvate kinase isozymes M2  
Pml: promyelocytic leukemia protein  
PPAR $\gamma$ : peroxisome proliferator-activated receptor gamma

## **Q**

qPCR: quantitative polymerase chain reaction

## **R**

ROS: reactive oxygen species  
RXR: retinoid X receptor

## **S**

Sirt1: Sirtuin 1  
SMRT: silencing mediator for retinoid and thyroid receptors  
SN: sympathetic neuron  
SRCs: steroid receptor coactivators  
SREBP1: sterol regulatory element binding protein 1  
SREBP2: sterol response element-binding protein 2  
STAT5A: Signal transducer and activator of transcription 5A  
STZ: Streptozotocin  
SVF: stromal vascular fraction

## **T**

T2DM: type 2 diabetes mellitus  
Tam: Tamoxifen  
Tfeb: transcription factor EB  
TR: thyroid hormone receptor  
TZD: Thiazolidinedione

## **U**

UCP: uncoupling protein  
ULK: Unc-51-like kinase

## **V**

VLDL: very-low-density lipoprotein

## **W**

WAT: white adipose tissue  
Wnts: Wingless and INT-1 proteins

## Chapter 1 Introduction

Obesity (BMI>30) is a rapidly growing epidemic not only in the USA, but around the world<sup>1</sup>. In 2014 there were more than 1.9 billion adults (aged 18 years and older) overweight, of those more than 600 million obese adults around the world, and more than 2.8 million adults die of overweight or obesity each year (www.who.int). It is estimated that about \$210 billion per year is spent on the medical care of obesity-related illness in USA<sup>2</sup>. Prevention and treatment of obesity and its-related diseases are challenging tasks around the world. Characterized by excess adiposity, obese individuals tend to develop metabolic syndromes including insulin resistance, cardiovascular diseases, fatty liver diseases, and type II diabetes<sup>3</sup>. Therefore, control of adiposity is very important to prevent obesity and related diseases. Although the molecular mechanism of obesity is not fully understood, excess adiposity may be attributed to increased adipogenesis (hyperplasia) and adipocyte size (hypertrophy)<sup>4,5</sup>. Recent studies suggest that autophagy, a process that recycles or remodels cytoplasmic constituents, contributes to adipogenesis<sup>6-8</sup>. However, it is unknown how adipocyte autophagy is regulated, and the pathway by which autophagy regulates adipocyte biology remains largely unclear. Previous research from our lab and others have shown that metabolic stress activates transcription factor FoxO1 (forkhead box O1) in obesity<sup>9-11</sup>. Therefore, we hypothesize that FoxO1 may play an important role in adipocyte autophagy and biology. In this chapter, I will present a broader view of FoxO transcription factors and their role in metabolic and autophagy regulation, followed by a brief proposal of my dissertation project.

## 1. The FoxO family

The forkhead box O (FoxO) family is a subclass of winged helix/forkhead transcription factors. The mammalian FoxO family currently includes four members (FoxO1, FoxO3, FoxO4 and FoxO6), which are homologues of the *Caenorhabditis elegans* transcription factor Dauer Formation-16 (DAF-16)<sup>12-16</sup>. FoxOs consist of four domains, including a highly conserved DNA binding domain (DBD), a nuclear localization signal (NLS) domain, a nuclear export sequence (NES) domain and a C-terminal transactivation domain<sup>17, 18</sup>. The expression of FoxOs is highly tissue-specific and they play different roles in specific tissues. FoxOs can regulate glucose and lipid metabolism in liver, muscle and adipose tissue responding to nutritional status or external stimuli<sup>19-21</sup>. FoxOs acted as transcriptional factors can regulate many specific genes expression to promote cell cycle arrest, resistant to oxidative stress and apoptosis, and activate autophagy to promote cell survival and extend the cellular lifespan<sup>22-27</sup>. FoxOs can be modified by many post-translational modifications, including phosphorylation, acetylation, ubiquitination, etc., and these modifications will affect the transcriptional activity of FoxOs<sup>11, 18</sup>. For instance, Insulin-phosphatidylinositol 3 kinase (PI3K)-Akt/protein kinase B (PKB) pathway can regulate the activity of FoxOs. Akt/PKB, which is a serine-threonine kinase, can phosphorylate FoxOs at different sites, one of which is located at NLS, and inhibit the transcriptional activity of FoxOs by excluding FoxOs from nucleus<sup>11, 18, 28</sup>. Deacetylation of FoxO3 by Sirt1 can increase FoxO3's induction of cell cycle arrest and resistance to cell stress, but inhibits FoxO3's induction of cell death<sup>29</sup>. Ubiquitination of FoxOs will promote the degradation of FoxOs and affect their function in tumorigenesis<sup>30</sup>. S-phase kinase-associated protein 2 (SKP2), a subunit of the Skp1/Cul1/F-box protein ubiquitin complex, can ubiquitinate FoxO1 and increase the degradation of FoxO1 after its phosphorylation at Ser-256 by Akt.<sup>30</sup> The

ubiquitination of FoxO1 by SKP2 will promote tumorigenesis.<sup>30</sup> These different forms of modification on FoxOs can regulate their activity or protein to adjust their physiological roles under certain conditions.

## **2. The role of FoxOs in metabolism**

### **2.1 FoxOs in adipose tissue**

Adipose tissue plays an important role in energy metabolism. Not only can adipose tissue store energy in form of triglycerides, but it also can secrete various adipokines, such as adiponectin and leptin, to regulate energy homeostasis<sup>11</sup>. The best studied FoxO isoform in adipose tissue is FoxO1, yet its role in adipogenesis and metabolism has been controversial and under investigation<sup>20, 31-38</sup>.

#### *2.1.1 Adipogenesis*

Adipogenesis is the process of fibroblast-like preadipocytes differentiating into mature lipid laden and insulin-responsive adipocytes, which includes roughly six stages: mesenchymal precursor, committed preadipocyte, growth-arrested preadipocyte, mitotic clonal expansion, cell-cycle arrest and mature adipocyte<sup>39, 40</sup>. Adipogenesis is a very complicated, but well-orchestrated process which requires the regulation of many transcriptional factors, such as peroxisome proliferator-activated receptor gamma (PPAR $\gamma$ ) and CCAAT/enhancer-binding proteins (C/EBPs). Although the details of adipogenesis are still not well studied, more and more activators or repressors have been identified, including Wingless and INT-1 proteins (Wnts) and  $\beta$ -catenin, cell-cycle proteins, Kruppel-like factors (KLFs), sterol regulatory element binding protein 1 (SREBP1), etc.<sup>39, 40</sup> (Figure 1). Previous studies have shown that PPAR $\gamma$  is both

required and sufficient to induce adipogenesis. PPAR $\gamma$  belongs to the nuclear factor superfamily of ligand activated transcription factors and includes three domains: the N-terminal domain, a DNA binding domain and a C-terminal ligand binding domain<sup>41</sup>. Transcribed from alternative promoters, the PPAR $\gamma$  gene gives rise to two protein isoforms, PPAR $\gamma$ 1 and PPAR $\gamma$ 2. Both PPAR $\gamma$ 1 and PPAR $\gamma$ 2 are highly expressed in adipocytes, and PPAR $\gamma$ 2 is almost adipocyte specific<sup>42</sup>. PPAR $\gamma$  forms a heterodimer with retinoid X receptor (RXR) to bind DNA on thousands of sites in mature adipocytes based on the genome-wide mapping data<sup>43,44</sup>. The endogenous PPAR $\gamma$  ligand is still unknown, although some lipid metabolites have been implicated as PPAR $\gamma$  ligands, including polyunsaturated fatty acids (FAs), eicosanoids and 15-deoxy- $\Delta$  12, 14- prostaglandin J2. However, these molecules either have low affinity for PPAR $\gamma$  or low expression in adipocytes, making them uncertain as endogenous PPAR $\gamma$  ligands<sup>45-47</sup>. Thiazolidinedione (TZD), a potent insulin sensitizer, targets and activates PPAR $\gamma$  to regulate adipogenesis in the adipocyte<sup>48</sup>. In the absence of ligand, PPAR $\gamma$  binds to target genes and represses transcription by interacting with corepressors such as nuclear receptor corepressor (NCoR), silencing mediator for retinoid and thyroid receptors (SMRT), and histone deacetylases. When the ligand binds, the conformation of PPAR $\gamma$  is changed. This switch allows the binding of coactivators, such as steroid receptor coactivators (SRCs) and peroxisome proliferator-activated receptor- $\gamma$  coactivator-1 $\alpha$  (PGC-1 $\alpha$ )<sup>41,49</sup>. PPAR $\gamma$  is induced during adipogenesis in adipocyte cell lines such as 3T3-L1<sup>50</sup>. PPAR $\gamma$  is also required for differentiation of adipose tissue *in vivo*. Although PPAR $\gamma$  knockout caused embryonic lethality due to placental vascularization, a mice chimeric study showed that PPAR $\gamma$  deficient cells didn't contribute to adipose tissue development<sup>51,52</sup>. Furthermore, fat specific knockout PPAR $\gamma$  reduced BAT and WAT and PPAR $\gamma$ 2 specific knockout showed that PPAR $\gamma$ 1 could almost compensate the

function of PPAR $\gamma$ 2 in the development of adipose tissue<sup>53-56</sup>. In conclusion, PPAR $\gamma$  is a major regulator for adipogenesis.

CCAAT/enhancer-binding proteins (C/EBPs) belong to a family of basic-leucine zipper proteins, which include at least six protein isoforms (C/EBP $\alpha$ ,  $\beta$ ,  $\gamma$ ,  $\delta$ ,  $\epsilon$  and  $\zeta$ )<sup>57</sup>. Many of the C/EBPs (i.e.  $\alpha$ ,  $\beta$ ,  $\delta$ ) have shown to play important roles in adipogenesis<sup>57</sup>. C/EBP $\alpha$  and PPAR $\gamma$  are the two major regulators in adipogenesis. C/EBP $\alpha$  ChIP-chip study showed that 35-60% co-localization of C/EBP $\alpha$  and PPAR $\gamma$ , which suggested that both C/EBP $\alpha$  and PPAR $\gamma$  were required for expression of certain genes<sup>43</sup>. Whole body knockout of the C/EBP $\alpha$  gene caused mice to die of hypoglycemia in 8 hours after birth and failed to accumulate lipid in adipocytes<sup>58</sup>. And poly(I:C) induced whole body knockout C/EBP $\alpha$  cause hypophaga, weight loss, fat mass loss in white adipose tissue, and death 1 month after injection of poly(I:C)<sup>59</sup>. These studies showed that C/EBP $\alpha$  played important roles in maintenance the function of adipocytes. It was shown that overexpression of PPAR $\gamma$  can induce adipogenesis in C/EBP $\alpha$ -deficient cells; however, C/EBP $\alpha$  can't promote adipogenesis in PPAR $\gamma$ -deficient cells, indicating that C/EBP $\alpha$  is dispensable in adipogenesis<sup>60</sup>. C/EBP $\beta$  was shown to be required in adipogenesis both *in vitro* and *vivo* studies. Mouse embryo fibroblasts (MEFs) from C/EBP $\beta$  –deficient mice can't differentiate into mature adipocytes, while ectopic expression of C/EBP $\beta$  in MEFs from C/EBP $\beta$  –deficient mice restored adipogenesis<sup>61</sup>. About 85% of C/EBP $\beta$ ,  $\delta$  double knockout mice died at the early neonatal stage with no accumulation of droplets in brown adipose tissue (BAT) and reduced white adipose tissue (WAT)<sup>62</sup>, but loss of both C/EBP $\alpha$  and C/EBP $\beta$  can reduce adipocyte-specific genes, such as aP2 and adiponectin, which means that C/EBPs play an important role in adipogenesis<sup>43</sup>.

In addition to PPAR $\gamma$  and C/EBPs ( $\alpha$ ,  $\beta$ ,  $\delta$ ), many other transcription factors play emerging roles in adipogenesis. For instance, cAMP response element binding protein (CREB), which belongs to the bZIP transcription factor family, was able to promote adipogenesis in 3T3-L1 cells when expressed in a constitutively active CREB form, while a dominant-negative CREB alone blocked adipogenesis<sup>63</sup>. Further research showed that CREB induced the expression of C/EBP $\beta$  to regulate the adipogenesis<sup>64</sup>, and CREB was activated in adipocytes in the obese condition. Transgenic mice with a dominant-negative CREB transgene promoted insulin sensitivity in diet-induced or genetic obesity<sup>65</sup>. The above mentioned data showed that CREB could promote adipogenesis. Glucocorticoid Receptor (GR), which is a member of steroid receptor family of nuclear receptors, also plays important role in adipogenesis through transient function with other enhancers to induce gene expression including PPAR $\gamma$ <sup>266</sup>. Further studies have shown that GR can recruit cell cycle and apoptosis regulator 1 (CCAR1), which is a transcription co-regulator, to the GR binding regions (GBRs) of PPAR to induce the expression of PPAR $\gamma$ ; while CCAR1 deficient inhibited adipogenesis in mouse mesenchymal stem cell and 3T3-L1 cells<sup>67</sup>. Recently, a study showed that Foxa3 was a direct target of GR in adipose tissue<sup>68</sup>. Signal transducer and activator of transcription 5A (STAT5A), a member of STAT family of transcription factors, is also required for adipogenesis. Overexpression of wild-type STAT5A could promote adipogenesis, while dominant-negative STAT5A attenuated adipogenesis in adipocytes<sup>69</sup>. A further study showed that STAT5A associated with GR to promote adipogenesis<sup>70</sup>. Other proteins are involved in the process of adipogenesis as activators or repressors, such as the KLFs, Krox20, SREBP-1c, thyroid hormone receptor (TR), Wnts,  $\beta$ -catenin and cell cycle proteins<sup>39, 71</sup>. All of these regulators should be fine-tuned to control the process of adipogenesis. The

dysfunction of one or more regulators may cause dysfunction of adipogenesis and related obesity and metabolic diseases, such as type 2 diabetes.

### *2.1.2 FoxO1 regulates adipogenesis*

FoxO1 is regulated by insulin through phosphorylated Akt and plays an important role in adipocyte differentiation (Figure 2). Overexpressing a constitutively active form of FoxO1 inhibits the differentiation of preadipocytes, while dominant-negative FoxO1 rescues the differentiation of fibroblast from insulin-receptor knockout mice<sup>20</sup>. FoxO1 haploinsufficiency can protect mice from diet-induced diabetes. A further study showed that FoxO1 can disrupt the DNA binding of PPAR $\gamma$ /RXR $\alpha$  complex to inhibit the differentiation<sup>34</sup>. FoxO1 can transrepress PPAR $\gamma$  by direct protein-protein interaction, which can be disrupted by insulin-induced phosphorylation of FoxO1<sup>36</sup>. Furthermore, FoxO1 can inhibit the expression of PPAR $\gamma$ 1 and PPAR $\gamma$ 2 in rat primary adipocytes and increase the expression of Glut 4, thereby improving insulin sensitivity<sup>35</sup>. Overexpression of a mutant FoxO1 in adipose tissue-specific FoxO1 transgenic mice can increase Glut 4 and improve glucose tolerance and insulin sensitivity<sup>72</sup>. Other studies have shown that the acetylation of Foxo1 also affects the FoxO1 activity in adipocyte differentiation. Overexpression of Sirt2, which is a cytoplasmic predominant sirtuin in adipocytes, decreases the acetylation of FoxO1 and reduces the expression of PPAR $\gamma$ , CEBP $\alpha$  and other genes involved in terminal adipocyte differentiation as well as inhibits differentiation. Knockdown of Sirt2 promotes adipogenesis<sup>73</sup>. Resveratrol increases Sirt1, but decreases FoxO1 and PPAR $\gamma$ 2 and inhibits differentiation. However, nicotinamide can decrease Sirt1 mRNA but increase FoxO1 and PPAR $\gamma$ 2 to stimulate the differentiation in pig preadipocytes<sup>74</sup>. However, other studies show that FoxO1 is required during adipocyte differentiation. Knockdown of

FoxO1 using adenovirus FoxO1-siRNA inhibits the differentiation of 3T3-L1 preadipocyte and is accompanied by decreased PPAR $\gamma$  and CEBP $\alpha$ , especially when exposing cells to FoxO1-siRNA before the differentiation induction<sup>32</sup>. Epigallocatechin gallate (EGCG) treatment can inhibit the adipocyte differentiation via FoxO1 and SREBP1-c inactivation<sup>31</sup>. These seemingly controversial data indicate the complex role of FoxO1 in adipocyte differentiation, especially in different stages of adipogenesis.

## **2.2 FoxOs in liver**

The liver is a major organ for glucose and lipid metabolism (Figure 3). Plasma glucose levels are maintained well through glucose production and uptake by peripheral tissues such as the liver, adipose tissue, and skeletal muscle in normal conditions<sup>9</sup>. During a fasting period, the liver will break down glycogen and increase gluconeogenesis to increase the glucose levels; while under postprandial condition, the liver can store glucose through glycogen synthesis and reduce glucose level in the bloodstream<sup>11</sup>. Glucose-6-phosphatase (G6Pase), fructose-1, 6-biophosphatase and phosphoenolpyruvate carboxykinase (PEPCK) are three major gluconeogenic enzymes in liver. Overexpression of a constitutively active form of FoxO1 in the liver of transgenic mice increases fasting glucose levels and glucose intolerance. The genes involved in gluconeogenesis, such as G6Pase and PEPCK, are also increased; while de novo lipogenesis is decreased after re-feeding<sup>21</sup>. Inhibition of FoxO1 expression using antisense oligonucleotides (ASOs) in mouse hepatocytes can decrease mRNA levels of G6Pase and PEPCK and lipolysis, while increasing insulin sensitivity and glucose tolerance in mice with diet-induced obesity<sup>75</sup>. Recently, similar results have shown that liver-specific ablation of insulin receptor (LIRKO) increases glucose intolerance and insulin resistance, while liver-specific

double knockout insulin receptor and FoxO1 (LIRFKO) rescue glucose tolerance, reduce hepatic glucose production, and decrease gluconeogenic gene expression, such as G6Pase and PEPCK<sup>76</sup>. The above-mentioned data show that FoxO1 can increase hepatic glucose production through upregulating G6Pase and PEPCK.

FoxOs also play roles in lipid metabolism. Adenoviral delivery of FoxO1 to mouse liver can induce steatosis through increasing triglyceride accumulation but decreasing fatty acid oxidation<sup>77</sup>. Another study showed that in HepG2 cells, FoxO1 can induce the expression of microsomal tryglyceride transfer protein (MTP), by directly binding to the MTP promoter<sup>78</sup>. MTP is a rate-limiting protein involved in very-low-density lipoprotein (VLDL) production. Overexpression of a constitutively active FoxO1 in mice can increase the expression of MTP, VLDL production, and plasma triglyceride levels<sup>78</sup>. Adenovirus-mediated FoxO1 delivered to hepatocytes stimulates the expression of apoC-III through directly binding to the promoter of apoC-III, which plays an important role in triglyceride metabolism, and results in increased triglyceride levels in the plasma and fat intolerance<sup>79</sup>. A mutation or deletion of the FoxO1 binding site on the apoC-III promoter can abolish the insulin response and FoxO1-mediated stimulation. A further study showed that PPAR $\alpha$  interacts with FoxO1 to regulate the apoC-III expression<sup>80</sup>. Interestingly, it was shown that FoxO1 deletion in the liver using Cre/LoxP genetic approach decreases glucose concentration in blood but has little effect on lipid homeostasis. Deletion both FoxO1 and FoxO3 decreases glucose concentrations and elevates serum tryglyceride and cholesterol concentration, which indicates that FoxO3 has a role in lipid metabolism<sup>81</sup>. A further study showed that FoxO3 can recruit Sirt6 to regulate sterol response element-binding protein 2 (SREBP2) by binding to the Srebp2 gene promoter where Sirt6 can

deacetylates lysine 9 and 56 on histone H3, and further cholesterol homeostasis<sup>82</sup>. It was shown that FoxO1 can increase insulin sensitivity by inhibiting tribbles homolog 3 (Trb3), which prevents the phosphorylation of Akt by binding to it, to increase the phosphorylation of Akt<sup>77</sup>. Above data show the important roles of FoxOs in the regulation of glucose and lipid metabolism.

### **2.3 FoxOs in muscle**

Skeletal muscle is a major peripheral tissue that is responsible for insulin-mediated energy homeostasis, which contributes more than 30% of resting metabolic rate and 80% whole body glucose uptake<sup>83</sup>. FoxO1 plays important roles in regulating glucose and lipid metabolism in skeletal muscle (Figure 4). Under starvation or glucocorticoid treatment, FoxO1 is induced and pyruvate dehydrogenase kinase 4 (PDK4) is upregulated by FoxO1 which can directly bind to the promoter of PDK4 and further inhibit glucose oxidation<sup>19</sup>. A further study shows that the effect of RXR $\gamma$  on enhanced glucose tolerance may be at least in part due to upregulated Glut1 in skeletal muscle<sup>84</sup>. Another study showed that ectopic expression of FoxO1 increased the gene expression of lipoprotein lipase (LPL), which plays an important role in lipid usage in skeletal muscle<sup>85</sup>. Overexpression of FoxO1 using inducible constructs in C2C12 cells increases the fatty acid translocase FAT/cluster of differentiation 36 (CD36), Acyl-CoA oxidase (ACO) and PPAR $\delta$ , and enhances the uptake of oleate and oleate oxidation<sup>86</sup>. These effects of enhanced FA utilization induced by FoxO1 can be abolished by the CD36 inhibitor. SREBP1c also plays a role in regulation of lipid metabolism via FoxO1. RXR $\alpha$  or RXR $\gamma$ , together with liver X receptor  $\alpha$  (LXR $\alpha$ ), can activate the promoter of SREBP1c<sup>87</sup>. Overexpression of RXR $\gamma$  in skeletal muscle increases SREBP1c and triglyceride concentrations; and overexpression of FoxO1 decreases the expression of RXR $\gamma$  and SREBP1c<sup>87</sup>. The above-mentioned data show that FoxO1 prevents the

RXR/LXR-mediated SREBP1c in the regulation of lipogenesis. AMP-activated protein kinase (AMPK), which is a master regulator of glucose and lipid metabolism, can upregulate FoxOs (including FoxO1 and FoxO3a) and atrogin-1 as well as muscle RING finger enzyme-1 (MuRF-1) and leads to a further increase in the protein degradation in skeletal muscle<sup>88</sup>. Short-term cold stimulation can reduce the phosphorylation of Akt and increase the activity of FoxO1, which increases the expression of atrogin-1 and MuRF-1, thereby increasing the protein degradation in skeletal muscle<sup>89</sup>. Overexpression of FoxO1 in skeletal muscle can reduce the body weight and skeletal muscle mass, decrease type I muscles. Overexpression of FoxO1 can also increase the expression of cathepsin L, which is a lysosomal proteinase, leading to increased protein degradation in skeletal muscle<sup>90</sup>. Hence, Not only do FoxOs play important roles in switching from glucose oxidation to fatty acid utilization, but they also increase muscle atrophy in skeletal muscle.

## **2.4 FoxOs in pancreatic $\beta$ cells**

The pancreas plays a critical role in glucose homeostasis and contains at least five different types of cells:  $\alpha$ -cell,  $\beta$ -cell,  $\delta$ -cell,  $\epsilon$ -cell and PP-cell<sup>91</sup>.  $\beta$  cells can sense the blood glucose concentration and secrete insulin to regulate glucose homeostasis. Generally,  $\beta$  cells can uptake and metabolize glucose, thereby increasing the cellular ratio of ATP/ADP to close the  $K^+$ -ATP channel and depolarize the cell. Depolarization of the cell leads to the opening of the voltage-dependent  $Ca^{2+}$  channel and a subsequent increase the cytosolic  $Ca^{2+}$  concentration, leading to the release of insulin<sup>92</sup>. Previous studies show that insulin signaling is required to maintain  $\beta$  cell mass. Mice with insulin receptor substrate-2 knockout (IRS2KO) develop  $\beta$  cell failure. While haploinsufficiency of FoxO1 can reverse  $\beta$  cell failure in IRS2KO mice through the increase in  $\beta$

cell proliferation as well as increase the expression of pancreas/duodenum homeobox gene-1 (Pdx1), which is a pancreatic transcription factor<sup>93</sup>. Overexpressing a constitutively active form of FoxO1 decreases the Pdx1 expression by acting as a repressor of Foxa2-dependent Pdx1 transcription. These data show that insulin signaling can increase the expression of Pdx1 to maintain  $\beta$  cell mass through inhibition of FoxO1. A further study showed that the deletion of FoxO1 in the domain of the Pdx1 promoter (P-FoxO1-KO) improved glucose tolerance under high-fat high-sucrose diet (HFHSD). Additionally, this led to an increased  $\beta$  cell mass. Mice with P-FoxO1-KO crossed with db/db showed more severe glucose intolerance than in the control mice, indicating that FoxO1 functions as a double-edged sword in the pancreas<sup>94</sup>. FoxO1 can also regulate  $\beta$  cell function, survival, and compensation through the inhibition of PPAR $\gamma$  and its target genes, such as Pdx1 and pyruvate carboxylase<sup>95</sup>. Impaired FoxO1 may cause or exacerbate diabetes<sup>95</sup>. Controversially, upregulated FoxO1 in  $\beta$ -cell-specific FoxO1-transgenic mice can increase  $\beta$ -cell mass, improve glucose tolerance, and protect the mice from HFD-induced glucose disorder<sup>96</sup>. Furthermore, FoxO1 plays other roles in  $\beta$  cell function. It was shown that FoxO1 can protect  $\beta$  cell from oxidative stress by increasing two insulin2 gene transcription factors, NeuroD and MafA, through forming a complex with promyelocytic leukemia protein (Pml) and Sirt1. Acetylated FoxO1 can bind to Pml and prevent FoxO1 from degradation. While Sirt1 can deacetylate FoxO1 and accelerate its degradation, thereby prevent unchecked FoxO1 transcription<sup>97</sup>. Another study shows that the c-Jun N-terminal kinase (JNK) pathway can regulate FoxO1 translocation from the cytosol to the nucleus. Overexpression of JNK can induce the nuclear localization of FoxO1, while inhibiting JNK can decrease the oxidative stress-induced FoxO1 nuclear localization<sup>98</sup>. Generally, more studies are needed to elucidate the

complicated roles of FoxO1 in  $\beta$  cell function, proliferation, and compensation, especially under different physiological conditions, such as diabetes.

### **3. FoxOs regulate autophagy**

#### **3.1 Autophagy**

Autophagy (from the Latin words “auto,” means oneself and “phagy,” meaning to eat) refers to physiological degradative processes during which cytosolic components are degraded in bulk. This includes the degradation of proteins, lipids, sugars, and some organelles (mitochondria, peroxisomes, ribosomes, et c) <sup>99</sup>. Generally, there are three types of autophagy, including microautophagy, macroautophagy, and chaperone-mediated autophagy. Microautophagy is the process where the lysosome membrane engulfs part of cytoplasm. Macroautophagy is the degradative process that involves a formation of autophagosome. Finally, chaperone-mediated autophagy is a selective degradative process that can specifically degrade proteins recognized by the chaperone protein Hsc70. Macroautophagy (referred to as autophagy hereafter) is a self-protective mechanism for cells under nutrition deprivation.

Autophagy is a well-regulated degradative system and many factors are involved in this process, which can be divided into several steps: initiation; elongation; maturation; autophagosome-lysosome fusion and degradation <sup>99</sup> (Figure 5). Although the sources of isolation membranes are still not fully understood, endoplasmic reticulum (ER) is the most important isolation membrane contributor to initiate the autophagy under starvation. The Golgi complex, endosome, mitochondria, plasma and nuclear membranes are also possible membrane sources <sup>100</sup>. Under starvation, following the induction of autophagy, a  $\Omega$ -like shape domain on ER is formed which

termed as omegasome. Phosphatidylinositol 3-phosphate (PI3P), autophagy related protein 14 L (Atg14L), beclin1, vacuolar proteins 34 (Vps34) and Unc-51-like kinase 1 (ULK1) are required for the formation of omegasome<sup>101-106</sup>. Among many factors involved in the initiation of autophagy, Atg1/Unc-51-like kinase (ULK) complex plays a central role. In mammals, ULK1-atg13- the focal adhesion kinase family interacting protein of 200 kD (FIP200)-atg101 kinase complex is negatively regulated by the mammalian target of rapamycin complex 1 (mTORC1) depending on nutrient status. For instance, under nutrient sufficiency, high mTOR activity can phosphorylate ULK1 at Ser757 to prevent ULK1 activity and disrupt the ULK1-AMPK interaction, resulting in inhibition of autophagy<sup>107</sup>. Under starvation, AMPK can phosphorylate ULK1 at Ser317 and Ser777 directly and activate ULK1 to induce autophagy. Ser467 and Ser 555 on ULK1 can be also phosphorylated by AMPK to promote autophagy<sup>108</sup>.

Following the formation of the isolation membrane, it will elongate to engulf cytosol components. During the elongation of autophagy, Atg12-Atg5 translocates to the outside of the isolation membrane and detaches from the membrane before or after the autophagosome is formed completely<sup>109</sup>. The Atg12-Atg5 complex is required for targeting microtubule-associated protein 1A/1B-light chain 3-phosphatidylethanolamine conjugate (LC3) (a mammalian homolog of Atg8) onto the isolation membrane. LC3 is synthesized as a preform of ProLC3, which can be cleaved by Atg4 to expose the C-terminal Gly of LC3 (LC3-I). LC3I can conjugate with PE to form LC3-II (LC3-PE) activated by Atg7 (E1-like enzyme) and Atg3 (E2-like enzyme)<sup>110</sup>. During the elongation to maturation of autophagosome, the amount of LC3-II is increased. Atg4 can then delipidate LC3-II to LC3-I on the surface of autophagosome to recycle LC3-I.

Following the maturation of autophagosome, the outer membrane can fuse with the lysosome to form an autolysosome. The process of fusion can be positively regulated by UVRAG-Vps34-beclin1 PI3K complex, but can be also negatively regulated by Rubicon- UVRAG-Vps34-beclin1 PI3K complex<sup>101, 102</sup>. The engulfed cytosolic components, including part of LC3-II which locates on the intra-autophagosome surface, can be degraded by hydrolyses in the autolysosome. During the degradation process, the amount of LC3-II will be decreased.

In addition to nonselective autophagy, selective autophagy is also physiologically important. P62/SQSTM1, an important ubiquitin and LC3-binding protein as an autophagy adaptor, can be selectively degraded by the autolysosome<sup>111, 112</sup>. When autophagy is impaired, P62 accumulates in the cell and serves as an important biomarker for autophagy. Based on the different organelles or cytosol components involved in selective degradation, the selective autophagy family includes mitophagy (specifically for mitochondria), pexophagy (for peroxisomes), ribophagy (for ribosomes) and etc. For most of these selective autophagy processes, P62 is a critical autophagy adaptor<sup>113</sup>.

### **3.2 FoxOs regulate autophagy in liver**

FoxO1 plays an important role in hepatic lipid metabolism partly through the autophagy pathway (Figure 3). FoxOs can regulate a key autophagy-related regulator, Atg14, through binding at its promoter, which has been revealed through luciferase reporter analysis and chromatin immunoprecipitation (ChIP)<sup>114</sup>. Either knockdown Atg14 or liver-specific FoxO1/3/4 triple knockout elevated triglycerides in the liver and serum<sup>114</sup>. Overexpression of Atg14 improved hepertriglyceridemia in liver-specific FoxO1/3/4 triple knockout mice<sup>114</sup>. A ketogenic amino acid (KAA) replacement diet ameliorated autophagy deficiency in HFD-fed mice accompanied

by decreased FoxO3, increased Sirtuin 1 (Sirt1), and inhibition of the phosphorylation of the mammalian target of rapamycin (mTOR)<sup>115</sup>. Metformin alleviated hepatosteatosis through Sirt1-mediated, AMP-activated kinase (AMPK)-independent autophagy machinery<sup>116</sup>.

### 3.3 FoxOs regulate autophagy in muscle

During fasting or denervation, FoxO3 can be activated to induce autophagy in skeletal muscle and cause muscle atrophy both *in vitro* and *in vivo*<sup>117, 118</sup> (Figure 4). Phosphorylation of Akt can block FoxO3 to induce autophagy. However, rapamycin, which is a specific mTOR inhibitor, cannot rescue the effect of Akt on FoxO3 and autophagy, which indicates that FoxO3 can induce autophagy in an mTOR-independent way. FoxO3 regulates the expression of many autophagy-related genes, including LC3 and Bnip3<sup>117, 118</sup>. Recently, triple FoxO1, 3, 4 muscle-specific knockout mice were generated to study the role of FoxOs in autophagy<sup>119</sup>. It was shown that FoxOs (FoxO1, 3, 4) knockouts can prevent muscle loss after fasting through inhibition of autophagy and protein ubiquitination. Inhibition of FoxOs decreases many important autophagy-related genes such as LC3, Gabarapl, Bnip3, and P62/SQSTM1. A further study shows that FoxO1, 3, 4 are redundant in regulation of autophagy in skeletal muscle<sup>119</sup>. More studies show that histone deacetylase 6 (HDAC6) is a downstream target of FoxO3 in autophagy<sup>120</sup>. During denervation, HDAC6 is upregulated during muscle atrophy and FoxO3 can directly bind to the HDAC6 promoter to regulate the expression of HDAC6, while knockdown of HDAC6 using shRNA reduces muscle atrophy<sup>120</sup>. The role of FoxOs and the insulin or insulin-like growth factor-1 (IGF-1) signaling pathway in autophagy is further confirmed *in vivo*. Muscle-specific knockout of the insulin receptor (M-IR<sup>-/-</sup>), but not the IGF-1 receptor (M-IGF1R<sup>-/-</sup>), displays a moderate reduction in muscle mass, while both IR and IGF-1R knockout mice (MIGIRKO)

shows a marked reduction of muscle mass<sup>121</sup>. However, combined muscle-specific knockout FoxO1, 3, 4 in MIGIRKO mice reverses the increased autophagy and rescues the muscle mass loss<sup>121</sup>. These results further confirm the importance of insulin or IGF-1 mediated FoxOs' activity in autophagy in skeletal muscle. More studies show that PGC1 $\alpha$  and PGC1 $\beta$  can block the effect of FoxO3 or starvation on autophagy to prevent muscle atrophy, which indicates that exercise can increase the expression of PGC1 $\alpha$  to inhibit FoxO3 activity to prevent muscle atrophy<sup>122</sup>. Interestingly, Wei et al showed that Mammalian Sterile 20-like kinase 1 (MST1) can regulate FoxO3 activity through phosphorylation of FoxO3 at Ser207<sup>123</sup>. MST1 kinase is upregulated in fast twitch skeletal muscles immediately after denervation. Activated MST1 increases FoxO3 phosphorylation at Ser207 and promotes FoxO3's nuclear translocation to induce autophagy. Notably, MST1-mediated phosphorylation of FoxO3 at Ser 207 can promote FoxO3 nuclear translocation, while pAkt-mediated phosphorylation of FoxO3 at Thr32, Ser253, and Ser315 can inhibit FoxO3 nuclear translocation. This difference may be due to the phosphorylation occurring at different sites which may lead to impaired interactions with protein 14-3-3.

In addition to the effects that phosphorylation has on FoxO3 activity and localization, the acetylation of FoxO3 also plays a role. During fasting, the expression of Sirt1 is decreased dramatically in type II skeletal muscle which leads to increased atrophy<sup>124</sup>. Maintenance of Sirt1 can prevent atrophy induced by fasting or denervation in the skeletal muscle of mice. Overexpression of Sirt1 can block the activity of FoxO1 and FoxO3 during atrophy and further prevent the induction of expression of autophagy genes. Sirt1-mediated FoxO1 and FoxO3 deacetylation inhibits their activity to induce autophagy during fasting or denervation in skeletal

muscle. During denervation, acetylation of FoxO1 is increased, leading to an increase in the cytosolic localization of FoxO3 and its degradation via the proteasome system<sup>125</sup>. However, Hussain et al show that, in the diaphragm and limb muscles of humans, prolonged controlled mechanical ventilation (CMV) triggers autophagy, which is associated with increased gene expression of FoxO1, but not FoxO3<sup>126</sup>.

Recently, it was shown that calcitonin gene-related peptide (CGRP) can decrease FoxOs-mediated autophagy through protein kinase A (PKA)/CREB signaling *in vitro* and *in vivo* in skeletal muscle<sup>127</sup>. CGRP can elevate cAMP levels, stimulate PKA/CREB signaling, and increase FoxO1 phosphorylation to reduce the FoxO1 activity on autophagy-related gene expression in a concentration-dependent manner, while PKA inhibitors can abolish the effect of CGRP on FoxO1, 3, 4 and autophagy<sup>127</sup>.

### **3.4 FoxOs regulate autophagy in heart**

FoxO transcription factors were found to regulate autophagy in the heart under starvation or ischemia/reperfusion in mice. In cultured rat neonatal cardiomyocytes, overexpression of either FoxO1 or FoxO3 reduced cell size and induced the autophagy pathway, showing increased genes *LC3*, *Gabarapl* and *atg12*. These effects of overexpression of either FoxO1 or FoxO3 were similar to the condition of glucose deprivation<sup>128</sup>. Moreover, FoxO1 and FoxO3 directly bound to the promoters of *Gabarapl* and *atg12*. Inhibition of FoxO1 activity by overexpression of dominant negative FoxO1 ( $\Delta 256$ ) reversed the effect of starvation on cardiomyocyte size<sup>128</sup>. Under cellular stress, such as starvation or ischemia/reperfusion *in vivo*, autophagy was induced accompanied with increased FoxO1 and FoxO3 activity. Thus, FoxO1 and FoxO3 regulated autophagy and cell size in cardiomyocytes<sup>128</sup>. A further study showed that Sirt1 induced

deacetylation of FoxO1, while the upregulation of Rab7 also played a role in starvation-induced autophagy in cardiomyocytes<sup>129</sup>. FoxO3 induced autophagy via AMPK signaling pathway under conditions of hypoxia in H9C2 cells<sup>130</sup>. Insulin suppressed autophagy-related genes such as LC3 and *Gabarapl* in cardiomyocytes through phosphorylation of Akt and downstream FoxO3, while acute insulin deficiency caused by Streptozotocin (STZ) and increased autophagy genes LC3 and *Gabarapl* as well as the muscle-specific Ub-ligases atrogin-1 and MuRF1<sup>131</sup>. A further study showed that cardiac sympathetic neuron (SN) ablation caused a reduction in cardiomyocyte size through FoxO-mediated atrogin-1 and MuRF1 but decreased stimulation of cardiomyocyte  $\beta$ 2-adrenoceptor (AR)<sup>132</sup>. Consistently,  $\beta$ 2-AR agonist clenbuterol treatment prevented atrophy in denervated mice, while  $\beta$ 2-AR knockout mice showed cardiac atrophy<sup>132</sup>. FoxO transcription factors played roles in oxidative stress resistance in cardiomyocytes. FoxO1 and FoxO3 and their target genes' activities were promoted by oxidative stress. Overexpression of FoxO1 and FoxO3 reduced reactive oxidative species (ROS) and cell death, while dominant-negative FoxO1 ( $\Delta$ 256) increased ROS and cell death significantly in cardiomyocytes. Cardiomyocyte-specific FoxO1/3 knockout mice subjected to myocardial infarction (MI) showed reduced cardiac function and increased ROS and cell death compared to control. Thus, FoxO1 and FoxO3 promote cardiomyocyte survival under oxidative stress<sup>133</sup>. A further study confirmed the role of FoxO1 in protecting cardiomyocytes from oxidative stress in cardiomyocyte H9C2 cells<sup>134</sup>.

### **3.5 FoxOs regulate autophagy in cancers**

FoxOs can regulate autophagy to inhibit colorectal cancer growth<sup>135</sup>. Previous studies show that the activity of p38 $\alpha$  is required for proliferation and survival of colorectal cancer cell (CRC). P38 $\alpha$  can increase the expression of hypoxia-inducible factor 1 $\alpha$  (HIF1 $\alpha$ ) and its target glycolytic

rate-limiting genes such as GLUT1, Hexokinase (HK) 1/2, Pyruvate kinase isozymes M2 (PKM2) and Lactate dehydrogenase A (LDHA). Blockage of p38 $\alpha$  using a p38 $\alpha$  inhibitor SB202190 can decrease the expression of HIF1  $\alpha$  and its target genes, while activation of FoxO3 and its target autophagy-related genes, such as MAP1LC3, GABARAPL1, ATG 12, BNIP3, and BNIP3L induces autophagy and inhibits colorectal cancer growth. Similar results are also shown in ovarian cancer cells<sup>136</sup>. Histone deacetylase inhibitors (HDACIs) can induce autophagy through increasing the expression of FoxO1 and its transcriptional activity in HCT116 colon cancer cells<sup>137</sup>. Knockdown FoxO1 using FoxO1-specific siRNA can block HDACIs –induced autophagy. These data show that FoxO1 and FoxO3 can induce autophagy in different cancer cells. Interestingly, it is shown that cytosolic FoxO1 is required for its induction of FoxO1 and tumor suppressor activity which is independent of its transcriptional activity in different cancer cell lines (such as HCT116, Hela and H1299 cells)<sup>138</sup>. Under oxidative stress or serum starvation, cytosolic FoxO1 can dissociate with Sirt 2 which leads to the acetylation of FoxO1. The acetylated FoxO1 binds to Atg7 to induce autophagy.<sup>138</sup> Furthermore, FoxO3 can induce autophagy in a FoxO1-dependent way at least in the HEK293T human embryonic kidney cell line and mouse embryonic fibroblast (MEF) cell lines<sup>139</sup>. Controversially, other study shows that FoxO3 can negatively regulate autophagy in PC3 prostate cancer cells, HCT116 colon, and MDA-MB-231 breast cancer cell lines, as FoxO3 inhibits the expression of FoxO1<sup>140</sup>. These controversial data from different research groups indicate that the roles of FoxO1 and FoxO3 in autophagy of cancer cells are complicated and may be due to their cell-type dependent expression pattern or specific signaling pathways.

### 3.6 FoxOs regulate autophagy in immunity

The role of DAF-16 (a homologous protein of FoxO) in pathogen resistance via autophagy was initially illustrated in *C. elegans*. Overexpression of DAF-16 increased autophagy in TJ356 animals (a strain of *C. elegans*) indicated by an increased number of GFP::LGG1 punctuate dots<sup>141</sup>. This DAF-16 overexpressed TJ356 showed resistance to *Salmonella* infection, while this pathogen resistance was blocked by the autophagy genes *bec-1* and *lgg-1* RNAi<sup>141</sup>. Thus, DAF-16 (FoxO) transcription factor induced autophagy to resistant pathogen infection.

Recently, one study showed that FoxO1-mediated autophagy was required for natural killer (NK) cell maturation. Strong autophagy was found in immature NK (iNK) cells, while autophagy deficiency in NK-specific Atg5 knockout mice (*Atg5<sup>fllox/fllox</sup>, NKp46-Cre*) resulted in damaged mitochondria and an increase in ROS, as well as cell death<sup>142</sup>. Interestingly, phosphorylated FoxO1 in the cytoplasm of iNK interacted with Atg7 to induce autophagy, which is independent of the transcriptional activity of FoxO1<sup>142</sup>. Of note, another group showed that FoxO1 regulated NK maturation negatively<sup>143</sup>. Further studies are needed to confirm the role of FoxO1 in NK maturation.

### 3.7 FoxOs regulate autophagy in aging

It was shown that dFoxO regulates autophagy to affect longevity in *Drosophila*<sup>27</sup>. While the characterization of muscle aging in *Drosophila* is ongoing, accumulation of protein aggregates and overexpression of dFoxO in the muscle can delay the accumulation of protein aggregates, at least partly through autophagy<sup>27</sup>. Both dFoxO and its target- 4E-BP can delay aging-related muscle function decay and expand lifespan in *Drosophila*. Other studies show that dFoxO may activate autophagy through inhibition of the Activin signaling pathway to expand the lifespan in

*Drosophila*<sup>144</sup>. DFoxO1 can bind and repress dawdle, an Activin ligand, to prevent the inhibition of the Smad binding element on autophagy-related gene Atg8a, leading to an increased lifespan<sup>144</sup>. During human joint aging from 23-90, the expression of FoxO1 and FoxO3 are markedly decreased in the superficial zone of cartilage. In the cartilage during osteoarthritis (OA), the activity of FoxO is highly inhibited with increased phosphorylation of FoxO1 and increased cytosolic localization<sup>145</sup>. Since FoxOs can activate autophagy in many tissues, it is possible that FoxOs-mediated autophagy is decreased during the aging of knee joints.

### **3.8 FoxOs regulate autophagy in neurology**

FoxO is shown to play a role in the elimination of neural stem cells (neuroblasts) in *Drosophila*<sup>146</sup>. Inhibition of FoxO and reaper family proapoptotic genes can increase the survival of neuroblasts and maintain neurogenesis in adult mushroom body (mb), which is possibly through autophagy and apoptosis, since inhibition of autophagy-related gene Atg1 and apoptosis can also promote neuroblast survival<sup>146</sup>. FoxO1-mediated autophagy is also required for the survival of neurons in mice or MEFs<sup>147</sup>. The cJun N-terminal kinase (JNK) may act as a negative regulator of FoxO1-dependent autophagy in neurons. Triple ablation of Jnk1, Jnk2 and Jnk3 in neurons can increase the nuclear localization of FoxO1 and its target gene Bnip3 to activate autophagy and increase the neuron lifespan<sup>147</sup>.

## **4. Dissertation proposal**

As mentioned above, obesity and its related diseases are pressing health issues around the world. Understanding the molecular and cellular mechanism of obesity is the key to developing effective strategy to treat or prevent the diseases. Recent studies suggest that adipose tissues from obese and type 2 diabetic subjects have higher autophagy activity<sup>148-154</sup>. Consistently,

genetic inhibition of autophagy by targeting autophagy related 5 (Atg5) or Atg7 in adipose tissue can reduce adipocyte size and prevent mice from diet-induced obesity<sup>6-8</sup>. Ablation of Atg5 or Atg7 also prevents adipocyte differentiation<sup>8, 155</sup>. Whereas these data underline autophagy as an important regulator of adiposity, the mechanism of autophagy induction remains elusive, and it is largely unclear how altered autophagy affects adipocyte biology. Given that FoxO1 is activated in obesity and type 2 diabetes<sup>9-11</sup>, we hypothesize that FoxO1 may regulate adipocyte autophagy. Indeed, FoxO transcription factors were recently shown to mediate autophagy in liver, skeletal muscle, heart and cancer cells<sup>114, 118, 128, 138</sup>. However, a role of FoxO1 in adipocyte autophagy has not been established. This dissertation project was designed to investigate the effects of FoxO1 inhibition on adipocyte autophagy and adipocyte differentiation using 3T3L1 cell line and primary adipocytes (stromal vascular fractions). Research efforts were also made to explore the pathway by which FoxO1 regulates autophagy, and the pathway that FoxO1-autophagy axis regulates adipocyte biology.

## **Abbreviations**

ACO: Acyl-CoA oxidase  
AMPK: AMP-activated protein kinase  
AR: adrenoceptor  
ASOs: antisense oligonucleotides  
Atg5: autophagy related 5  
BAT: brown adipose tissue  
C/EBPs: CCAAT/enhancer-binding proteins  
CCAR1: cell cycle and apoptosis regulator 1  
CD36: cluster of differentiation 36  
CGRP: calcitonin gene-related peptide  
ChIP: chromatin immunoprecipitation  
CMV: controlled mechanical ventilation  
CRC: colorectal cancer cell  
CREB: cAMP response element binding protein  
DAF-16: Dauer Formation-16  
EGCG: Epigallocatechin gallate

Fas: fatty acids  
FAT: fatty acid translocase  
FIP200: the focal adhesion kinase family interacting protein of 200 kD  
FoxO1: factor forkhead box O1  
G6Pase: Glucose-6-phosphatase  
GR: Glucocorticoid Receptor  
HDAC6: histone deacetylase 6  
HDACIs: Histone deacetylase inhibitors  
HFHSD: high-fat high-sucrose diet  
HIF1 $\alpha$ : hypoxia-inducible factor 1 $\alpha$   
IGF-1: insulin-like growth factor-1  
iNK: immature NK  
JNK: c-Jun N-terminal kinase  
KAA: ketogenic amino acid  
KLFs: Krupel-like factors  
LC3: light chain 3  
LDHA: Lactate dehydrogenase A  
LPL: lipoprotein lipase  
mb: mushroom body  
MEFs: Mouse embryo fibroblasts  
MI: myocardial infarction  
MST1: Mammalian Sterile 20-like kinase 1  
mTORC1: mammalian target of rapamycin complex 1  
MTP: microsomal triglyceride transfer protein  
MuRF-1: muscle RING finger enzyme-1  
NCoR: nuclear receptor corepressor  
NK: natural killer  
OA: osteoarthritis  
PDK4: pyruvate dehydrogenase kinase 4  
Pdx1: pancreas/duodenum homeobox gene-1  
PEPCK: phosphoenolpyruvate carboxykinase  
PGC-1 $\alpha$ : peroxisome proliferator-activated receptor- $\gamma$  coactivator-1 $\alpha$   
PI3P: Phosphatidylinositol 3-phosphate  
PKA: protein kinase A  
PKM2: Pyruvate kinase isozymes M2  
Pml: promyelocytic leukemia protein  
PPAR $\gamma$ : peroxisome proliferator-activated receptor gamma  
ROS: reactive oxidative species  
RXR: retinoid X receptor  
Sirt1: Sirtuin 1  
SMRT: silencing mediator for retinoid and thyroid receptors  
SN: sympathetic neuron  
SRCs: steroid receptor coactivators  
SREBP1: sterol regulatory element binding protein 1  
SREBP2: sterol response element-binding protein 2

STAT5A: Signal transducer and activator of transcription 5A  
STZ: Streptozotocin  
TR: thyroid hormone receptor  
TZD: Thiazolidinedione  
ULK: Unc-51-like kinase  
VLDL: very-low-density lipoprotein  
WAT: white adipose tissue  
Wnts: Wingless and INT-1 proteins

**Figures:**

**Figure 1**

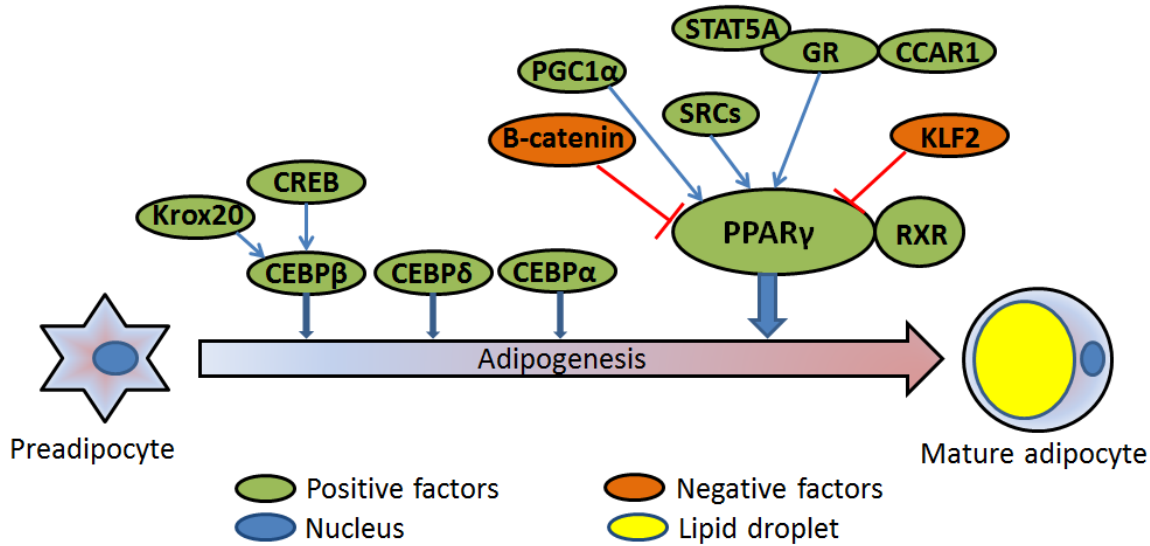


**Figure 1 Multiple transcription factors regulate the process of adipogenesis.** Adipogenesis is the process of preadipocytes differentiating into mature adipocytes, which requires many different factors. PPAR $\gamma$  is a major positive regulator of adipogenesis. Many other factors, such as PGC1 $\alpha$ , SRCs, GR, STAT5A and CCAR1, can promote adipogenesis through PPAR $\gamma$ ; CEBPs ( $\alpha$ ,  $\beta$ ,  $\delta$ ) can also promote adipogenesis; while Krox20 and CREB can increase adipogenesis through activating CEBP $\beta$ . However,  $\beta$ -catenin and KLF2 can suppress adipogenesis via inhibition of PPAR $\gamma$ . CREB: cAMP response element binding protein; C/EBP: CCAAT/enhancer-binding protein; CCAR1: cell cycle and apoptosis regulator 1; GR: Glucocorticoid Receptor; KLF: Krupel-like factor; PGC-1 $\alpha$ : peroxisome proliferator-activated receptor- $\gamma$  coactivator-1 $\alpha$ ; PPAR $\gamma$ : peroxisome proliferator-activated receptor gamma; RXR: retinoid X receptor; SRCs: steroid receptor coactivators; STAT5A: Signal transducer and activator of transcription 5A.

**Figure 2**

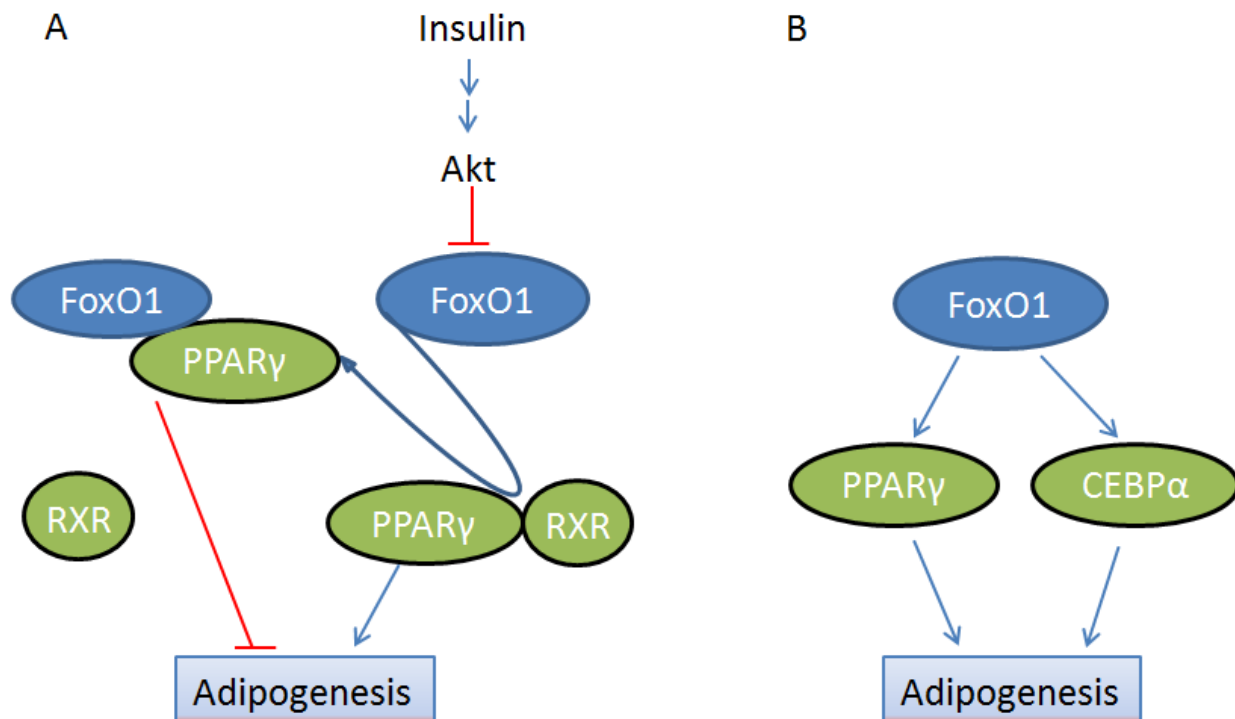


**Figure 2 A paradoxical views of FoxO1 regulating adipogenesis.** (A) FoxO1 may transrepress PPAR $\gamma$  by forming complex with PPAR $\gamma$ , thereby inhibiting adipogenesis; insulin can promote adipogenesis by inhibiting FoxO1. (B) FoxO1 is required for adipogenesis. Knockdown of FoxO1 reduces PPAR $\gamma$  and CEBP $\alpha$  expression, and prevents adipogenesis. RXR: retinoid X receptor.

**Figure 3**

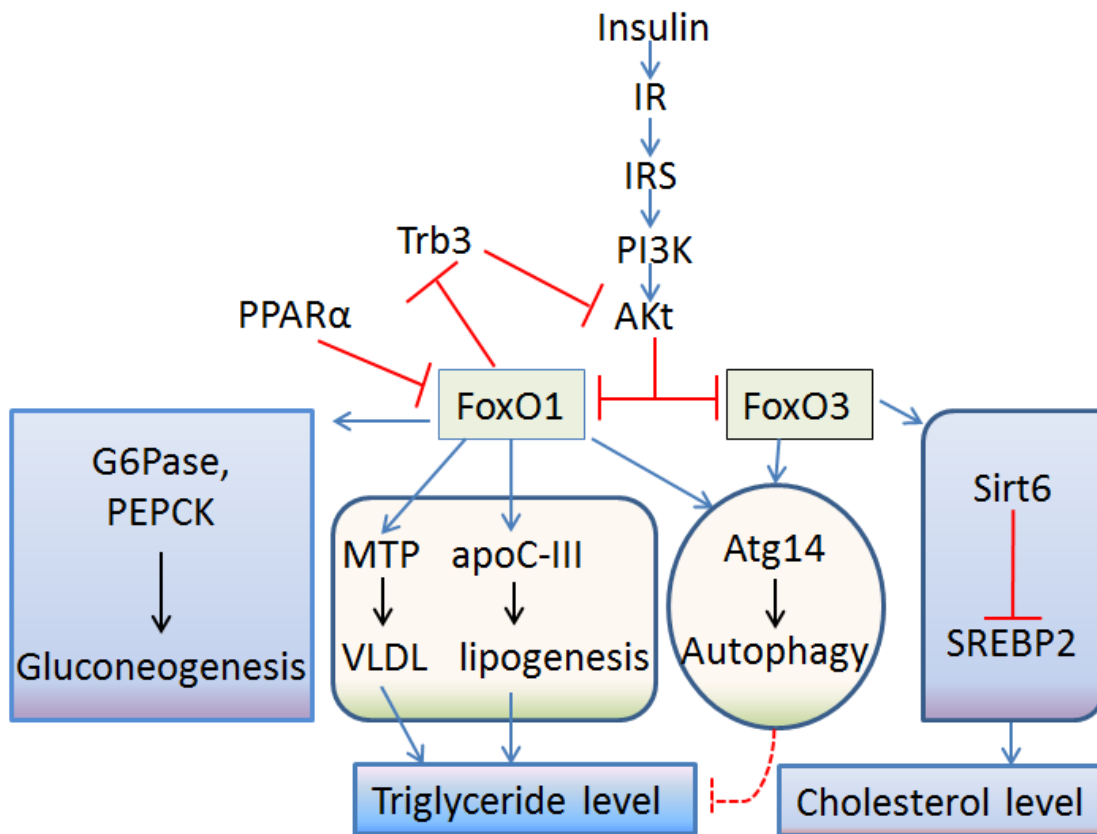


**Figure 3 FoxOs regulate glucose and lipid metabolism in the liver.** Under postprandial condition, insulin signaling pathway is activated to inhibit FoxO1 and FoxO3. In fasting state, FoxO1 is activated to upregulate gluconeogenesis through G6Pase and PEPCK. FoxO1 can activate MTP/VLDL pathway and promote lipogenesis through apoC-III, thereby increasing triglyceride level in serum. However, other evidence suggests FoxOs can regulate autophagy via Atg14 that decreases triglyceride level in serum. Moreover, FoxO1 was shown to enhance insulin sensitivity by inhibiting Trb3. FoxO3 can reduce cholesterol level through Sirt6 and inhibition of SREBP2. Atg14: autophagy related 14; G6Pase: Glucose-6-phosphatase; MTP: microsomal triglyceride transfer protein; PEPCK: phosphoenolpyruvate carboxykinase; Sirt6:

Sirtuin 6; SREBP2: sterol response element-binding protein 2; Trb3: tribbles homolog 3; VLDL: very-low-density lipoprotein.

**Figure 4**

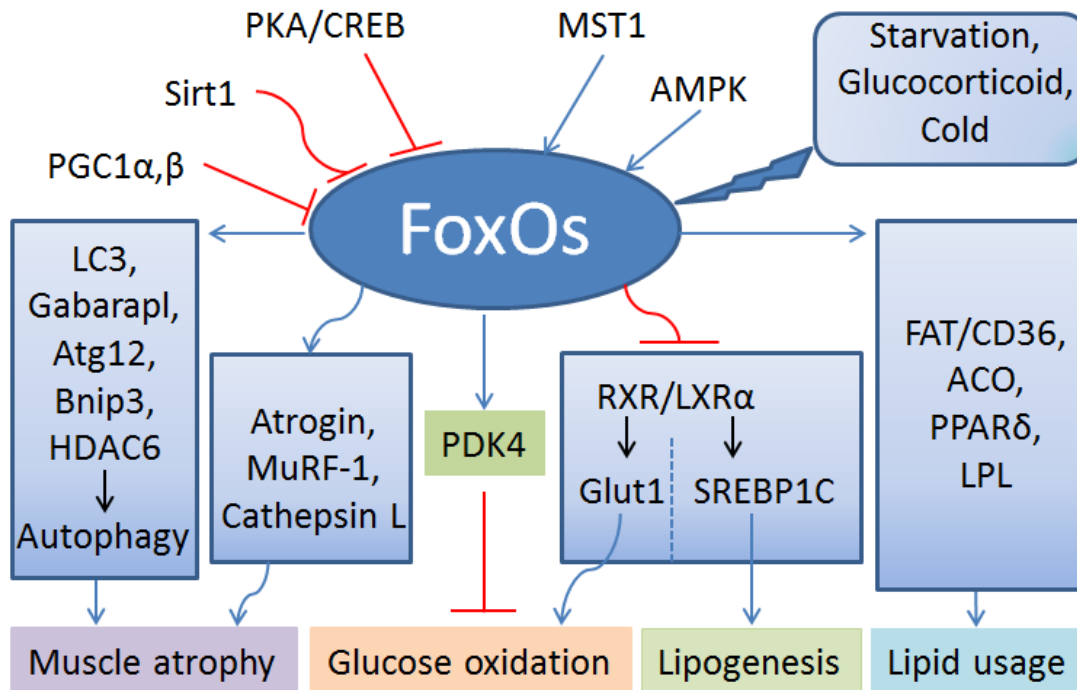


**Figure 4 The role of FoxOs regulating muscle and metabolism.** Under starvation, denervation or cold condition, FoxOs (such as FoxO1 and FoxO3) are activated and can switch from glucose oxidation to fatty acid utilization. Activation of FoxOs inhibits glucose oxidation via PDK4 and RXR/LXR $\alpha$  complex, which also reduces SREBP1C-mediated lipogenesis. By contrast, FoxOs increase lipid utilization through activating FAT, CD36, ACO, PPAR $\delta$  and LPL. It has been shown that FoxOs regulate muscle mass through autophagy (LC3, Gabarapl, Atg12, Bnip3 and HDAC6), and ubiquitin-proteasome pathway (Atrogin, MuRF-1 and Cathepsin L). Activation of autophagy and ubiquitin-proteasome pathways by FoxOs leads to muscle atrophy. The

upstream regulators of FoxOs include AMPK, MST1, PGC1, Sirt1, PKA and CREB. ACO: Acyl-CoA oxidase; AMPK: AMP-activated protein kinase; CD36: cluster of differentiation 36; FAT: fatty acid translocase; HDAC6: histone deacetylase 6; LPL: lipoprotein lipase; LXR $\alpha$ : liver X receptor  $\alpha$ ; MST1: Mammalian Sterile 20-like kinase 1; MuRF-1: muscle RING finger enzyme-1; PDK4: pyruvate dehydrogenase kinase 4; PKA: protein kinase A.

**Figure 5**

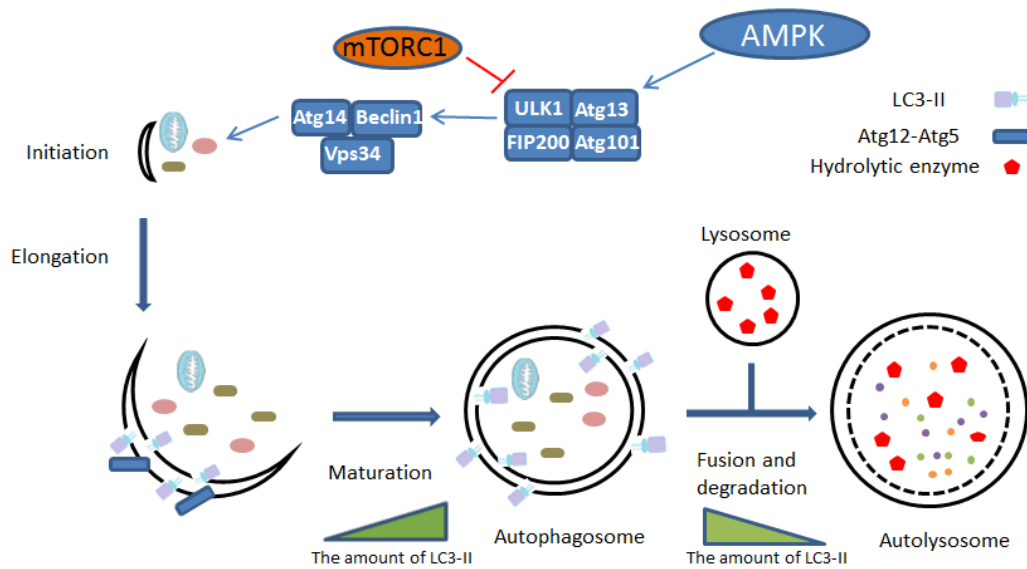


**Figure 5 The process of autophagy.** Autophagy (macroautophagy) is a physiological degradative process, which can degrade cytosolic components (such as dysfunctional proteins, organelles). Autophagy can be generally divided into several steps: initiation, elongation, maturation, fusion and degradation. Under nutrient sufficiency, mTORC1 inhibits ULK1 complex and prevents the initiation of autophagy. During starvation, AMPK activates ULK1 complex and induces autophagy by recruiting Atg14-beclin1-Vps34 complex. Atg12-Atg5 complex and LC3-II are important for elongation and maturation stages. At the end of

maturation, autophagosome is fused with lysosome to form autolysosome, where the engulfed cytosolic components (including part of intra-autophagosome located LC3-II) are degraded.

AMPK: AMP-activated protein kinase; Atgs: autophagy related proteins; FIP200: the focal adhesion kinase family interacting protein of 200 kD;

LC3: microtubule-associated protein 1A/1B-light chain 3-phosphatidylethanolamine conjugate;

mTORC1: mammalian target of rapamycin complex 1; ULK1: Unc-51-like kinase 1; Vps34: vacuolar proteins 34.

## References

1. Ogden CL, Carroll MD, Kit BK, Flegal KM. Prevalence of childhood and adult obesity in the United States, 2011-2012. *JAMA* 2014; 311:806-14.
2. Cawley J, Meyerhoefer C. The medical care costs of obesity: an instrumental variables approach. *J Health Econ* 2012; 31:219-30.
3. Niswender K. Diabetes and obesity: therapeutic targeting and risk reduction - a complex interplay. *Diabetes Obes Metab* 2010; 12:267-87.
4. Wang QA, Tao C, Gupta RK, Scherer PE. Tracking adipogenesis during white adipose tissue development, expansion and regeneration. *Nat Med* 2013; 19:1338-44.
5. Rutkowski JM, Stern JH, Scherer PE. The cell biology of fat expansion. *J Cell Biol* 2015; 208:501-12.
6. Singh R, Xiang Y, Wang Y, Baikati K, Cuervo AM, Luu YK, et al. Autophagy regulates adipose mass and differentiation in mice. *The Journal of clinical investigation* 2009; 119:3329-39.
7. Zhang Y, Goldman S, Baerga R, Zhao Y, Komatsu M, Jin S. Adipose-specific deletion of autophagy-related gene 7 (*atg7*) in mice reveals a role in adipogenesis. *Proceedings of the National Academy of Sciences of the United States of America* 2009; 106:19860-5.
8. Baerga R, Zhang Y, Chen PH, Goldman S, Jin S. Targeted deletion of autophagy-related 5 (*atg5*) impairs adipogenesis in a cellular model and in mice. *Autophagy* 2009; 5:1118-30.
9. Gross DN, van den Heuvel AP, Birnbaum MJ. The role of FoxO in the regulation of metabolism. *Oncogene* 2008; 27:2320-36.
10. Battiprolu PK, Hojaye B, Jiang N, Wang ZV, Luo X, Iglewski M, et al. Metabolic stress-induced activation of FoxO1 triggers diabetic cardiomyopathy in mice. *The Journal of clinical investigation* 2012; 122:1109-18.
11. Cheng Z, White MF. Targeting Forkhead box O1 from the concept to metabolic diseases: lessons from mouse models. *Antioxid Redox Signal* 2011; 14:649-61.
12. Jacobs FM, van der Heide LP, Wijchers PJ, Burbach JP, Hoekman MF, Smidt MP. FoxO6, a novel member of the FoxO class of transcription factors with distinct shuttling dynamics. *The Journal of biological chemistry* 2003; 278:35959-67.
13. Kaestner KH, Knochel W, Martinez DE. Unified nomenclature for the winged helix/forkhead transcription factors. *Genes Dev* 2000; 14:142-6.
14. Kenyon C, Chang J, Gensch E, Rudner A, Tabtiang R. A *C. elegans* mutant that lives twice as long as wild type. *Nature* 1993; 366:461-4.
15. Lin K, Dorman JB, Rodan A, Kenyon C. *daf-16*: An HNF-3/forkhead family member that can function to double the life-span of *Caenorhabditis elegans*. *Science* 1997; 278:1319-22.
16. Ogg S, Paradis S, Gottlieb S, Patterson GI, Lee L, Tissenbaum HA, et al. The Fork head transcription factor DAF-16 transduces insulin-like metabolic and longevity signals in *C. elegans*. *Nature* 1997; 389:994-9.
17. Furuyama T, Nakazawa T, Nakano I, Mori N. Identification of the differential distribution patterns of mRNAs and consensus binding sequences for mouse DAF-16 homologues. *Biochem J* 2000; 349:629-34.
18. Obsil T, Obsilova V. Structure/function relationships underlying regulation of FOXO transcription factors. *Oncogene* 2008; 27:2263-75.

19. Furuyama T, Kitayama K, Yamashita H, Mori N. Forkhead transcription factor FOXO1 (FKHR)-dependent induction of PDK4 gene expression in skeletal muscle during energy deprivation. *Biochem J* 2003; 375:365-71.
20. Nakae J, Kitamura T, Kitamura Y, Biggs WH, 3rd, Arden KC, Accili D. The forkhead transcription factor Foxo1 regulates adipocyte differentiation. *Dev Cell* 2003; 4:119-29.
21. Zhang W, Patil S, Chauhan B, Guo S, Powell DR, Le J, et al. FoxO1 regulates multiple metabolic pathways in the liver: effects on gluconeogenic, glycolytic, and lipogenic gene expression. *J Biol Chem* 2006; 281:10105-17.
22. Kops GJ, Dansen TB, Polderman PE, Saarloos I, Wirtz KW, Coffey PJ, et al. Forkhead transcription factor FOXO3a protects quiescent cells from oxidative stress. *Nature* 2002; 419:316-21.
23. Kops GJ, Medema RH, Glassford J, Essers MA, Dijkers PF, Coffey PJ, et al. Control of cell cycle exit and entry by protein kinase B-regulated forkhead transcription factors. *Molecular and cellular biology* 2002; 22:2025-36.
24. Schmidt M, Fernandez de Mattos S, van der Horst A, Klomp maker R, Kops GJ, Lam EW, et al. Cell cycle inhibition by FoxO forkhead transcription factors involves downregulation of cyclin D. *Mol Cell Biol* 2002; 22:7842-52.
25. Medema RH, Kops GJ, Bos JL, Burgering BM. AFX-like Forkhead transcription factors mediate cell-cycle regulation by Ras and PKB through p27kip1. *Nature* 2000; 404:782-7.
26. Miyauchi H, Minamino T, Tateno K, Kunieda T, Toko H, Komuro I. Akt negatively regulates the in vitro lifespan of human endothelial cells via a p53/p21-dependent pathway. *The EMBO journal* 2004; 23:212-20.
27. Demontis F, Perrimon N. FOXO/4E-BP signaling in *Drosophila* muscles regulates organism-wide proteostasis during aging. *Cell* 2010; 143:813-25.
28. van der Vos KE, Coffey PJ. The extending network of FOXO transcriptional target genes. *Antioxid Redox Signal* 2011; 14:579-92.
29. Brunet A, Sweeney LB, Sturgill JF, Chua KF, Greer PL, Lin Y, et al. Stress-dependent regulation of FOXO transcription factors by the SIRT1 deacetylase. *Science* 2004; 303:2011-5.
30. Huang H, Regan KM, Wang F, Wang D, Smith DI, van Deursen JM, et al. Skp2 inhibits FOXO1 in tumor suppression through ubiquitin-mediated degradation. *Proceedings of the National Academy of Sciences of the United States of America* 2005; 102:1649-54.
31. Kim H, Hiraishi A, Tsuchiya K, Sakamoto K. (-) Epigallocatechin gallate suppresses the differentiation of 3T3-L1 preadipocytes through transcription factors FoxO1 and SREBP1c. *Cytotechnology* 2010; 62:245-55.
32. Munekata K, Sakamoto K. Forkhead transcription factor Foxo1 is essential for adipocyte differentiation. *In Vitro Cell Dev Biol Anim* 2009; 45:642-51.
33. Higuchi M, Dusing GJ, Peshavariya H, Jiang F, Hsiao ST, Chan EC, et al. Differentiation of human adipose-derived stem cells into fat involves reactive oxygen species and Forkhead box O1 mediated upregulation of antioxidant enzymes. *Stem cells and development* 2013; 22:878-88.
34. Dowell P, Otto TC, Adi S, Lane MD. Convergence of peroxisome proliferator-activated receptor gamma and Foxo1 signaling pathways. *The Journal of biological chemistry* 2003; 278:45485-91.

35. Armoni M, Harel C, Karni S, Chen H, Bar-Yoseph F, Ver MR, et al. FOXO1 represses peroxisome proliferator-activated receptor-gamma1 and -gamma2 gene promoters in primary adipocytes. A novel paradigm to increase insulin sensitivity. *The Journal of biological chemistry* 2006; 281:19881-91.
36. Fan W, Imamura T, Sonoda N, Sears DD, Patsouris D, Kim JJ, et al. FOXO1 transrepresses peroxisome proliferator-activated receptor gamma transactivation, coordinating an insulin-induced feed-forward response in adipocytes. *The Journal of biological chemistry* 2009; 284:12188-97.
37. Kim JJ, Li P, Huntley J, Chang JP, Arden KC, Olefsky JM. FoxO1 haploinsufficiency protects against high-fat diet-induced insulin resistance with enhanced peroxisome proliferator-activated receptor gamma activation in adipose tissue. *Diabetes* 2009; 58:1275-82.
38. Ortega-Molina A, Efeyan A, Lopez-Guadamillas E, Munoz-Martin M, Gomez-Lopez G, Canamero M, et al. Pten positively regulates brown adipose function, energy expenditure, and longevity. *Cell metabolism* 2012; 15:382-94.
39. Lefterova MI, Lazar MA. New developments in adipogenesis. *Trends Endocrinol Metab* 2009; 20:107-14.
40. Ali AT, Hochfeld WE, Myburgh R, Pepper MS. Adipocyte and adipogenesis. *Eur J Cell Biol* 2013; 92:229-36.
41. Tontonoz P, Spiegelman BM. Fat and beyond: the diverse biology of PPARgamma. *Annu Rev Biochem* 2008; 77:289-312.
42. Poulsen L, Siersbaek M, Mandrup S. PPARs: fatty acid sensors controlling metabolism. *Semin Cell Dev Biol* 2012; 23:631-9.
43. Lefterova MI, Zhang Y, Steger DJ, Schupp M, Schug J, Cristancho A, et al. PPARgamma and C/EBP factors orchestrate adipocyte biology via adjacent binding on a genome-wide scale. *Genes Dev* 2008; 22:2941-52.
44. Nielsen R, Pedersen TA, Hagenbeek D, Moulos P, Siersbaek R, Megens E, et al. Genome-wide profiling of PPARgamma:RXR and RNA polymerase II occupancy reveals temporal activation of distinct metabolic pathways and changes in RXR dimer composition during adipogenesis. *Genes Dev* 2008; 22:2953-67.
45. Schupp M, Lazar MA. Endogenous ligands for nuclear receptors: digging deeper. *The Journal of biological chemistry* 2010; 285:40409-15.
46. Willson TM, Brown PJ, Sternbach DD, Henke BR. The PPARs: from orphan receptors to drug discovery. *J Med Chem* 2000; 43:527-50.
47. Bell-Parikh LC, Ide T, Lawson JA, McNamara P, Reilly M, FitzGerald GA. Biosynthesis of 15-deoxy-delta12,14-PGJ2 and the ligation of PPARgamma. *The Journal of clinical investigation* 2003; 112:945-55.
48. Cariou B, Charbonnel B, Staels B. Thiazolidinediones and PPARgamma agonists: time for a reassessment. *Trends Endocrinol Metab* 2012; 23:205-15.
49. Puigserver P, Wu Z, Park CW, Graves R, Wright M, Spiegelman BM. A cold-inducible coactivator of nuclear receptors linked to adaptive thermogenesis. *Cell* 1998; 92:829-39.
50. Chawla A, Schwarz EJ, Dimaculangan DD, Lazar MA. Peroxisome proliferator-activated receptor (PPAR) gamma: adipose-predominant expression and induction early in adipocyte differentiation. *Endocrinology* 1994; 135:798-800.

51. Barak Y, Nelson MC, Ong ES, Jones YZ, Ruiz-Lozano P, Chien KR, et al. PPAR gamma is required for placental, cardiac, and adipose tissue development. *Mol Cell* 1999; 4:585-95.
52. Rosen ED, Sarraf P, Troy AE, Bradwin G, Moore K, Milstone DS, et al. PPAR gamma is required for the differentiation of adipose tissue in vivo and in vitro. *Mol Cell* 1999; 4:611-7.
53. He W, Barak Y, Hevener A, Olson P, Liao D, Le J, et al. Adipose-specific peroxisome proliferator-activated receptor gamma knockout causes insulin resistance in fat and liver but not in muscle. *Proceedings of the National Academy of Sciences of the United States of America* 2003; 100:15712-7.
54. Jones JR, Barrick C, Kim KA, Lindner J, Blondeau B, Fujimoto Y, et al. Deletion of PPARgamma in adipose tissues of mice protects against high fat diet-induced obesity and insulin resistance. *Proceedings of the National Academy of Sciences of the United States of America* 2005; 102:6207-12.
55. Medina-Gomez G, Virtue S, Lelliott C, Boiani R, Campbell M, Christodoulides C, et al. The link between nutritional status and insulin sensitivity is dependent on the adipocyte-specific peroxisome proliferator-activated receptor-gamma2 isoform. *Diabetes* 2005; 54:1706-16.
56. Zhang J, Fu M, Cui T, Xiong C, Xu K, Zhong W, et al. Selective disruption of PPARgamma 2 impairs the development of adipose tissue and insulin sensitivity. *Proceedings of the National Academy of Sciences of the United States of America* 2004; 101:10703-8.
57. Ramji DP, Foka P. CCAAT/enhancer-binding proteins: structure, function and regulation. *Biochem J* 2002; 365:561-75.
58. Wang ND, Finegold MJ, Bradley A, Ou CN, Abdelsayed SV, Wilde MD, et al. Impaired energy homeostasis in C/EBP alpha knockout mice. *Science* 1995; 269:1108-12.
59. Yang J, Croniger CM, Lekstrom-Himes J, Zhang P, Fenyus M, Tenen DG, et al. Metabolic response of mice to a postnatal ablation of CCAAT/enhancer-binding protein alpha. *The Journal of biological chemistry* 2005; 280:38689-99.
60. Rosen ED, Hsu CH, Wang X, Sakai S, Freeman MW, Gonzalez FJ, et al. C/EBPalpha induces adipogenesis through PPARgamma: a unified pathway. *Genes Dev* 2002; 16:22-6.
61. Tang QQ, Otto TC, Lane MD. CCAAT/enhancer-binding protein beta is required for mitotic clonal expansion during adipogenesis. *Proceedings of the National Academy of Sciences of the United States of America* 2003; 100:850-5.
62. Tanaka T, Yoshida N, Kishimoto T, Akira S. Defective adipocyte differentiation in mice lacking the C/EBPbeta and/or C/EBPdelta gene. *The EMBO journal* 1997; 16:7432-43.
63. Reusch JE, Colton LA, Klemm DJ. CREB activation induces adipogenesis in 3T3-L1 cells. *Molecular and cellular biology* 2000; 20:1008-20.
64. Zhang JW, Klemm DJ, Vinson C, Lane MD. Role of CREB in transcriptional regulation of CCAAT/enhancer-binding protein beta gene during adipogenesis. *The Journal of biological chemistry* 2004; 279:4471-8.
65. Qi L, Saberi M, Zmuda E, Wang Y, Altarejos J, Zhang X, et al. Adipocyte CREB promotes insulin resistance in obesity. *Cell metabolism* 2009; 9:277-86.
66. Steger DJ, Grant GR, Schupp M, Tomaru T, Lefterova MI, Schug J, et al. Propagation of adipogenic signals through an epigenomic transition state. *Genes Dev* 2010; 24:1035-44.

67. Ou CY, Chen TC, Lee JV, Wang JC, Stallcup MR. Coregulator cell cycle and apoptosis regulator 1 (CCAR1) positively regulates adipocyte differentiation through the glucocorticoid signaling pathway. *The Journal of biological chemistry* 2014; 289:17078-86.
68. Ma X, Xu L, Mueller E. Forkhead box A3 mediates glucocorticoid receptor function in adipose tissue. *Proceedings of the National Academy of Sciences of the United States of America* 2016; 113:3377-82.
69. Nanbu-Wakao R, Morikawa Y, Matsumura I, Masuho Y, Muramatsu MA, Senba E, et al. Stimulation of 3T3-L1 adipogenesis by signal transducer and activator of transcription 5. *Mol Endocrinol* 2002; 16:1565-76.
70. Floyd ZE, Stephens JM. STAT5A promotes adipogenesis in nonprecursor cells and associates with the glucocorticoid receptor during adipocyte differentiation. *Diabetes* 2003; 52:308-14.
71. Siersbaek R, Nielsen R, Mandrup S. Transcriptional networks and chromatin remodeling controlling adipogenesis. *Trends Endocrinol Metab* 2012; 23:56-64.
72. Nakae J, Cao Y, Oki M, Orba Y, Sawa H, Kiyonari H, et al. Forkhead transcription factor FoxO1 in adipose tissue regulates energy storage and expenditure. *Diabetes* 2008; 57:563-76.
73. Jing E, Gesta S, Kahn CR. SIRT2 regulates adipocyte differentiation through FoxO1 acetylation/deacetylation. *Cell metabolism* 2007; 6:105-14.
74. Bai L, Pang WJ, Yang YJ, Yang GS. Modulation of Sirt1 by resveratrol and nicotinamide alters proliferation and differentiation of pig preadipocytes. *Mol Cell Biochem* 2008; 307:129-40.
75. Samuel VT, Choi CS, Phillips TG, Romanelli AJ, Geisler JG, Bhanot S, et al. Targeting foxo1 in mice using antisense oligonucleotide improves hepatic and peripheral insulin action. *Diabetes* 2006; 55:2042-50.
76. Titchenell PM, Chu Q, Monks BR, Birnbaum MJ. Hepatic insulin signalling is dispensable for suppression of glucose output by insulin in vivo. *Nature communications* 2015; 6:7078.
77. Matsumoto M, Han S, Kitamura T, Accili D. Dual role of transcription factor FoxO1 in controlling hepatic insulin sensitivity and lipid metabolism. *The Journal of clinical investigation* 2006; 116:2464-72.
78. Kamagate A, Qu S, Perdomo G, Su D, Kim DH, Slusher S, et al. FoxO1 mediates insulin-dependent regulation of hepatic VLDL production in mice. *J Clin Invest* 2008; 118:2347-64.
79. Altomonte J, Cong L, Harbaran S, Richter A, Xu J, Meseck M, et al. Foxo1 mediates insulin action on apoC-III and triglyceride metabolism. *The Journal of clinical investigation* 2004; 114:1493-503.
80. Qu S, Su D, Altomonte J, Kamagate A, He J, Perdomo G, et al. PPAR{alpha} mediates the hypolipidemic action of fibrates by antagonizing FoxO1. *American journal of physiology Endocrinology and metabolism* 2007; 292:E421-34.
81. Zhang K, Li L, Qi Y, Zhu X, Gan B, DePinho RA, et al. Hepatic suppression of Foxo1 and Foxo3 causes hypoglycemia and hyperlipidemia in mice. *Endocrinology* 2012; 153:631-46.
82. Tao R, Xiong X, DePinho RA, Deng CX, Dong XC. Hepatic SREBP-2 and cholesterol biosynthesis are regulated by FoxO3 and Sirt6. *J Lipid Res* 2013; 54:2745-53.

83. de Lange P, Moreno M, Silvestri E, Lombardi A, Goglia F, Lanni A. Fuel economy in food-deprived skeletal muscle: signaling pathways and regulatory mechanisms. *FASEB J* 2007; 21:3431-41.
84. Sugita S, Kamei Y, Akaike F, Suganami T, Kanai S, Hattori M, et al. Increased systemic glucose tolerance with increased muscle glucose uptake in transgenic mice overexpressing RXR $\gamma$  in skeletal muscle. *PLoS One* 2011; 6:e20467.
85. Kamei Y, Mizukami J, Miura S, Suzuki M, Takahashi N, Kawada T, et al. A forkhead transcription factor FKHR up-regulates lipoprotein lipase expression in skeletal muscle. *FEBS Lett* 2003; 536:232-6.
86. Bastie CC, Nahle Z, McLoughlin T, Esser K, Zhang W, Unterman T, et al. FoxO1 stimulates fatty acid uptake and oxidation in muscle cells through CD36-dependent and -independent mechanisms. *The Journal of biological chemistry* 2005; 280:14222-9.
87. Kamei Y, Miura S, Suganami T, Akaike F, Kanai S, Sugita S, et al. Regulation of SREBP1c gene expression in skeletal muscle: role of retinoid X receptor/liver X receptor and forkhead-O1 transcription factor. *Endocrinology* 2008; 149:2293-305.
88. Nakashima K, Yakabe Y. AMPK activation stimulates myofibrillar protein degradation and expression of atrophy-related ubiquitin ligases by increasing FOXO transcription factors in C2C12 myotubes. *Biosci Biotechnol Biochem* 2007; 71:1650-6.
89. Manfredi LH, Zanon NM, Garofalo MA, Navegantes LC, Kettelhut IC. Effect of short-term cold exposure on skeletal muscle protein breakdown in rats. *J Appl Physiol* (1985) 2013; 115:1496-505.
90. Kamei Y, Miura S, Suzuki M, Kai Y, Mizukami J, Taniguchi T, et al. Skeletal muscle FOXO1 (FKHR) transgenic mice have less skeletal muscle mass, down-regulated Type I (slow twitch/red muscle) fiber genes, and impaired glycemic control. *The Journal of biological chemistry* 2004; 279:41114-23.
91. Murtaugh LC. Pancreas and beta-cell development: from the actual to the possible. *Development* 2007; 134:427-38.
92. Straub SG, Sharp GW. Glucose-stimulated signaling pathways in biphasic insulin secretion. *Diabetes Metab Res Rev* 2002; 18:451-63.
93. Kitamura T, Nakae J, Kitamura Y, Kido Y, Biggs WH, 3rd, Wright CV, et al. The forkhead transcription factor Foxo1 links insulin signaling to Pdx1 regulation of pancreatic beta cell growth. *The Journal of clinical investigation* 2002; 110:1839-47.
94. Kobayashi M, Kikuchi O, Sasaki T, Kim HJ, Yokota-Hashimoto H, Lee YS, et al. FoxO1 as a double-edged sword in the pancreas: analysis of pancreas- and beta-cell-specific FoxO1 knockout mice. *American journal of physiology Endocrinology and metabolism* 2012; 302:E603-13.
95. Gupta D, Leahy AA, Monga N, Peshavaria M, Jetton TL, Leahy JL. Peroxisome proliferator-activated receptor gamma (PPAR $\gamma$ ) and its target genes are downstream effectors of FoxO1 protein in islet beta-cells: mechanism of beta-cell compensation and failure. *The Journal of biological chemistry* 2013; 288:25440-9.
96. Liu Y, Wang X, Wu H, Chen S, Zhu H, Zhang J, et al. Glycine enhances muscle protein mass associated with maintaining Akt-mTOR-FOXO1 signaling and suppressing TLR4 and NOD2 signaling in piglets challenged with LPS. *Am J Physiol Regul Integr Comp Physiol* 2016; 311:R365-73.

97. Kitamura YI, Kitamura T, Kruse JP, Raum JC, Stein R, Gu W, et al. FoxO1 protects against pancreatic beta cell failure through NeuroD and MafA induction. *Cell metabolism* 2005; 2:153-63.
98. Kawamori D, Kaneto H, Nakatani Y, Matsuoka TA, Matsuhisa M, Hori M, et al. The forkhead transcription factor Foxo1 bridges the JNK pathway and the transcription factor PDX-1 through its intracellular translocation. *The Journal of biological chemistry* 2006; 281:1091-8.
99. Tanida I. Autophagosome formation and molecular mechanism of autophagy. *Antioxidants & redox signaling* 2011; 14:2201-14.
100. Mizushima N, Yoshimori T, Ohsumi Y. The role of Atg proteins in autophagosome formation. *Annu Rev Cell Dev Biol* 2011; 27:107-32.
101. Itakura E, Kishi C, Inoue K, Mizushima N. Beclin 1 forms two distinct phosphatidylinositol 3-kinase complexes with mammalian Atg14 and UVRAG. *Mol Biol Cell* 2008; 19:5360-72.
102. Matsunaga K, Saitoh T, Tabata K, Omori H, Satoh T, Kurotori N, et al. Two Beclin 1-binding proteins, Atg14L and Rubicon, reciprocally regulate autophagy at different stages. *Nature cell biology* 2009; 11:385-96.
103. Obara K, Noda T, Niimi K, Ohsumi Y. Transport of phosphatidylinositol 3-phosphate into the vacuole via autophagic membranes in *Saccharomyces cerevisiae*. *Genes Cells* 2008; 13:537-47.
104. Sun Q, Fan W, Chen K, Ding X, Chen S, Zhong Q. Identification of Barkor as a mammalian autophagy-specific factor for Beclin 1 and class III phosphatidylinositol 3-kinase. *Proceedings of the National Academy of Sciences of the United States of America* 2008; 105:19211-6.
105. Sun Q, Fan W, Zhong Q. Regulation of Beclin 1 in autophagy. *Autophagy* 2009; 5:713-6.
106. Itakura E, Mizushima N. Characterization of autophagosome formation site by a hierarchical analysis of mammalian Atg proteins. *Autophagy* 2010; 6:764-76.
107. Kim J, Kundu M, Viollet B, Guan KL. AMPK and mTOR regulate autophagy through direct phosphorylation of Ulk1. *Nat Cell Biol* 2011; 13:132-41.
108. Egan DF, Shackelford DB, Mihaylova MM, Gelino S, Kohnz RA, Mair W, et al. Phosphorylation of ULK1 (hATG1) by AMP-activated protein kinase connects energy sensing to mitophagy. *Science* 2011; 331:456-61.
109. Mizushima N, Yamamoto A, Hatano M, Kobayashi Y, Kabeya Y, Suzuki K, et al. Dissection of autophagosome formation using Apg5-deficient mouse embryonic stem cells. *J Cell Biol* 2001; 152:657-68.
110. Hanada T, Noda NN, Satomi Y, Ichimura Y, Fujioka Y, Takao T, et al. The Atg12-Atg5 conjugate has a novel E3-like activity for protein lipidation in autophagy. *The Journal of biological chemistry* 2007; 282:37298-302.
111. Bjorkoy G, Lamark T, Brech A, Outzen H, Perander M, Overvatn A, et al. p62/SQSTM1 forms protein aggregates degraded by autophagy and has a protective effect on huntingtin-induced cell death. *J Cell Biol* 2005; 171:603-14.
112. Pankiv S, Clausen TH, Lamark T, Brech A, Bruun JA, Outzen H, et al. p62/SQSTM1 binds directly to Atg8/LC3 to facilitate degradation of ubiquitinated protein aggregates by autophagy. *The Journal of biological chemistry* 2007; 282:24131-45.

113. Rogov V, Dotsch V, Johansen T, Kirkin V. Interactions between autophagy receptors and ubiquitin-like proteins form the molecular basis for selective autophagy. *Mol Cell* 2014; 53:167-78.
114. Xiong X, Tao R, DePinho RA, Dong XC. The autophagy-related gene 14 (Atg14) is regulated by forkhead box O transcription factors and circadian rhythms and plays a critical role in hepatic autophagy and lipid metabolism. *J Biol Chem* 2012; 287:39107-14.
115. Xu L, Kanasaki M, He J, Kitada M, Nagao K, Jinzu H, et al. Ketogenic essential amino acids replacement diet ameliorated hepatosteatosis with altering autophagy-associated molecules. *Biochim Biophys Acta* 2013; 1832:1605-12.
116. Song YM, Lee YH, Kim JW, Ham DS, Kang ES, Cha BS, et al. Metformin alleviates hepatosteatosis by restoring SIRT1-mediated autophagy induction via an AMP-activated protein kinase-independent pathway. *Autophagy* 2015; 11:46-59.
117. Zhao J, Brault JJ, Schild A, Cao P, Sandri M, Schiaffino S, et al. FoxO3 coordinately activates protein degradation by the autophagic/lysosomal and proteasomal pathways in atrophying muscle cells. *Cell Metab* 2007; 6:472-83.
118. Mammucari C, Milan G, Romanello V, Masiero E, Rudolf R, Del Piccolo P, et al. FoxO3 controls autophagy in skeletal muscle in vivo. *Cell Metab* 2007; 6:458-71.
119. Milan G, Romanello V, Pescatore F, Armani A, Paik JH, Frasson L, et al. Regulation of autophagy and the ubiquitin-proteasome system by the FoxO transcriptional network during muscle atrophy. *Nature communications* 2015; 6:6670.
120. Ratti F, Ramond F, Moncollin V, Simonet T, Milan G, Mejat A, et al. Histone deacetylase 6 is a FoxO transcription factor-dependent effector in skeletal muscle atrophy. *The Journal of biological chemistry* 2015; 290:4215-24.
121. O'Neill BT, Lee KY, Klaus K, Softic S, Krumpoch MT, Fentz J, et al. Insulin and IGF-1 receptors regulate FoxO-mediated signaling in muscle proteostasis. *The Journal of clinical investigation* 2016; 126:3433-46.
122. Brault JJ, Jespersen JG, Goldberg AL. Peroxisome proliferator-activated receptor gamma coactivator 1alpha or 1beta overexpression inhibits muscle protein degradation, induction of ubiquitin ligases, and disuse atrophy. *The Journal of biological chemistry* 2010; 285:19460-71.
123. Wei B, Dui W, Liu D, Xing Y, Yuan Z, Ji G. MST1, a key player, in enhancing fast skeletal muscle atrophy. *BMC Biol* 2013; 11:12.
124. Lee D, Goldberg AL. SIRT1 protein, by blocking the activities of transcription factors FoxO1 and FoxO3, inhibits muscle atrophy and promotes muscle growth. *The Journal of biological chemistry* 2013; 288:30515-26.
125. Bertaggia E, Coletto L, Sandri M. Posttranslational modifications control FoxO3 activity during denervation. *Am J Physiol Cell Physiol* 2012; 302:C587-96.
126. Hussain SN, Mofarrahi M, Sigala I, Kim HC, Vassilakopoulos T, Maltais F, et al. Mechanical ventilation-induced diaphragm disuse in humans triggers autophagy. *Am J Respir Crit Care Med* 2010; 182:1377-86.
127. Machado J, Manfredi LH, Silveira WA, Goncalves DA, Lustrino D, Zanon NM, et al. Calcitonin gene-related peptide inhibits autophagic-lysosomal proteolysis through cAMP/PKA signaling in rat skeletal muscles. *Int J Biochem Cell Biol* 2016; 72:40-50.
128. Sengupta A, Molkentin JD, Yutzey KE. FoxO transcription factors promote autophagy in cardiomyocytes. *J Biol Chem* 2009; 284:28319-31.

129. Hariharan N, Maejima Y, Nakae J, Paik J, Depinho RA, Sadoshima J. Deacetylation of FoxO by Sirt1 Plays an Essential Role in Mediating Starvation-Induced Autophagy in Cardiac Myocytes. *Circ Res* 2010; 107:1470-82.
130. Chi Y, Shi C, Zhao Y, Guo C. Forkhead box O (FOXO) 3 modulates hypoxia-induced autophagy through AMPK signalling pathway in cardiomyocytes. *Biosci Rep* 2016; 36.
131. Paula-Gomes S, Goncalves DA, Baviera AM, Zanon NM, Navegantes LC, Kettelhut IC. Insulin suppresses atrophy- and autophagy-related genes in heart tissue and cardiomyocytes through AKT/FOXO signaling. *Horm Metab Res* 2013; 45:849-55.
132. Zaglia T, Milan G, Franzoso M, Bertaggia E, Pianca N, Piasentini E, et al. Cardiac sympathetic neurons provide trophic signal to the heart via beta2-adrenoceptor-dependent regulation of proteolysis. *Cardiovasc Res* 2013; 97:240-50.
133. Sengupta A, Molkentin JD, Paik JH, DePinho RA, Yutzey KE. FoxO transcription factors promote cardiomyocyte survival upon induction of oxidative stress. *The Journal of biological chemistry* 2011; 286:7468-78.
134. Ning Y, Li Z, Qiu Z. FOXO1 silence aggravates oxidative stress-promoted apoptosis in cardiomyocytes by reducing autophagy. *J Toxicol Sci* 2015; 40:637-45.
135. Chiacchiera F, Matrone A, Ferrari E, Ingravallo G, Lo Sasso G, Murzilli S, et al. p38alpha blockade inhibits colorectal cancer growth in vivo by inducing a switch from HIF1alpha- to FoxO-dependent transcription. *Cell Death Differ* 2009; 16:1203-14.
136. Matrone A, Grossi V, Chiacchiera F, Fina E, Cappellari M, Caringella AM, et al. p38alpha is required for ovarian cancer cell metabolism and survival. *Int J Gynecol Cancer* 2010; 20:203-11.
137. Zhang J, Ng S, Wang J, Zhou J, Tan SH, Yang N, et al. Histone deacetylase inhibitors induce autophagy through FOXO1-dependent pathways. *Autophagy* 2015; 11:629-42.
138. Zhao Y, Yang J, Liao W, Liu X, Zhang H, Wang S, et al. Cytosolic FoxO1 is essential for the induction of autophagy and tumour suppressor activity. *Nat Cell Biol* 2010; 12:665-75.
139. Zhou J, Liao W, Yang J, Ma K, Li X, Wang Y, et al. FOXO3 induces FOXO1-dependent autophagy by activating the AKT1 signaling pathway. *Autophagy* 2012; 8:1712-23.
140. Zhu WL, Tong H, Teh JT, Wang M. Forkhead box protein O3 transcription factor negatively regulates autophagy in human cancer cells by inhibiting forkhead box protein O1 expression and cytosolic accumulation. *PLoS One* 2014; 9:e115087.
141. Jia K, Thomas C, Akbar M, Sun Q, Adams-Huet B, Gilpin C, et al. Autophagy genes protect against Salmonella typhimurium infection and mediate insulin signaling-regulated pathogen resistance. *Proceedings of the National Academy of Sciences of the United States of America* 2009; 106:14564-9.
142. Wang S, Xia P, Huang G, Zhu P, Liu J, Ye B, et al. FoxO1-mediated autophagy is required for NK cell development and innate immunity. *Nature communications* 2016; 7:11023.
143. Deng Y, Kerdiles Y, Chu J, Yuan S, Wang Y, Chen X, et al. Transcription factor Foxo1 is a negative regulator of natural killer cell maturation and function. *Immunity* 2015; 42:457-70.
144. Bai H, Kang P, Hernandez AM, Tatar M. Activin signaling targeted by insulin/dFOXO regulates aging and muscle proteostasis in Drosophila. *PLoS Genet* 2013; 9:e1003941.
145. Akasaki Y, Hasegawa A, Saito M, Asahara H, Iwamoto Y, Lotz MK. Dysregulated FOXO transcription factors in articular cartilage in aging and osteoarthritis. *Osteoarthritis Cartilage* 2014; 22:162-70.

146. Siegrist SE, Haque NS, Chen CH, Hay BA, Hariharan IK. Inactivation of both Foxo and reaper promotes long-term adult neurogenesis in *Drosophila*. *Current biology : CB* 2010; 20:643-8.
147. Xu P, Das M, Reilly J, Davis RJ. JNK regulates FoxO-dependent autophagy in neurons. *Genes Dev* 2011; 25:310-22.
148. Cummins TD, Holden CR, Sansbury BE, Gibb AA, Shah J, Zafar N, et al. Metabolic remodeling of white adipose tissue in obesity. *American journal of physiology Endocrinology and metabolism* 2014; 307:E262-77.
149. Jansen HJ, van Essen P, Koenen T, Joosten LA, Netea MG, Tack CJ, et al. Autophagy activity is up-regulated in adipose tissue of obese individuals and modulates proinflammatory cytokine expression. *Endocrinology* 2012; 153:5866-74.
150. Ost A, Svensson K, Ruishalme I, Brannmark C, Franck N, Krook H, et al. Attenuated mTOR signaling and enhanced autophagy in adipocytes from obese patients with type 2 diabetes. *Mol Med* 2010; 16:235-46.
151. Kovsan J, Bluher M, Tarnovscki T, Kloting N, Kirshtein B, Madar L, et al. Altered autophagy in human adipose tissues in obesity. *J Clin Endocrinol Metab* 2011; 96:E268-77.
152. Nunez CE, Rodrigues VS, Gomes FS, Moura RF, Victorio SC, Bombassaro B, et al. Defective regulation of adipose tissue autophagy in obesity. *Int J Obes (Lond)* 2013; 37:1473-80.
153. Kosacka J, Kern M, Kloting N, Paeschke S, Rudich A, Haim Y, et al. Autophagy in adipose tissue of patients with obesity and type 2 diabetes. *Mol Cell Endocrinol* 2015; 409:21-32.
154. Kosacka J, Koch K, Gericke M, Nowicki M, Heiker JT, Kloting I, et al. The polygenetically inherited metabolic syndrome of male WOKW rats is associated with enhanced autophagy in adipose tissue. *Diabetology & metabolic syndrome* 2013; 5:23.
155. Zhang C, He Y, Okutsu M, Ong LC, Jin Y, Zheng L, et al. Autophagy is involved in adipogenic differentiation by repressing proteasome-dependent PPARgamma2 degradation. *American journal of physiology Endocrinology and metabolism* 2013; 305:E530-9.

## Chapter 2 Targeting FoxO1 with AS1842856 Suppresses Adipogenesis

Peng Zou,<sup>1,3</sup> Longhua Liu,<sup>1,3</sup> Louise Zheng,<sup>1</sup> Lu Liu,<sup>1</sup> Rebecca E. Stoneman,<sup>1</sup> Alicia Cho,<sup>1</sup>  
Ashley Emery,<sup>1</sup> Elizabeth R. Gilbert,<sup>2</sup> Zhiyong Cheng<sup>1\*</sup>

<sup>1</sup> Department of Human Nutrition, Foods and Exercise, Fralin Life Science Institute, College of Agriculture and Life Science, Virginia Tech, Blacksburg, Virginia, USA.

<sup>2</sup> Department of Animal and Poultry Sciences, Virginia Tech, Blacksburg, Virginia, USA.

<sup>3</sup> The authors contributed to the work equally.

Correspondence: Dr. Zhiyong Cheng, 1981 Kraft Drive, Blacksburg, VA 24061, USA. Phone: (540) 231 9445; Fax: (540) 231 5522; email: [zcheng@vt.edu](mailto:zcheng@vt.edu).

---

**This chapter has been published in *Cell Cycle*. 2014; 13(23):3759-67.**

**Abstract:** Hyperplasia (i.e., increased adipogenesis) contributes to excess adiposity, the hallmark of obesity that can trigger metabolic complications. As FoxO1 has been implicated in adipogenic regulation, we investigated the kinetics of FoxO1 activation during adipocyte differentiation, and tested the effects of FoxO1 antagonist (AS1842856) on adipogenesis. We found for the first time that the kinetics of FoxO1 activation follows a series of sigmoid curves, and reveals the phases relevant to clonal expansion, cell cycle arrest, and the regulation of PPAR $\gamma$ , adiponectin, and mitochondrial proteins (complexes I and III). In addition, multiple activation-inactivation transitions exist in the stage of terminal differentiation. Importantly, persistent inhibition of FoxO1 with AS1842856 almost completely suppressed adipocyte differentiation, while selective inhibition in specific stages had differential effects on adipogenesis. Our data present a new view of FoxO1 in adipogenic regulation, and suggest AS1842856 can be an anti-obesity agent that warrants further investigation.

**Keywords:** FoxO1, AS1842856, mitochondria, adipogenesis, obesity

## Introduction

Obesity is a rapidly growing epidemic.<sup>1-3</sup> Characterized by excess adiposity, obese individuals show aberrant glucose and lipid metabolism.<sup>4</sup> The resultant glucotoxicity and lipotoxicity have been found to impair endocrine (e.g., insulin secretion and signaling pathway) and cardiovascular functions, linking obesity to higher risks of type 2 diabetes mellitus (T2DM) and heart diseases.<sup>4</sup> Thus, control of adiposity and glycemia is critical to prevent obesity and related metabolic complications.

It has been recognized that hyperplasia — an increase in *de novo* adipocyte formation (i.e., adipogenesis) contributes to excess white adipose tissue in obese subjects.<sup>3</sup> During the development of adipose tissue, pre-adipocytes or precursor/stem cells differentiate into mature adipocytes through complex adipogenic programs that regulate signaling transduction, transcriptional regulation, cell cycle and mitochondrial metabolism.<sup>5-10</sup> The transcription factor forkhead box O1 (FoxO1) regulates an array of genes and integrates insulin signaling with metabolic homeostasis, which has been shown to play an important role in adipogenesis.<sup>5, 11-15</sup> In particular, FoxO1 controls adipogenesis through interacting with peroxisome proliferator-activated receptor gamma (PPAR $\gamma$ ) and the cell cycle inhibitor p21 (CDKN1A).<sup>15-18</sup> FoxO1 haploinsufficiency protects mice from diet induced insulin resistance and diabetes.<sup>15, 19</sup> In the liver, activated FoxO1 can regulate lipid metabolism by manipulating mitochondrial function,<sup>20, 21</sup> and it also increases blood glucose by upregulating glucose 6-phosphatase (G6P) and phosphoenolpyruvate carboxykinase (PEPCK), the gluconeogenic enzymes that promote glucose production.<sup>22</sup> These multiple roles in regulating metabolism demonstrate the great potential to target FoxO1 for new therapeutics for obesity and T2DM.<sup>5</sup>

A selective FoxO1 antagonist, 5-amino-7-(cyclohexylamino)-1-ethyl-6-fluoro-4-oxo-1,4-dihydroquinoline-3-carboxylic acid (commercially AS1842856), was discovered recently.<sup>23</sup> It can potently inhibit the DNA binding of FoxO1 and its transactivation.<sup>23-25</sup> In hepatic cells, AS1842856 inhibits glucose production by suppressing G6P and PEPCK mRNA levels, and administration of AS1842856 to diabetic db/db mice significantly reduces fasting blood glucose.<sup>23</sup> However, the effect of AS1842856 on adipogenesis has not been examined. In the present study, we targeted FoxO1 with AS1842856 and investigated its effects on adipogenesis. We found that persistent inhibition of FoxO1 by AS1842856 almost completely inhibited adipogenesis, which was accompanied with significant suppression of the adipogenic regulator PPAR $\gamma$  and mitochondrial proteins (complexes I and III). By contrast, selective inhibition at different stages of adipocyte differentiation imposed differential effects on adipogenesis, suggesting that FoxO1 plays stage-dependent roles in adipogenesis. Indeed, we found for the first time that the kinetics of FoxO1 activation and inactivation follows a series of sigmoid curves, which reveals the phases specifically relevant to clonal expansion, cell cycle arrest and PPAR $\gamma$  and mitochondrial regulation. Furthermore, additional sigmoid phases exist in the late stage of kinetics, which warrants future investigation.

## **Results and Discussion**

### **Persistent inhibition of FoxO1 by AS1842856 prevented adipocyte**

**differentiation.** Following an established protocol we cultured 3T3L1 preadipocytes in basal media (days 0-2, BMI), and adipocyte differentiation was induced with differentiation media I

(days 3-4, DMI) and differentiation media (days 5-6, DMII), and then the cells were maintained in basal media (days 7-12, BMII) (Figure 1s, A).<sup>26</sup> BMI and BMII are the same chemically but different in cell differentiation stages. Compared with the preadipocytes, the fully differentiated cells (mature adipocytes) showed significant accumulation of lipid droplets and strong oil red O staining (Figure 1, A-B; Figure 1s, B-C). However, persistent treatment of cells with AS1842856 (days 0-12) almost completely prevented the adipogenesis (Figure 1, C-D; Figure 1s, D). In line with AS1842856 predominantly blocking dephosphorylated FoxO1 and interfering with its interaction with DNA binding sites to suppress Foxo1-mediated transactivation,<sup>23</sup> treatment of the cells with AS1842856 locked FoxO1 in a state of being highly dephosphorylated, and the phosphorylation level was less than 10% of that in untreated adipocytes ( $p < 0.0001$ ; Figures 1, E, F). In addition, the level of total FoxO1 protein was reduced by 52% ( $p < 0.05$ ) (Figure 1, E, G). Therefore, AS1842856 induced prevention of adipogenesis was associated with its inhibitory effects on FoxO1.

**AS1842856 reduced PPAR $\gamma$  protein levels.** The transcription factor PPAR $\gamma$  plays a key role in adipogenesis,<sup>27</sup> and its expression and activity can be regulated by FoxO1.<sup>5, 16-18</sup> To test whether AS1842856 affects PPAR $\gamma$ , we measured the protein level of PPAR $\gamma$  after induction of differentiation (Figure 2, A-B). In fully differentiated (or mature) adipocytes, the expression of PPAR $\gamma$  was about 10 fold greater ( $p < 0.0001$ ) than in pre-adipocytes. However, treatment of cells with AS1842856 (days 0-12) significantly suppressed PPAR $\gamma$  (Figure 2, A-B). Loss of PPAR $\gamma$  function may account largely for AS1842856 induced inhibition of adipogenesis (Figure 1, C). Consistently, adiponectin — the adipokine that is secreted predominantly by mature adipocytes<sup>6</sup>

<sup>7</sup> — was highly expressed in the fully differentiated cells but barely detected in AS1842856 treated cells (Figure 2, A, B). These data suggest that suppression of adipogenesis by AS1842856 involves interference with the FoxO1-PPAR $\gamma$  axis.

**AS1842856 reduced mitochondrial protein levels.** Mitochondria underpin adipogenesis and adipocyte function.<sup>6,7</sup> As FoxO1 was implicated in mitochondrial regulation,<sup>12,20</sup> we asked if AS1842856 interferes with mitochondrial function in adipocytes. Western blot analysis of mitochondrial proteins revealed 2.6-fold ( $p < 0.01$ ) upregulation of respiration chain complex I (C1) and 3.9-fold ( $p < 0.01$ ) elevation of complex III (C3) in matured adipocytes when compared with pre-adipocytes (Figure 2, A, C-D). However, treatment with AS1842856 substantially reduced the levels of C1 (24%,  $p < 0.05$ ) and C3 (46%,  $p < 0.01$ ) when compared with the fully differentiated adipocytes, indicative of an impaired mitochondrial function or efficiency (Figure 2, A, C-D). Thus, inhibition of FoxO1 by AS1842856 seems to prevent adipogenesis by interfering with mitochondrial function in addition to PPAR $\gamma$  expression.

**FoxO1 underwent sigmoid activation during adipocyte differentiation.** FoxO1 can repress PPAR $\gamma$  expression and transrepress its transactivation,<sup>15-18</sup> implying that silencing FoxO1 may stimulate PPAR $\gamma$  and promotes adipogenesis. However, persistent inhibition of FoxO1 (days 0-12) with AS1842856 markedly suppressed PPAR $\gamma$  and prevented adipogenesis, suggesting FoxO1 activation was indispensable for adipogenesis (Figures 1-2; Figure 1s). In line with this, silencing FoxO1 in preadipocytes with siRNA severely prevents the cells from

differentiation.<sup>14</sup> To better understand the physiological role of FoxO1, we studied the kinetics of FoxO1 activation (i.e., dephosphorylation) and inactivation (i.e., phosphorylation) during 3T3L1 cell differentiation.<sup>5</sup> As shown in Figure 3, A-B, FoxO1 activation followed a series of sigmoid curves, revealing 3 inactivation peaks (days 1, 5 and 9) and 3 activation peaks (days 3, 7 and 10). FoxO1 was most inactive on day 1 (IP1), when the cells reentered into cell cycle with clonal expansion (Figure 3, B).<sup>15</sup> By contrast, FoxO1 reached the first activation peak (AP1) on day 3, when postmitotic growth arrest takes place (Figure 3, B).<sup>15</sup> These data strongly support the notion that FoxO1 regulates the cell cycle.<sup>5, 15</sup>

The second inactivation phase took place during days 3-5 and peaked on day 5 (IP2), which was accompanied with gradual upregulation of PPAR $\gamma$  and adiponectin (Figure 3, B; Figure 4, A-B). Concomitantly, the expression of mitochondrial C1 and C3 increased (Figure 4, A, C). Interestingly, the expression of PPAR $\gamma$  and mitochondrial proteins was minimally changed in phase IP1 (days 0-2; Figure 4, A-C). Thus, phase IP2 seems to be relevant primarily to PPAR $\gamma$  and mitochondrial regulation, while phase IP1 to clonal expansion.

A third inactivation peak (IP3) appeared on day 9, before which FoxO1 activation reached the second maximum (AP2) on day 7 and after which was AP3 on day 10 (Figure 3, B).

Interestingly, the expression of PPAR $\gamma$  and adiponectin continuously increased in the phase transition of IP2  $\rightarrow$  AP2 (days 5-7; Figure 4, A-B), so did mitochondrial proteins C1 and C3 (Figure 4, A, C). The observation of additional transitions (IP2  $\rightarrow$  AP2, AP2  $\rightarrow$  IP3 and IP3  $\rightarrow$  AP3) is novel, which fall into the same stage of “terminal differentiation” (days 4-12),<sup>15</sup> and warrants further study to advance our understanding of FoxO1 in adipogenic regulation.

**AS1842856 had stage-dependent effects on adipogenesis.** To test the importance of the additional transitions of IP2→AP3 for adipogenesis, we added AS1842856 (0.1 μM) to BMII at the end of day 6, locking FoxO1 in an inhibited state during days 7-12 (Figure 2s, A). As controls, mature adipocytes showed significant accumulation of lipid droplets and strong Oil red O staining, which were not observed in the pre-adipocytes (Figure 5, A-B; Figure 3s, A-B). By contrast, treatment of the cells with AS1842856 from day 7 to day 12 potently prevented adipogenesis regardless of differentiation induction (Figure 5, C; Figure 3s, C). Thus, FoxO1 re-activation and the progression to IP2→AP3 are critical for adipogenesis. We then moved the treatments to earlier stages (Figure 2s, B-D). Addition of AS1842856 (0.1 μM) to DMI led to a similar phenotype than to BMII (Figure 5, D; Figure 3s, D). However, when it was supplemented in BMI and DMII, AS1842856 suppressed adipogenesis to a lesser extent than in BMII, suggestive of a milder disturbance of FoxO1 action in adipogenesis (Figure 5, E-F; Figure 3s, E-F).

Aligning stages BMI, DMI, DMII and BMII with FoxO1 activation trajectory (Figure 2s, E), one can see the same primary mark in stages BMI and DMII, i.e., to inactivate FoxO1 at IP1 and IP2, respectively. Evidently, addition of AS1842856 to media BMI and DMII promotes FoxO1 inactivation in stages BMI and DMII, in concert with the physiological role of FoxO1 thus favorable for adipogenesis. However, AS1842856 prevents FoxO1 re-activation in the late stages of BMI (day 2) and DMII (day 6), which counteracts the physiological role of FoxO1 and may account at least in part for the overtly mild suppression of adipogenesis (Figure 5, E-F; Figure 3s, E-F). By contrast, the primary mark in stages DMI and BMII is FoxO1 activation at AP1 and

AP2 (Figure 2s, E). Supplement of AS1842856 in media DMI and BMII prevents FoxO1 from reactivation, thereby largely inhibiting adipogenesis (Figure 5, C-D; Figure 3s, C-D). Thus, a finely tuned activity of FoxO1 is critical for its physiological role in adipogenesis.

## **Conclusion**

Our data suggest targeting FoxO1 with the selective antagonist AS1842856 dramatically suppresses adipogenesis. Antagonizing FoxO1 with AS1842856 also reduces the expression of mitochondrial proteins and adiponectin, supporting the notion that mitochondrial function is critical for adipocyte differentiation.<sup>6, 7</sup> Since excess adipogenesis contributes to obesity development, AS1842856 may be an anti-obesity candidate that warrants further investigation. It should be noted that the expression and activation of FoxO1 during adipocyte differentiation is fairly dynamic other than steady-state, which may explain the controversy arising from stable overexpression of FoxO1.<sup>13-15</sup> As FoxO1 activation and inactivation must follow sigmoid curves during the differentiation process, however, it is reasonable to observe that adipocytes overexpressing of constitutively active FoxO1 fail to differentiate.<sup>15</sup> The presence of multiple activation-inactivation transitions in the stage of “terminal differentiation” (days 4-12) suggests a complex regulation of FoxO1, and molecular events involved in these transitions remain largely unknown and warrant future study.

## Materials and Methods

**Materials** 3T3-L1 preadipocytes (ATCC<sup>®</sup> CL-173<sup>™</sup>) were purchased from ATCC (Manassas, VA). Dulbecco's modified Eagle's (DMEM) medium was from Corning Inc (Manassas, VA). Fetal bovine serum (FBS) was from GeneMate (Kaysville, UT). Dexamethasone, 3-isobutyl-1-methylxanthine (IBMX) and rosiglitazone were purchased from Cayman chemical (Ann Arbor, MI). Penicillin/streptomycin (P/S) was from GE Healthcare Life Sciences HyClone Laboratories (Logan, UT). Insulin was from Sigma-Aldrich (St. Louis, MO). FoxO1 inhibitor AS1842856 was from EMD Millipore (San Diego, CA).

**Cell culture and differentiation induction** 3T3-L1 preadipocytes were cultured in basal media (i.e., DMEM media supplemented with 10% FBS, 100 units/ml penicillin and 100 µg/ml streptomycin (1 × P/S)), at 37 °C in a humidified atmosphere of 5% CO<sub>2</sub>. The media were replaced every two days. Differentiation of 3T3-L1 cells was induced as described previously with slight modification (Figure 1s).<sup>26</sup> Briefly, 3T3-L1 cells were grown to confluence (day 0), and maintained in fresh basal media (BMI) for two days (days 1-2). On the end of day 2, BMI medium was changed to differentiation medium I (DMI): DMEM supplemented with 10% FBS, P/S (1 ×), IBMX (0.5 mM), dexamethasone (1 µM), insulin (1 µg/ml) and rosiglitazone (2 µM). On the end of day 4, DMI medium was changed to differentiation medium II (DMII): DMEM supplemented with 10% FBS, P/S (1 ×), and insulin (1 µg/ml). On the end of day 6, DMII medium was changed to basal media (BMII), and the cells were maintained in BMII (replaced with fresh basal medium every two days) until fully differentiated (day 12). As a control, preadipocytes were maintained in BMI till day 12, and the medium was replaced fresh one every

two days. Images of the cells were captured on day 12 with a Nikon ECLIPSE TS100 microscope.

**AS1842856 Treatments** AS1842856 has an IC<sub>50</sub> of 0.033  $\mu$ M to inhibit FoxO1 and can potently block FoxO1 at a final concentration of 0.05-1  $\mu$ M without showing cytotoxicity.<sup>23-25</sup>

We tested 0.1  $\mu$ M and 1  $\mu$ M, and found AS1842856 severely suppressed adipogenesis at both concentrations, thus choosing to use 0.1  $\mu$ M for the treatments if not specified elsewhere.

AS1842856 or the vehicle 0.1% DMSO as a treatment control was supplemented through the whole procedure of BMI→DMI→DMII→BMII (Figure 1s), or in the individual stage of BMI, DMI, DMII, BMII (Figure 2s). Other than the treatment stages, the cells were maintained in media identical to the protocol as described above. Images of the cells were captured on day 12 with a Nikon ECLIPSE TS100 microscope.

**Oil Red O staining** The Oil Red O working solution was freshly prepared by mixing 0.35% stock solution with dH<sub>2</sub>O (6:4) and filtered, and the staining was conducted as described.<sup>26</sup> At the end of differentiation procedure (day 12), the media were removed and the cells were washed once with phosphate buffered saline (PBS), and fixed in 4% formaldehyde at room temperature for 10 min and then at 4°C overnight. Subsequently, the cells were washed once with dH<sub>2</sub>O, once with 60% isopropanol, and air dried. Oil Red O working solution was added and the staining at room temperature lasted for 1 h. Afterwards, the stained cells were washed with dH<sub>2</sub>O for 4

times, and the images were captured with a Nikon ECLIPSE 80i microscope. Oil Red O retained in the cells was extracted with isopropanol, and quantified by the absorbance (O.D.) at 510 nm.<sup>28</sup>

**Western Blot** For cell lysates, the cells were washed with ice-cold PBS (Caisson Labs) and lysed with a Bullet Blender<sup>®</sup> (Next Advance, Inc.), in PLC lysis buffer:<sup>20, 29</sup> (30 mM Hepes, pH 7.5, 150 mM NaCl, 10% glycerol, 1% Triton X-100, 1.5 mM MgCl<sub>2</sub>, 1 mM EGTA, 10 mM NaPPi, 100 mM NaF, 1 mM Na<sub>3</sub>VO<sub>4</sub>) supplemented with protease inhibitor cocktail (Roche), 1 mM PMSF, 10 μM TSA (Trichostatin A, Selleckchem) and 5 mM Nicotinamide (Alfa Aesar). Total protein concentrations of the cell lysates were determined using the DC protein assay (Bio-Rad). Western blot and image analysis were conducted as described previously.<sup>20</sup> Antibody catalog numbers and vendors are as follows: C1 (A31857) and C3 (A21362) from Invitrogen; PPAR $\gamma$  (MA5-14889) and  $\beta$ -actin (MA5-15739) from Pierce; Adiponectin (2789s), phospho-FoxO1 (9464) and FoxO1 (9454) from Cell Signaling Technology.

**Statistical analyses** All results are expressed as means  $\pm$  s.d. and are analyzed by analysis of variance (ANOVA) to determine p values;  $p < 0.05$  was considered statistically significant.

## **Funding**

This work was supported by the start-up funds from HNFE, CALS, and Fralin Life Science Institute at Virginia Tech (Z.C.).

## **Conflict of Interest**

The authors declare no conflict of interest.

## **Abbreviations:**

AS1842856: 5-amino-7-(cyclohexylamino)-1-ethyl-6-fluoro-4-oxo-1,4-dihydroquinoline-3-carboxylic acid

BMI: basal media I

BMII: basal media II

C1: mitochondrial complex I

C3: mitochondrial complex III

DMI: differentiation media I

DMII: differentiation media II

FoxO1: forkhead box O1

G6P: glucose 6-phosphatase

PEPCK: phosphoenolpyruvate carboxykinase

PPAR $\gamma$ : peroxisome proliferator-activated receptor gamma

T2DM: type 2 diabetes mellitus

## Figures

### Figure 1

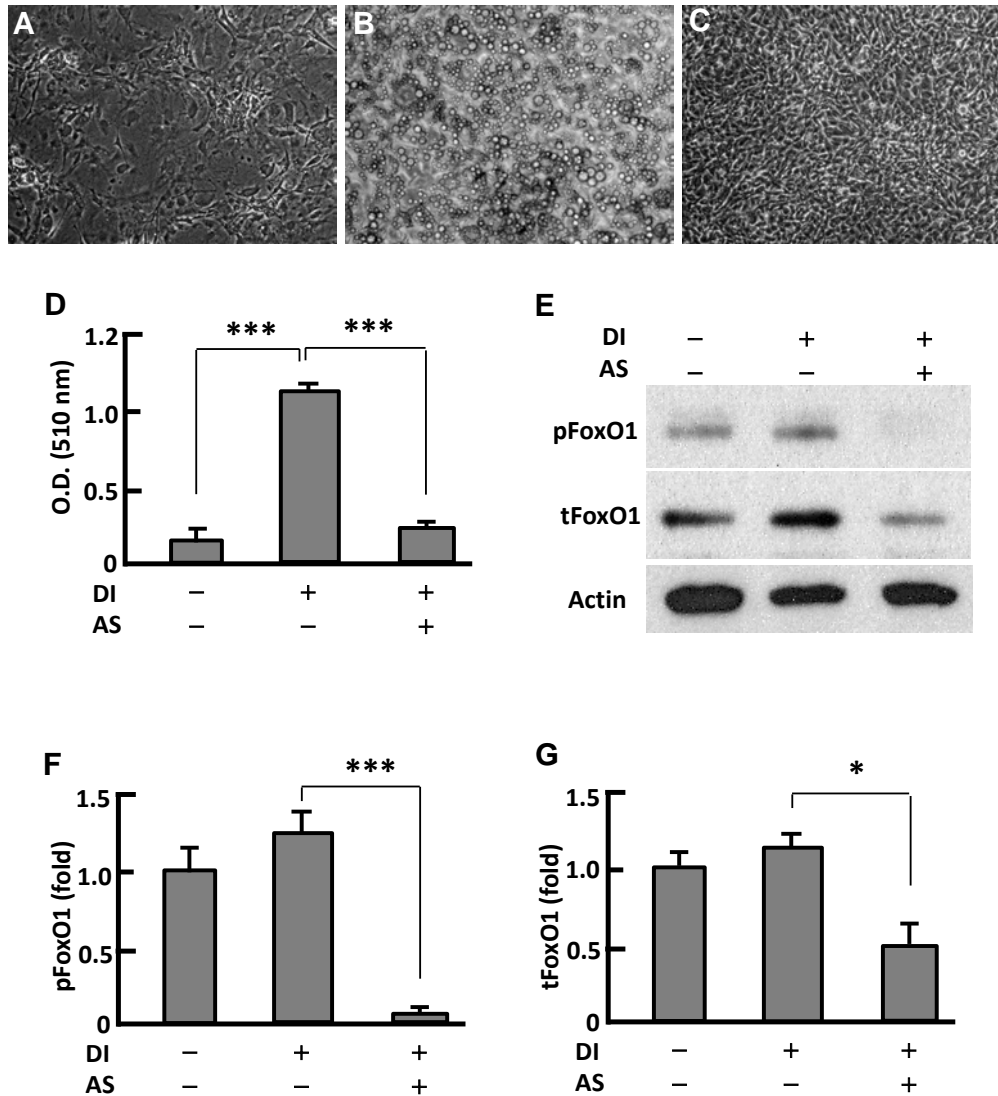


**Figure 1 Persistent inhibition of FoxO1 by AS1842856 largely suppressed adipogenesis.** (A-B) Microscopy images of preadipocytes that were maintained in basal medium (A), and that underwent differentiation induced with the protocol as described in Materials and Methods (B). (C) Microscopy images of cells that were treated with AS1842856 (0.1  $\mu$ M, days 0-12) and

underwent differentiation induction as in (B). All the images were captured on day 12, with the microscope set at 100X. (D) Measurement of extracted Oil red O retained in cells by the absorbance (O.D.) at 510 nm (n=6). (E) Representative western blot showing that AS1842856 inhibited FoxO1 through binding the de-phosphorylated sites, and to a lesser extent suppressed FoxO1 protein expression.  $\beta$ -actin was probed as the loading control. DI, differentiation induction; AS, AS1842856. (F-G) Densitometric analysis of western blot images with NIH ImageJ software; n=3-5. \*  $p < 0.05$ , and \*\*\*,  $p < 0.0001$ .

**Figure 2**

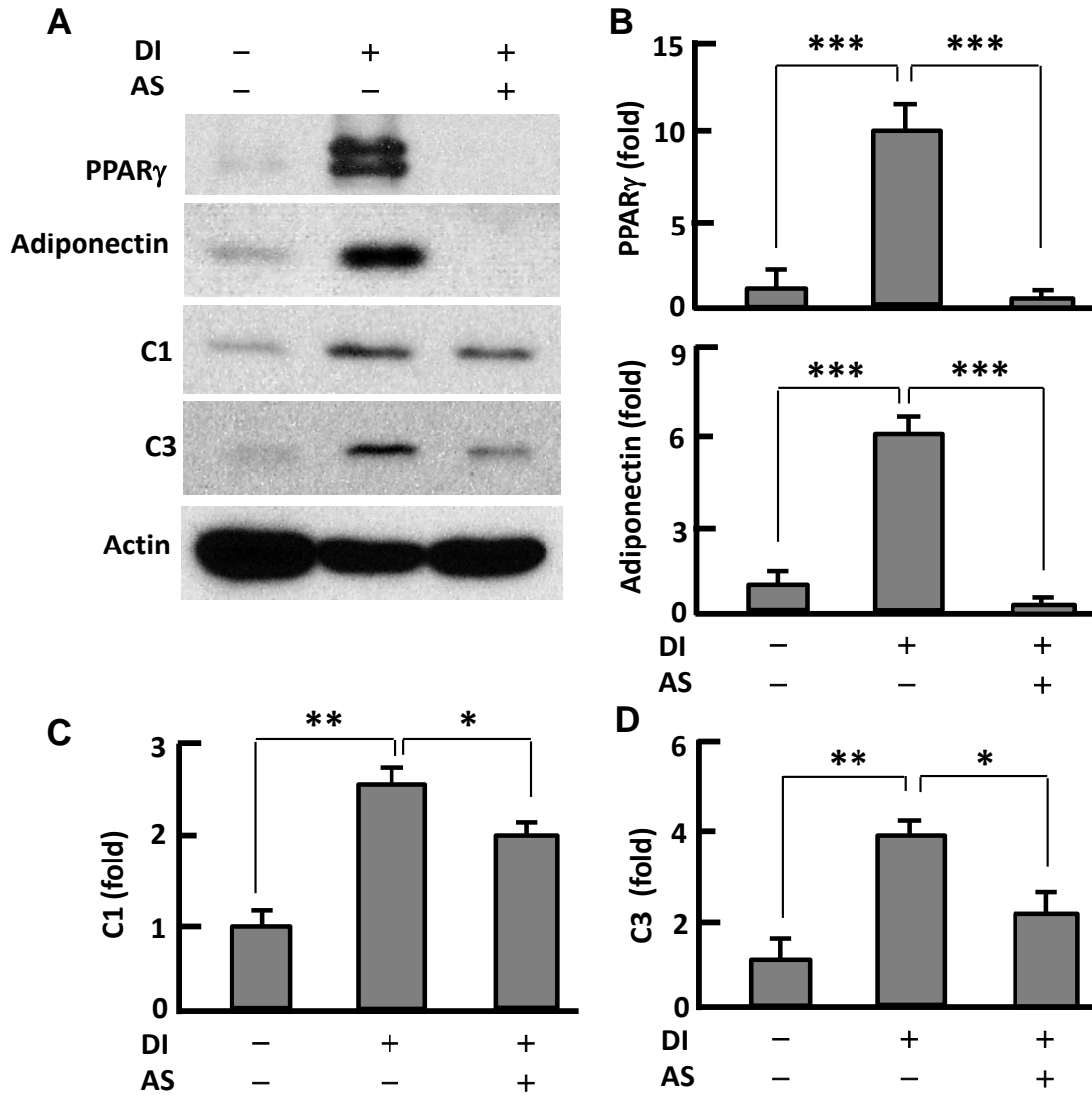


**Figure 2 AS1842856 suppressed PPAR $\gamma$  and mitochondrial protein expression.** (A) Western blots showing the effect of AS1842856 on PPAR $\gamma$ , adiponectin, mitochondrial proteins C1 and C3.  $\beta$ -actin was probed as the loading control. DI, differentiation induction; AS, AS1842856. (B-D) Densitometric analysis of western blot images with NIH ImageJ software; n=3-5. \* p<0.05; \*\*, p<0.01; and \*\*\*, p<0.0001.

## Figure 3

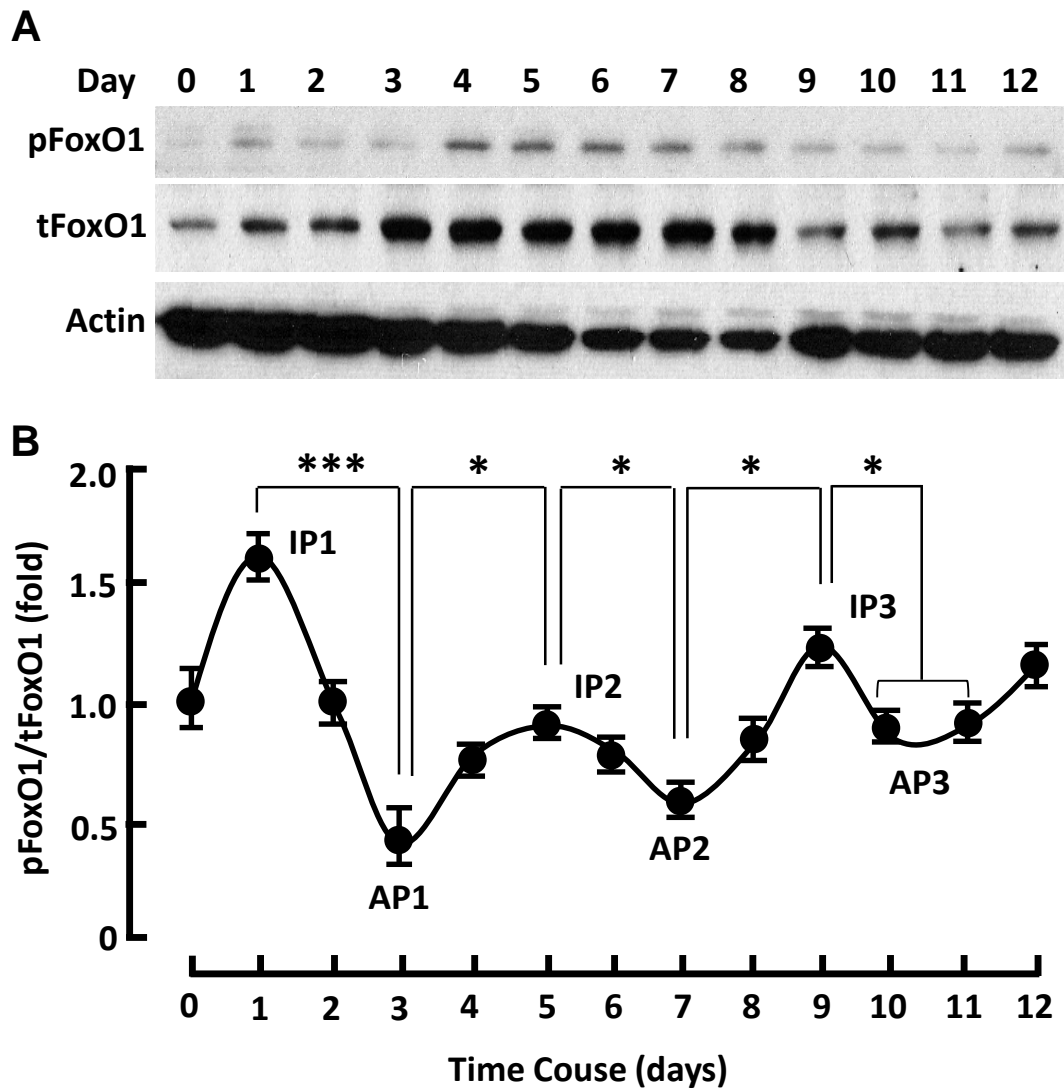


**Figure 3** The kinetics of FoxO1 activation followed a series of sigmoid curves during adipogenesis. (A) Western blots showing FoxO1 expression (i.e., tFoxO1), activation (i.e., dephosphorylation) and inactivation (i.e., phosphorylation) during adipogenesis.  $\beta$ -actin was probed as the loading control. (B) Densitometric analysis of western blot images with NIH ImageJ software;  $n=3-5$ . AP, activation peak; IP, inactivation peak. \*  $p<0.05$ ; and \*\*\*,  $p<0.0001$ .

**Figure 4**

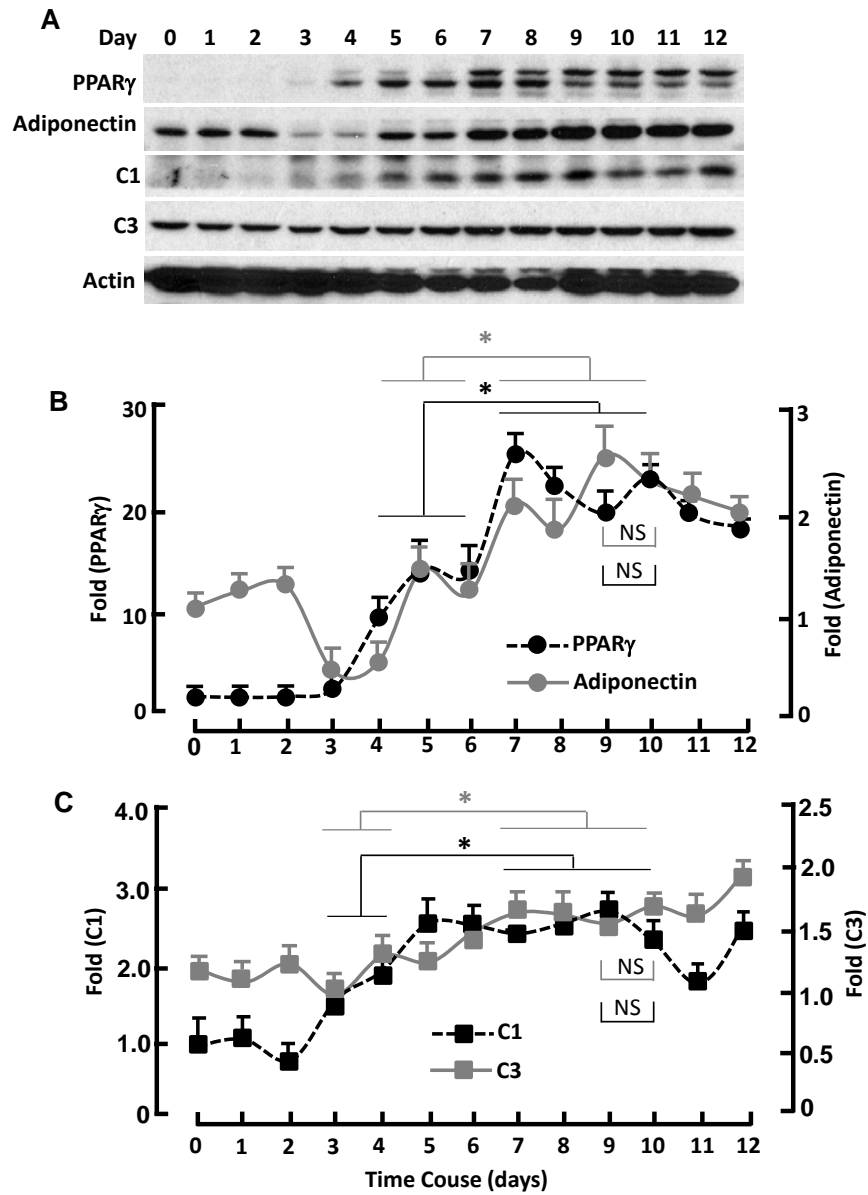


**Figure 4 Kinetics of FoxO1-regulated protein expression during adipogenesis.** (A) Western blots showing the expression of PPAR $\gamma$ , adiponectin, mitochondrial proteins C1 and C3.  $\beta$ -actin was probed as the loading control. (B) Densitometric analysis of western blot images for PPAR $\gamma$  and adiponectin with NIH ImageJ software. (C) Densitometric analysis of western blot images for C1 and C3 with NIH ImageJ software. n=3-5. \* p<0.05; NS, not significant.

**Figure 5**

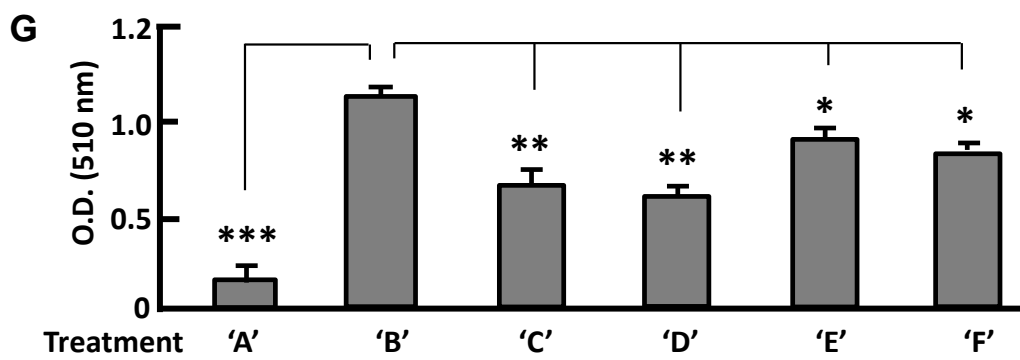
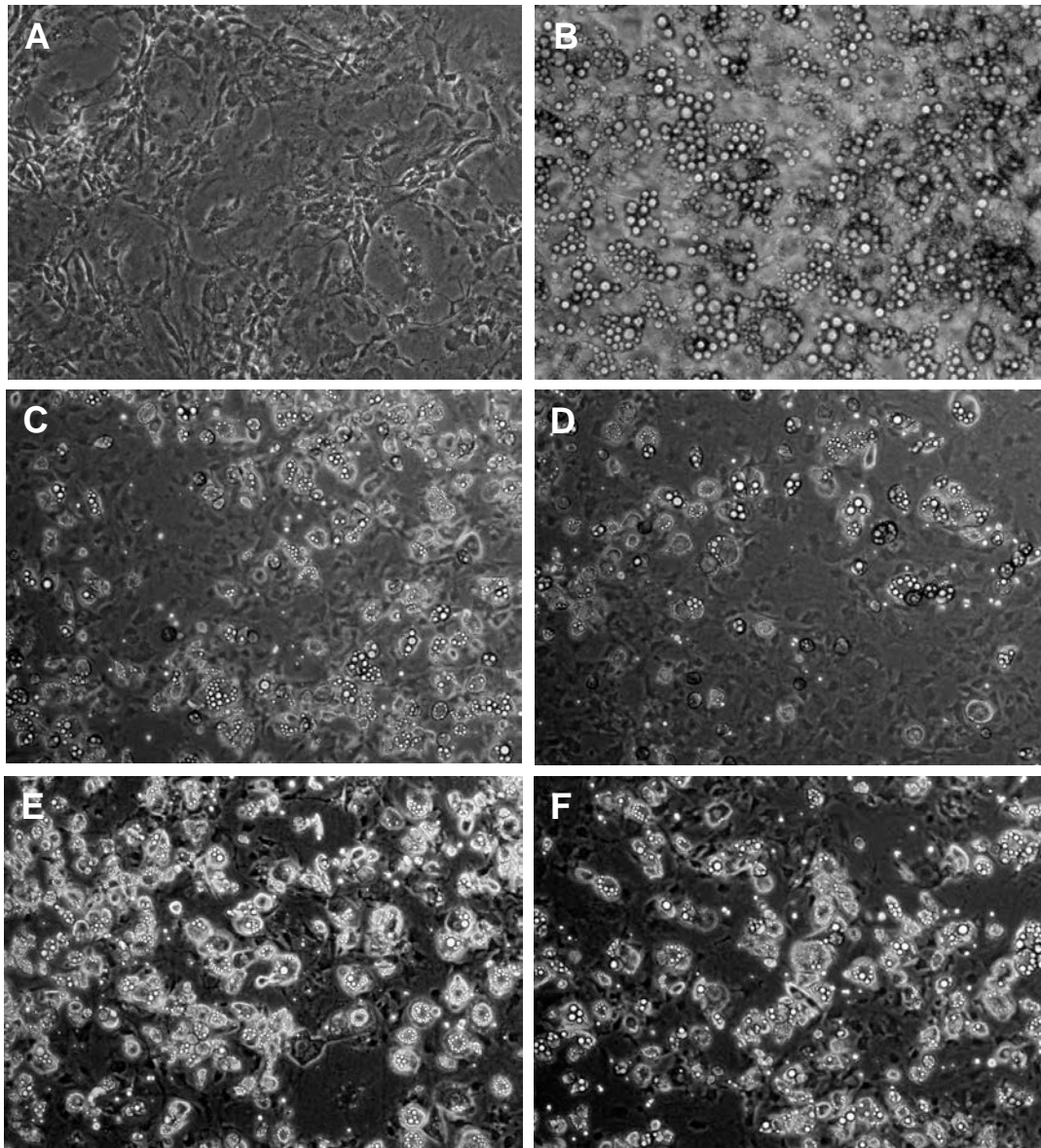


**Figure 5 Effects of phase-specific FoxO1 inhibition on adipogenesis.** (A-B) Images of cells that were maintained in basal medium (A), and that underwent differentiation induced with the protocol as described in Materials and Methods (B). (C) Images of cells that were treated with AS1842856 during stage BMII (days 7-12) and underwent differentiation induction as in (B). (D) Images of cells that were treated with AS1842856 during stage DMI (days 3-4) and underwent differentiation induction as in (B). (E) Images of cells that were treated with AS1842856 during stage BMI (days 1-2) and underwent differentiation induction as in (B). (F) Images of cells that were treated with AS1842856 during stage DMII (days 5-6) and underwent differentiation induction as in (B). The final concentration of AS1842856 was 0.1  $\mu$ M. All the images were captured on day 12, and the microscope was set at 100X. (G) Measurement of extracted Oil red O retained in cells by the absorbance (O.D.) at 510 nm (n=6). Treatments of 'A'-'F' refer to the individual treatments as described in panels A-F. \*  $p < 0.05$ ; \*\*,  $p < 0.01$ ; and \*\*\*,  $p < 0.0001$ .

**Figure 1s**

**A**

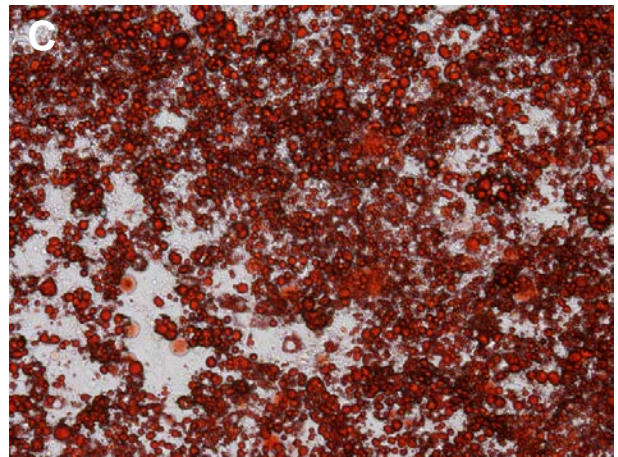
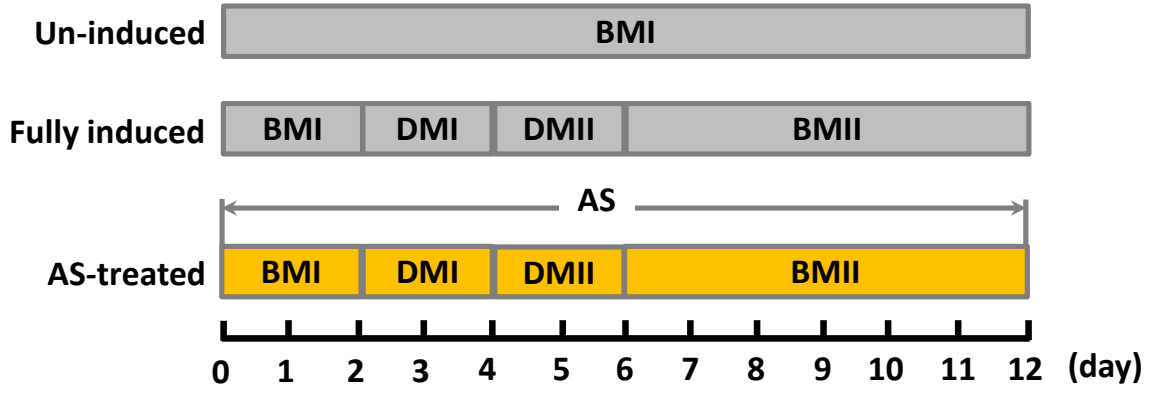


**Figure 1s Effects of persistent FoxO1 inhibition on adipogenesis.** (A) A diagram showing the conditions for cell culture, differentiation induction, and AS1842856 treatment. The grey color indicates the media as specified in Materials and Methods, while the yellow color refers to the modified media that contain AS1842856. BMI, basal medium I; DMI, differentiation medium I; DMII, differentiation medium II; BMII, basal medium II; AS, AS1842856. (B-D) Oil red O staining and microscopy images of preadipocytes that were maintained in basal medium (B), and that underwent full differentiation induced with the protocol as described in Materials and Methods (C), and that were treated with AS1842856 (0.1  $\mu$ M) throughout the cell culture (days 0-12) and underwent differentiation induction (D). All the images were captured on day 12, with the microscope set at 100X.

**Figure 2s**

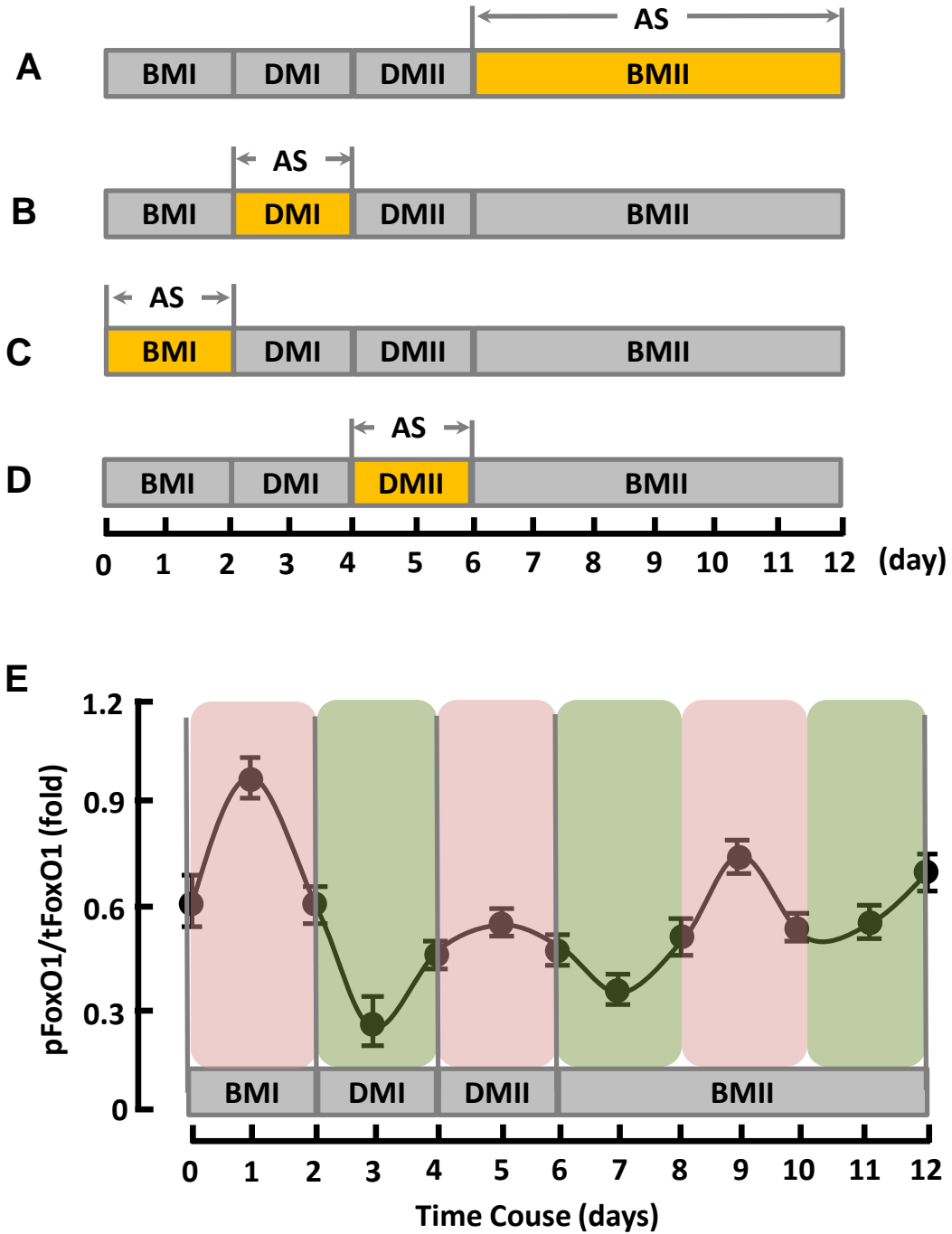
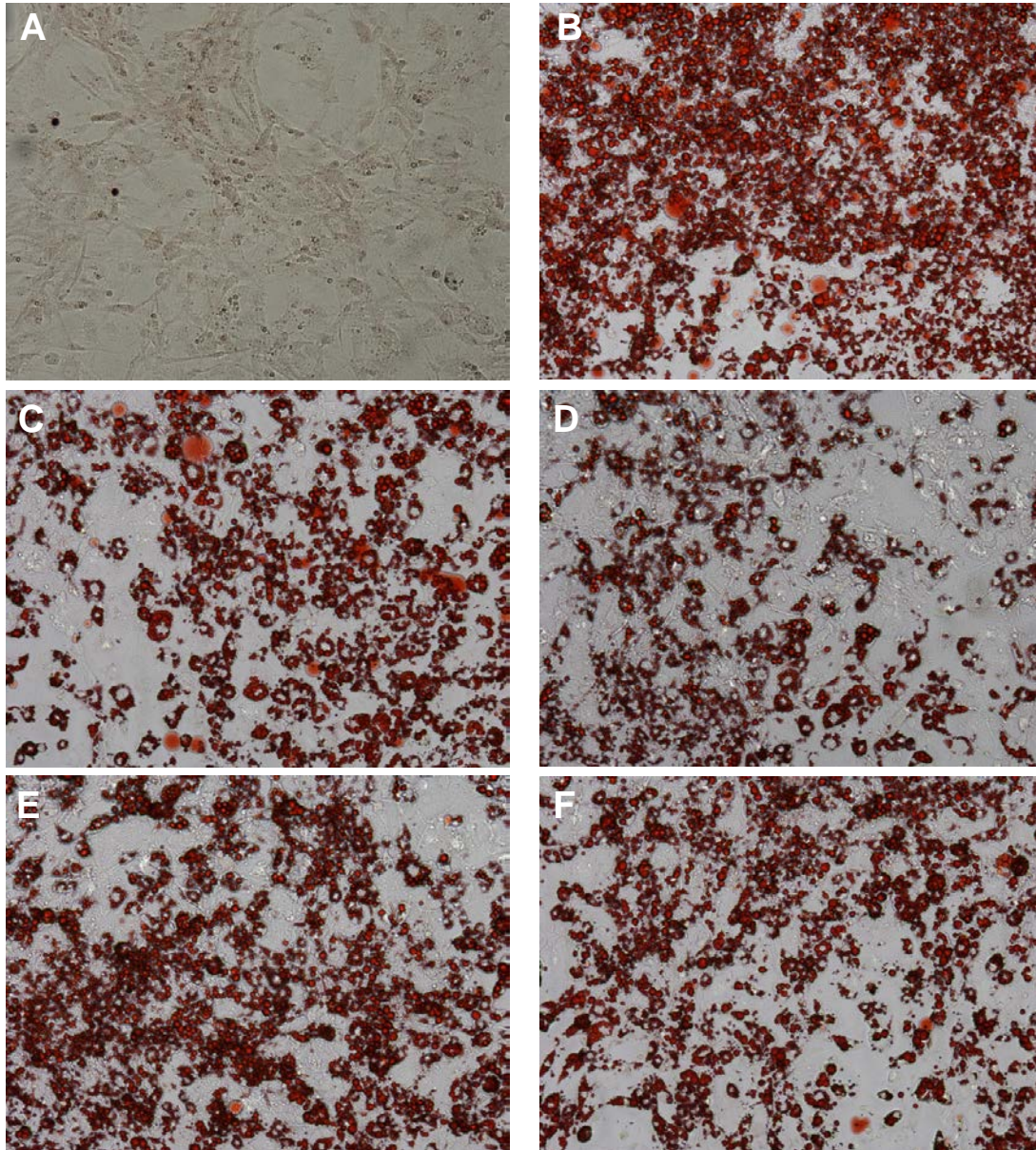


**Figure 2s Phase-specific inhibition of FoxO1 by AS1842856.** (A) A diagram showing the primary marks of FoxO1 regulation during adipogenesis. The phases in pink indicate a primary mark of inactivation, while the phases in green suggest a primary mark of activation. (B) A diagram showing the phase-specific treatment with AS1842856. The grey color indicates the media as specified in Materials and Methods, while the yellow color refers to the modified media that contain AS1842856. AS, AS1842856; BMI, basal medium I; DMI, differentiation medium I; DMII, differentiation medium II; BMII, basal medium II.

**Figure 3s**



**F**

**Figure 3s Examining effects of AS on adipogenesis by Oil Red O staining.** (A-B) Staining of cells that were maintained in basal medium (A), and that underwent differentiation induced with the protocol as described in Materials and Methods (B). (C) Staining of cells that underwent differentiation induction as in (B) and were treated with AS1842856 during stage BMII (days 7-

12). (D) Staining of cells that underwent differentiation induction as in (B) and were treated with AS1842856 during stage DMI (days 3-4). (E) Staining of cells that underwent differentiation induction as in (B) and were treated with AS1842856 during stage BMI (days 1-2). (F) Staining of cells that underwent differentiation induction as in (B) and were treated with AS1842856 during stage DMII (days 5-6). The final concentration of AS1842856 was 0.1  $\mu$ M. All the images were captured on day 12, and the microscope was set at 100X.

## References

1. Cheng Z, Almeida FA. Mitochondrial alteration in type 2 diabetes and obesity: an epigenetic link. *Cell Cycle* 2014; 13:890-7.
2. Cheng Z, Schmelz EM, Liu D, Hulver MW. Targeting mitochondrial alterations to prevent type 2 diabetes-Evidence from studies of dietary redox-active compounds. *Molecular nutrition & food research* 2014.
3. Wang QA, Tao C, Gupta RK, Scherer PE. Tracking adipogenesis during white adipose tissue development, expansion and regeneration. *Nature medicine* 2013; 19:1338-44.
4. Niswender K. Diabetes and obesity: therapeutic targeting and risk reduction - a complex interplay. *Diabetes, obesity & metabolism* 2010; 12:267-87.
5. Cheng Z, White MF. Targeting Forkhead box O1 from the concept to metabolic diseases: lessons from mouse models. *Antioxidants & redox signaling* 2011; 14:649-61.
6. De Pauw A, Tejerina S, Raes M, Keijer J, Arnould T. Mitochondrial (dys)function in adipocyte (de)differentiation and systemic metabolic alterations. *The American journal of pathology* 2009; 175:927-39.
7. Kusminski CM, Scherer PE. Mitochondrial dysfunction in white adipose tissue. *Trends in endocrinology and metabolism: TEM* 2012; 23:435-43.
8. Gesta S, Tseng YH, Kahn CR. Developmental origin of fat: tracking obesity to its source. *Cell* 2007; 131:242-56.
9. Farmer SR. Transcriptional control of adipocyte formation. *Cell metabolism* 2006; 4:263-73.
10. Rosen ED, Spiegelman BM. What we talk about when we talk about fat. *Cell* 2014; 156:20-44.
11. Cheng Z, White MF. The AKTion in non-canonical insulin signaling. *Nature medicine* 2012; 18:351-3.
12. Cheng Z, Tseng Y, White MF. Insulin signaling meets mitochondria in metabolism. *Trends in endocrinology and metabolism: TEM* 2010; 21:589-98.
13. Kim H, Hiraishi A, Tsuchiya K, Sakamoto K. (-) Epigallocatechin gallate suppresses the differentiation of 3T3-L1 preadipocytes through transcription factors FoxO1 and SREBP1c. *Cytotechnology* 2010; 62:245-55.
14. Munekata K, Sakamoto K. Forkhead transcription factor Foxo1 is essential for adipocyte differentiation. *In vitro cellular & developmental biology Animal* 2009; 45:642-51.
15. Nakae J, Kitamura T, Kitamura Y, Biggs WH, 3rd, Arden KC, Accili D. The forkhead transcription factor Foxo1 regulates adipocyte differentiation. *Developmental cell* 2003; 4:119-29.
16. Dowell P, Otto TC, Adi S, Lane MD. Convergence of peroxisome proliferator-activated receptor gamma and Foxo1 signaling pathways. *The Journal of biological chemistry* 2003; 278:45485-91.
17. Armoni M, Harel C, Karni S, Chen H, Bar-Yoseph F, Ver MR, et al. FOXO1 represses peroxisome proliferator-activated receptor-gamma1 and -gamma2 gene promoters in primary adipocytes. A novel paradigm to increase insulin sensitivity. *The Journal of biological chemistry* 2006; 281:19881-91.

18. Fan W, Imamura T, Sonoda N, Sears DD, Patsouris D, Kim JJ, et al. FOXO1 transrepresses peroxisome proliferator-activated receptor gamma transactivation, coordinating an insulin-induced feed-forward response in adipocytes. *The Journal of biological chemistry* 2009; 284:12188-97.
19. Kim JJ, Li P, Huntley J, Chang JP, Arden KC, Olefsky JM. FoxO1 haploinsufficiency protects against high-fat diet-induced insulin resistance with enhanced peroxisome proliferator-activated receptor gamma activation in adipose tissue. *Diabetes* 2009; 58:1275-82.
20. Cheng Z, Guo S, Copps K, Dong X, Kollipara R, Rodgers JT, et al. Foxo1 integrates insulin signaling with mitochondrial function in the liver. *Nature medicine* 2009; 15:1307-11.
21. Cheng Z, White MF. Foxo1 in hepatic lipid metabolism. *Cell Cycle* 2010; 9:219-20.
22. Dong XC, Copps KD, Guo S, Li Y, Kollipara R, DePinho RA, et al. Inactivation of hepatic Foxo1 by insulin signaling is required for adaptive nutrient homeostasis and endocrine growth regulation. *Cell metabolism* 2008; 8:65-76.
23. Nagashima T, Shigematsu N, Maruki R, Urano Y, Tanaka H, Shimaya A, et al. Discovery of novel forkhead box O1 inhibitors for treating type 2 diabetes: improvement of fasting glycemia in diabetic db/db mice. *Molecular pharmacology* 2010; 78:961-70.
24. Diep CH, Charles NJ, Gilks CB, Kalloger SE, Argenta PA, Lange CA. Progesterone receptors induce FOXO1-dependent senescence in ovarian cancer cells. *Cell Cycle* 2013; 12:1433-49.
25. Mortuza R, Chen S, Feng B, Sen S, Chakrabarti S. High glucose induced alteration of SIRT6 in endothelial cells causes rapid aging in a p300 and FOXO regulated pathway. *PloS one* 2013; 8:e54514.
26. Zebisch K, Voigt V, Wabitsch M, Brandsch M. Protocol for effective differentiation of 3T3-L1 cells to adipocytes. *Analytical biochemistry* 2012; 425:88-90.
27. Spiegelman BM. PPAR-gamma: adipogenic regulator and thiazolidinedione receptor. *Diabetes* 1998; 47:507-14.
28. Ramirez-Zacarias JL, Castro-Munozledo F, Kuri-Harcuch W. Quantitation of adipose conversion and triglycerides by staining intracytoplasmic lipids with Oil red O. *Histochemistry* 1992; 97:493-7.
29. Guo S, Copps KD, Dong X, Park S, Cheng Z, Poci A, et al. The Irs1 branch of the insulin signaling cascade plays a dominant role in hepatic nutrient homeostasis. *Molecular and cellular biology* 2009; 29:5070-83.

## **Chapter 3 FoxO1 antagonist suppresses autophagy and lipid droplet growth in adipocytes**

Longhua Liu,<sup>1</sup> Louise D. Zheng,<sup>1</sup> Peng Zou,<sup>1</sup> Joseph Brooke,<sup>1</sup> Cayleen Smith,<sup>1</sup> Yun Chau Long,<sup>2</sup>

Fabio A. Almeida,<sup>1</sup> Dongmin Liu,<sup>1</sup> Zhiyong Cheng<sup>1\*</sup>

<sup>1</sup> Department of Human Nutrition, Foods and Exercise, Fralin Life Science Institute, College of Agriculture and Life Science, Virginia Tech, Blacksburg, Virginia, USA.

<sup>2</sup> Department of Biochemistry, Yong Loo Lin School of Medicine, National University of Singapore, Singapore.

Correspondence: Dr. Zhiyong Cheng, 1981 Kraft Drive, Blacksburg, VA 24061, USA. Phone: (540) 231 9445; Fax: (540) 231 5522; email: [zcheng@vt.edu](mailto:zcheng@vt.edu).

---

**This chapter has been published in Cell Cycle. 2016 Aug 2; 15(15):2033-41.**

**Abstract:** Obesity and related metabolic disorders constitute one of the most pressing health concerns worldwide. Increased adiposity is linked to autophagy upregulation in adipose tissues. However, it is unknown how autophagy is upregulated and contributes to aberrant adiposity. Here we show a FoxO1-autophagy-FSP27 axis that regulates adipogenesis and lipid droplet (LD) growth in adipocytes. Adipocyte differentiation was associated with upregulation of autophagy and fat specific protein 27 (FSP27), a master regulator of adipocyte maturation and expansion by promoting LD formation and growth. However, FoxO1 specific Inhibitor AS1842856 potently suppressed autophagy, FSP27 expression, and adipocyte differentiation. In differentiated adipocytes, AS1842856 significantly reduced FSP27 level and LD size, which was recapitulated by autophagy inhibitors (bafilomycin-A1 and leupeptin, BL). Similarly, AS1842856 and BL dampened autophagy activity and FSP27 expression in explant cultures of white adipose tissue. To our knowledge, this is the first study addressing FoxO1 in adipose autophagy, shedding light on the mechanism of increased autophagy and adiposity in obese individuals. Given that adipogenesis and adipocyte expansion contribute to aberrant adiposity, targeting the FoxO1-autophagy-FSP27 axis may lead to new anti-obesity options.

**Keywords:** FoxO1, autophagy, adipogenesis, lipid droplet, FSP27, adipocyte expansion.

## Introduction

Obesity (a body mass index of > 30) is a pandemic in the US.<sup>1-3</sup> Obesity and its associated comorbidities including diabetes, heart disease, hypertension, liver disease, and infertility, exacerbate medical conditions and significantly increase healthcare costs.<sup>1,4</sup> By reducing life expectancy by 6 years at a body mass index (BMI) of 35-40, and 10 years at a BMI greater than 40, obesity has been one of the leading causes of death, which accounts for over 300,000 deaths per year in the US.<sup>5</sup> Thus, understanding the molecular mechanism of aberrant adiposity is of critical importance to treat obesity and related medical complications.

Aberrant expansion of adipose tissue may arise from an increase in adipocyte size (hypertrophy) or in adipocyte numbers (hyperplasia).<sup>6</sup> Recent studies show that expanded adiposity is associated with augmented autophagy in the adipose tissue from obese and type 2 diabetic humans and rodents.<sup>7-14</sup> Genetic suppression of autophagy by targeting autophagy related 5 (Atg5) or Atg7 in adipose tissue reduces adipocyte size, increases energy expenditure, and protects mice against diet-induced obesity.<sup>15-17</sup> Moreover, deletion of Atg5 suppresses adipogenesis (*de novo* formation of adipocytes).<sup>17, 18</sup> Consistently, pharmacological inhibition of autophagy prevented body weight gain and fat mass expansion, protecting against metabolic syndrome such as glucose intolerance and insulin resistance.<sup>15, 19</sup> These findings underscore autophagy as an important player in adiposity regulation.

To date it is unknown how autophagy is upregulated in adipose tissue and increases adiposity in obese subjects. Recent studies have implicated the transcription factor FoxO1 in autophagy regulation.<sup>22-25</sup> However, FoxO1 functions in a tissue-dependent way, and a role of FoxO1 in

adipose autophagy has not been reported.<sup>20-24</sup>. In this study we found that FoxO1 specific antagonist (AS1842856)<sup>3, 25</sup> potently suppressed autophagy and adipocyte differentiation, which was associated with downregulation of FSP27. In terminally differentiated adipocytes, targeting FoxO1 or autophagy with inhibitors significantly reduced FSP27 level and LD size. *Ex vivo* data from mouse white adipose tissues validated the existence of FoxO1-autophagy-FSP27 axis, which may regulate lipid droplet growth, adipocyte maturation and expansion. Further study of this regulatory pathway may lead to new anti-obesity option by preventing hyperplasia or adipocyte hypertrophy.

## Results

### **FoxO1 antagonist suppressed autophagy during adipocyte differentiation.**

Following an established protocol,<sup>3</sup> we induced 3T3L1 adipocyte differentiation and confirmed maturation of adipocytes by oil red O staining and analyzed adipogenic regulator PPAR $\gamma$  and adipocyte function marker adiponectin (Figure 1). Compared with preadipocytes, mature adipocytes showed significant lipid accumulation (Figure 1, A) and upregulation of PPAR $\gamma$  and adiponectin (Figure 1, B, E, F). Beclin 1, a critical autophagy promoter,<sup>26</sup> was upregulated in mature adipocytes, and it was accompanied by downregulation of p62 (or sequestosome 1, SQSTM1), a protein which is exclusively degraded by autophagy (Figure 1, B, C, D).<sup>10, 27, 28</sup> To measure autophagic flux, preadipocytes and mature adipocytes were treated with bafilomycin-A1 and leupeptin to inhibit autophagosome acidification and lysosomal proteases, respectively, followed by western blot analysis of p62.<sup>10, 27, 28</sup> Treatment with bafilomycin A1 and leupeptin prevented p62 from degradation by autophagy in a time-dependent manner (Figure 1s, A). A 12-

hr treatment restored p62 level in mature adipocytes (Figure 1s, B). In addition, the rate of p62 restoration was significantly higher in mature adipocytes than in preadipocytes, suggesting a higher turnover of p62 via autophagy (Figure 1s, C-F).<sup>10</sup> Intriguingly, inhibition of FoxO1 with a specific antagonist (AS1842856),<sup>3, 25</sup> prevented autophagy-mediated degradation of p62 during preadipocyte differentiation (Figure 1, B, D), and suppressed autophagy inducer beclin 1 and adipocyte maturation (Figure 1, A-C, E, F). These findings suggest that FoxO1-mediated autophagy is an important mechanism during 3T3L1 differentiation.

**FoxO1 antagonist reduced LD size in adipocytes.** Adipocyte maturation is characterized by lipid accumulation and LD growth in the cells.<sup>29</sup> Inhibition of FoxO1 prevents preadipocyte differentiation, resulting in minimal lipid accumulation and LD formation (Figure 1). This prompted us to ask whether FoxO1 regulates LD in mature (or terminally differentiated) adipocytes. To address this question, fully differentiated 3T3L1 adipocytes were treated with FoxO1 inhibitor AS1842856 or the vehicle (DMSO) for 4 days, followed by analysis of lipid accumulation, LD number and size, and western blot analysis of cell lysates (Figure 2). Consistent with the effects observed during preadipocyte differentiation (Figure 1), inhibition of FoxO1 in mature adipocytes suppressed autophagy, lowering beclin 1 level but increasing p62 abundance (Figure 2, A, B). In addition, treatment of FoxO1 antagonist AS1842856 led to smaller but more numerous LDs, although the total lipid content in the cells was not significantly changes (Figure 2, C, D, E). These results suggest that FoxO1 plays an important role in the regulation LD growth.

**Targeting autophagy with BL phenocopied the effects of FoxO1 antagonist on adipogenesis and LD size.** To determine whether inactivation of autophagy *per se* prevents adipocyte differentiation and reduces LD size, we used well-established autophagosome inhibitors BL (i.e., bafilomycin A1 and leupeptin) to treat 3T3L1 preadipocyte during differentiation (Figure 3, A-E). As expected, BL potently suppressed autophagy (Figure 3, B-D). Intriguingly, BL treatment drastically prevented preadipocyte differentiation, as indicated by marginal lipid accumulation and indiscernible PPAR $\gamma$  expression (Figure 3, A, B, E). When terminally differentiated adipocytes were treated with BL for 4 days, LD size was significantly reduced ( $54 \mu\text{m}^2$  vs  $36 \mu\text{m}^2$ ,  $p < 0.0001$ ) and LD number was increased by 72.7% ( $p < 0.0001$ ), while the total lipid content was not changes by BL treatment (Figure 3, F-H). These data recapitulated the effects of FoxO1 antagonist and suggest that targeting the FoxO1-autophagy axis with inhibitors accounts largely for the suppressed adipogenesis and reduced LD size in adipocytes (Figures 1-3).

**FSP27 was regulated by the FoxO1-autophagy axis in adipocytes.** Fat-specific protein 27 (FSP27) controls formation of large unilocular LDs by promoting LD clustering or fusion.<sup>30-32</sup> To examine whether FSP27 is responsible for the effects of FoxO1-autophagy axis on LD, we analyzed FSP27 in mature adipocytes treated with AS1842856, BL, or the vehicle (DMSO). Inhibition of FoxO1 with AS1842856 led to a 65% reduction in FSP27 protein level, an effect that is recapitulated by autophagy inhibitors BL (Figure 4, A). This may account for the reduced LD size in mature adipocytes (Figure 2, D, E; Figure 3, G, H), as downregulation of FSP27 prevents LD clustering or fusion.<sup>30-32</sup> In preadipocytes (day 0), FSP27 level was not

detectable but gradually upregulated during differentiation, reaching a plateau at day 10 through day 12 (Figure 4, B, C). However, treatment of preadipocytes with AS1842856 significantly suppressed FSP27 upregulation (Figure 4, D), consistent with AS1842856 induced absence of LD during adipocyte differentiation (Figure 1). Thus, the FoxO1-autophagy axis may regulate LD formation and expansion via FSP27.

**The FoxO1-autophagy-FSP27 axis functioned in SVF primary cells.** To examine if primary adipocytes share the FoxO1-autophagy-FSP27 regulatory pathway with 3T3L1 cell line, we isolated vascular fractions (SVF) from mouse adipose tissues as described previously.<sup>33, 34</sup> As observed in 3T3L1 cells, beclin 1 (4.2- fold,  $p < 0.0001$ ) and FSP27 (3.9-fold,  $p < 0.001$ ) were upregulated in differentiated SVF, which was associated with significant lipid accumulation and adiponectin expression (Figure 5). Inhibition of FoxO1 by AS1842856 suppressed the markers of autophagy (beclin 1, Figure 5-A,B) and adipogenesis (adiponectin expression, Figure 5-A,C; and lipid accumulation measured by Abs 510, Figure 5-D) (Figure 5, A-D). Accordingly, FSP27 upregulation was prevented in SVF treated with AS1842856 despite the presence of differentiation inducer (Figure 5, E-F). These findings suggest that FoxO1-autophagy-FSP27 axis is an important mechanism regulating adipocyte differentiation and LD size in both 3T3L1 cell line and SVF primary cells.

**FoxO1-autophagy axis regulated FSP27 in white adipose tissue.** To validate the findings in cells, we examined the FoxO1-autophagy-FSP27 axis in explant cultures of mouse white adipose tissues (Figure 6). When the explant cultures of adipose tissues were treated with FoxO1 inhibitor AS1842856, it significantly suppressed autophagy-mediated p62 degradation,

resulting in a 2.3-fold increase in p62 level ( $p < 0.05$ , Figure 6-A, B). Similarly, treatment with the autophagosome inhibitors BL led to a 2.0-fold elevation of p62 ( $p < 0.05$ , Figure 6-A, B). In line with the FoxO1-autophagy-FSP27 regulatory pathway, the AS1842856- and BL-induced suppression of autophagy was associated with downregulation of FSP27 (75% by AS1842856,  $p < 0.001$ ; and 61% by BL,  $p < 0.001$ ; Figure 6, C, D). Therefore, the FoxO1-autophagy-FSP27 axis represents a common mechanism regulating adipogenesis and LD expansion. Given that silencing adipose FSP27 reduces adiposity and protects against diet-induced obesity in mice,<sup>30, 35-37</sup> targeting this regulatory pathway may lead to effective anti-obesity strategies.

## Discussion

The transcription factor FoxO1 plays an important role in metabolic regulation and cell quality control.<sup>20, 21</sup> Previous studies demonstrated that FoxO1 activation dysregulates mitochondrial function and glucose and lipid metabolism in the liver; thus, ablation of FoxO1 in the liver reverses the adverse changes of mitochondria and metabolism.<sup>38-42</sup> We and others found that FoxO1 also regulated adipogenesis,<sup>3, 43, 44</sup> a process which may promote adipose expansion via hyperplasia.<sup>6, 29, 45</sup> Moreover, aberrant adiposity may result from adipocyte or LD hypertrophy.<sup>29, 45</sup> In this study, we showed for the first time that FoxO1 regulates LD size and number via an autophagy-FSP27 axis. Given that FoxO1 is activated by insulin resistance<sup>20, 46, 47</sup>, the FoxO1-autophagy-FSP27 axis may promote LD and adipocyte expansion in obese insulin resistant subjects, thereby casting new light on the mechanism of augmented autophagy in adipose tissues from obese subjects.<sup>7-12</sup> To the best of our knowledge, this is also the first study investigating the role of FoxO1 in the regulation of adipose autophagy.

Autophagic pathway begins with engulfment of cytoplasmic material by the phagophore (i.e., isolation membrane), which sequesters the cytoplasmic material in double-membraned vesicles (i.e., autophagosomes or autophagic vacuoles).<sup>23</sup> Among the multiple stages of autophagy, FoxO1 has been implicated in the steps of initiation, vesicle nucleation, and vesicle elongation.<sup>21,</sup><sup>23</sup> The autophagy genes which are regulated by FoxO1 include *Becn1* (encoding beclin1) and *Map1lc3* (encoding LC3).<sup>23</sup> In line with this, we found that inhibition of FoxO1 reduced the protein level of beclin 1, which suppressed the degradation of p62 by autophagy (Figures 1-2, Figures 5-6). The FoxO1-induced changes in autophagy seem to regulate LD formation and growth via FSP27 (Figures 4-6). While we cannot exclude the possibility that FoxO1 directly regulates FSP27, targeting either FoxO1 or autophagy with inhibitors similarly led to downregulation of FSP27, suggesting that FSP27 is a downstream effector of the FoxO1-autophagy axis (Figures 4-6). Like the adipogenic regulator PPAR $\gamma$ , FSP27 increases with autophagy during adipogenesis (Figure 1, Figures 4-5).<sup>3</sup> Given that activation of autophagy stabilizes PPAR $\gamma$  that promotes adipogenesis,<sup>18</sup> it would be of interest for future studies to investigate whether the FoxO1-autophagy axis increases FSP27 by affecting its stability. Taken together, our study reveals a FoxO1-autophagy-FSP27 axis that regulates adipogenesis and LD expansion. Silencing FoxO1 can potentially reduce autophagy activity and FSP27 level, suppressing adipocyte differentiation and LD growth. Given that LD expansion contributes to adipocyte hypertrophy and adipose expansion,<sup>6, 29, 45</sup> further study is warranted to targeting the FoxO1-autophagy axis to treat obesity.

## Materials and methods

**Mice.** Male C57BL6/J mice were purchased from Jackson Laboratory (Bar Harbor, Main) and housed as previously described.<sup>2</sup> Briefly, the mice were housed in plastic cages on a 12-h light–dark cycle, with free access to water and food. All the procedures followed NIH guidelines and were approved by the Virginia Tech Institutional Animal Care and Use Committee.

**SVF isolation and culture.** Primary preadipocytes (SVF) were isolated and cultured as previously described.<sup>33, 34</sup> Briefly, subcutaneous white adipose tissues from C57BL6/J mice (8-12 week old) were dissected, minced, and digested. Cells were suspended in growth media (DMEM/F12 containing 10% FPS and P/S), filtered through a 100-micron cell strainer, and centrifuged at 500 x g for 5 minutes. The pellet was then disrupted and resuspended in the growth media, and filtered through a 40-micron cell strainer. After centrifuge (500 x g) for 5 minutes, the pellet was resuspended in growth media and plated on 10 cm dishes. After subculture on 6-well plates, differentiation was induced as described previously.<sup>33, 34</sup>

**3T3L1 cell culture and treatment.** 3T3L1 preadipocytes (ATCC CL-173, Manassas, VA, USA) were cultured as previously described.<sup>2, 3</sup> Briefly, the cells were cultured in basal media (DMEM media supplemented with 10% FBS, 100 units/ml penicillin and 100 µg/ml streptomycin (1 × P/S)), at 37 °C in a humidified atmosphere of 5% CO<sub>2</sub>. The media were replaced every 2 days. 3T3L1 preadipocytes were grown to confluence (day 0), and further maintained in fresh basal media for 2 days (days 1–2). At the end of day 2, the medium was changed to differentiation medium I: DMEM supplemented with 10% FBS, P/S (1 ×), IBMX

(0.5 mM), dexamethasone (1  $\mu$ M), insulin (1  $\mu$ g/ml), and rosiglitazone (2  $\mu$ M). At the end of day 4, the medium was changed to differentiation medium II: DMEM supplemented with 10% FBS, P/S (1  $\times$ ), and insulin (1  $\mu$ g/ml). At the end of day 6, the medium was changed to basal media, and the cells were maintained in basal medium (replaced with fresh basal medium every 2 days) until fully differentiated (day 10). Control preadipocytes were maintained in basal media and supplied with fresh medium every other day till day 10. Depending on the experimental design, treatment with inhibitors (e.g., AS1842856 or bafilomycin A1 plus leupeptin) started on day 0 through day 10 (during differentiation), or on day 10 through day 14 (after adipocyte maturation). Images of the cells were captured on day 10 (if not specified elsewhere) with a Nikon ECLIPSE TS100 microscope (Melville, NY, USA), and the size and number of LDs were analyzed with the NIH ImageJ software (Bethesda, MD, USA) as described previously.<sup>48</sup>

**Oil red O staining.** The Oil Red O working solution was freshly prepared by mixing 0.35% stock solution with dH<sub>2</sub>O (6:4) and filtered, and the staining was conducted as described.<sup>3</sup> At the end of differentiation (day 10), the media were removed and the cells were washed once with phosphate buffered saline (PBS), and fixed in 4% formaldehyde at room temperature for 10 min and then at 4°C overnight. Subsequently, the cells were washed once with dH<sub>2</sub>O, once with 60% isopropanol, and air dried. Oil Red O working solution was added and the staining at room temperature lasted for 1 h. Afterwards, the stained cells were washed with dH<sub>2</sub>O for 4 times, and the images were captured with a Nikon ECLIPSE 80i microscope. Oil Red O retained in the cells was extracted with isopropanol, and quantified by the absorbance at 510 nm on a Synergy™ H4 Hybrid Multi-Mode Microplate Reader (BioTek Instruments, Inc).<sup>3</sup>

**Autophagy flux assay.** For cell culture, preadipocytes (day 10) and mature adipocytes (day 10) in basal media were treated with bafilomycin A1 (inhibitor of autophagosome acidification, at 0.1  $\mu$ M) plus leupeptin (the inhibitor of lysosomal proteases, at 10  $\mu$ g/ml) for 0, 2, 4, 8, and 12 hr; and the cell lysates were prepared as previously described.<sup>2, 3</sup> For *ex vivo* assay, adipose tissues were minced into small tissue fragments (2–3 mm<sup>3</sup>) and pre-incubated for 1 h in a CO<sub>2</sub> incubator (37°C, 5% CO<sub>2</sub>) in DMEM medium supplemented with 2 mM glutamine, 1% (vol/vol) antibiotic solution, and 10% (vol/vol) fetal bovine serum. Tissue fragments were then incubated for an additional 4 h in the same medium in the presence and absence of bafilomycin-A1 and leupeptin. Tissue lysates were prepared as we described previously,<sup>2, 3</sup> p62, the protein exclusively degraded by autophagy, was detected to assess autophagy flux by western blotting and image analysis.<sup>10, 27, 28</sup>

**Western blotting.** To prepare tissue lysates, snap-frozen adipose tissues were weighed and homogenized with a Bullet Blender (Next Advance, Averill Park, NY, USA) in PLC lysis buffer (30 mM HEPES, pH 7.5, 150 mM NaCl, 10% glycerol, 1% Triton X-100, 1.5 mM MgCl<sub>2</sub>, 1 mM EGTA, 10 mM NaPPi, 100 mM NaF, 1 mM Na<sub>3</sub>VO<sub>4</sub>) supplemented with protease inhibitor cocktail (Roche), 1 mM PMSF.<sup>2, 3</sup> For cell lysates, the 3T3L1 preadipocytes and mature adipocytes (at day 10) were washed with ice-cold PBS and homogenized with the Bullet Blender. Total protein concentrations of the lysates were determined using the DC protein assay (Bio-Rad). Western blotting and image analysis were conducted as described previously.<sup>2, 3</sup> Antibody catalog numbers and vendors are as follows: FSP27 (CIDE 3) (PA1-4316), PPAR $\gamma$  (MA5-14889), GAPDH (MA5-15738) and  $\beta$ -actin (MA5-15739) antibodies from Pierce

(Rockford, IL, USA); p62 (SQSTM1) (#5114) antibody from Cell Signaling Technology (Beverly, MA, USA); and adiponectin (AB3269P) and Beclin 1 (MABN16) antibodies from EMD Millipore (Billerica, MA, USA).

**Statistical analyses.** All results are expressed as means  $\pm$  SD. and are analyzed by analysis of variance (ANOVA) to determine p values;  $p < 0.05$  was considered statistically significant.

## **Funding**

Funding for this work was provided, in part, by USDA National Institute of Food and Agriculture Hatch Project 1007334 (ZC), NIH grant R18DK091811 (FAA), and NIH grant 1R01AT007077 (DL). Work in YCL lab was supported by grants Singapore Ministry of Education Academic Research Fund (T1-2011 Sep-05 and T1-2014 Apr -05).

## **Conflicts of Interest**

No potential conflicts of interest were disclosed.

## **Abbreviations:**

AS1842856: 5-amino-7-(cyclohexylamino)-1-ethyl-6-fluoro-4-oxo-1,4-dihydroquinoline-3-carboxylic acid

BL: bafilomycin-A1 and leupeptin

BMI: body mass index

FSP27: fat specific protein 27

FoxO1: forkhead box O1

GAPDH: glyceraldehyde 3-phosphate dehydrogenase

LC3: microtubule-associated protein 1A/1B-light chain 3-phosphatidylethanolamine conjugate

LD: lipid droplet

p62: sequestosome 1 (SQSTM1)

PPAR $\gamma$ : peroxisome proliferator-activated receptor gamma

SVF: stromal vascular fraction

## Figures

**Figure 1**

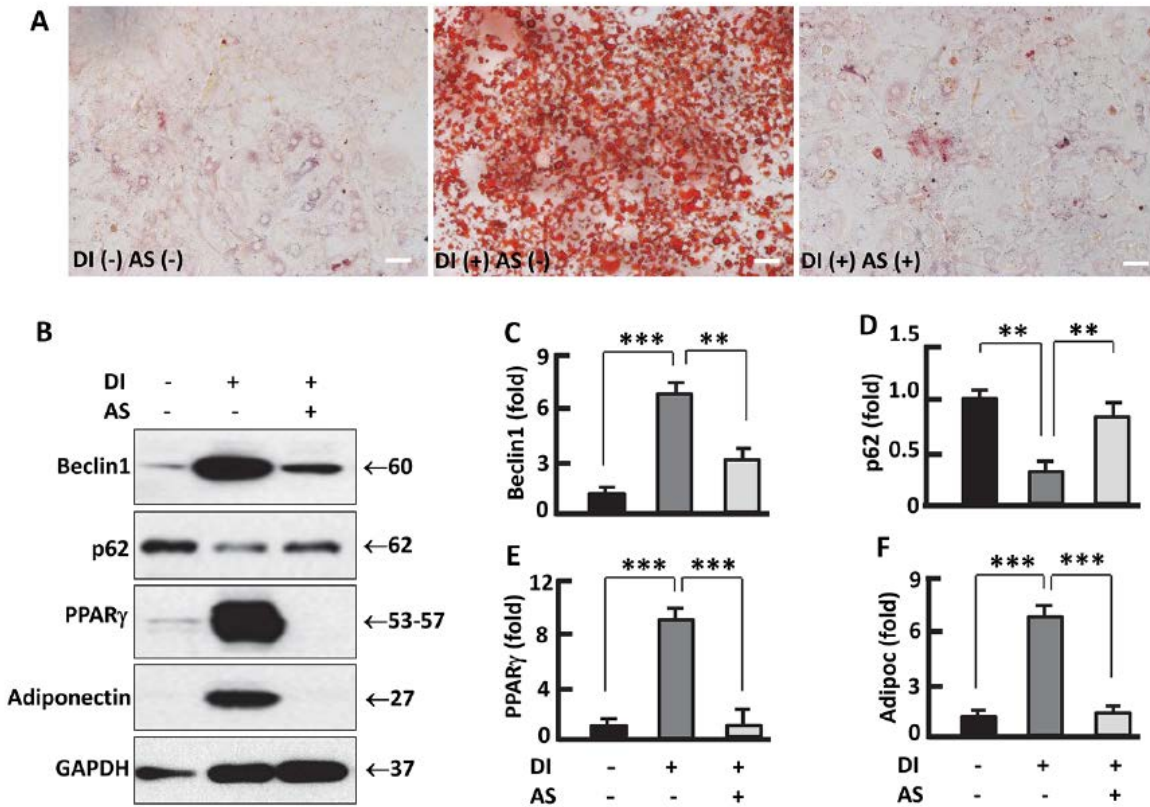


**Figure 1. Inhibition of FoxO1 with the antagonist AS1842856 suppressed autophagy and adipocyte maturation.** (A) Effect of antagonizing FoxO1 (AS1842856 treatment at 0.1  $\mu$ M from day 0 – 10) on 3T3L1 preadipocyte differentiation. The cells were stained with oil red O at day 10; DI, differentiation induction; AS, AS1842856. Scale bar = 50  $\mu$ m. (B) Western blot analysis of autophagy (beclin 1 and p62) and adipocyte maturation (PPAR $\gamma$ , adiponectin). (C-F) Densitometric analysis of western blot images as shown in panel B. Results are expressed as means  $\pm$  SD. \*\*,  $p < 0.01$ ; \*\*\*,  $p < 0.0001$ ,  $n = 3-5$ .

**Figure 2**

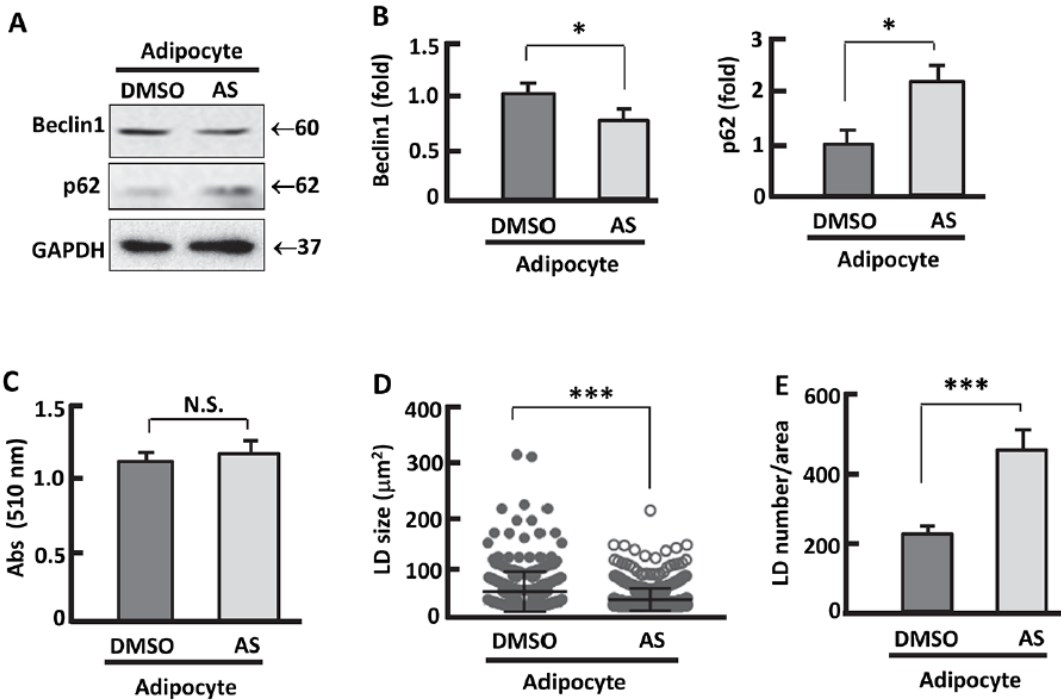


**Figure 2. Inhibition of FoxO1 suppressed autophagy, reduced the size but increased the number of lipid droplets in mature adipocytes.** (A-B) Western blotting (A) and densitometric analysis (B) of autophagy (beclin 1 and p62) in mature adipocytes. Fully differentiated 3T3L1 adipocytes (at day 10) were treated with AS1842856 (1  $\mu\text{M}$ ) for 4 days (day 11-14), followed by western blot analysis (control cells were treated with DMSO). AS, AS1842856. (C) Oil red O staining of mature adipocytes treated with AS1842856 (1  $\mu\text{M}$ ) for 4 days (at day 14), followed by the measurement of absorbance at 510 nm. (D-E) Measurement of lipid droplet size (D) and

number (E) after FoxO1 was inhibited for 4 days in adipocytes. The measurements were conducted on 8-10 images (0.04 mm<sup>2</sup>) for each treatment, and a representative distribution of lipid droplet size was shown in panel D, and the numbers were averaged and shown in panel E. Results are expressed as means  $\pm$  SD. \*,  $p < 0.05$ ; \*\*\*,  $p < 0.0001$ , NS, not significant;  $n = 3-5$ .

**Figure 3**

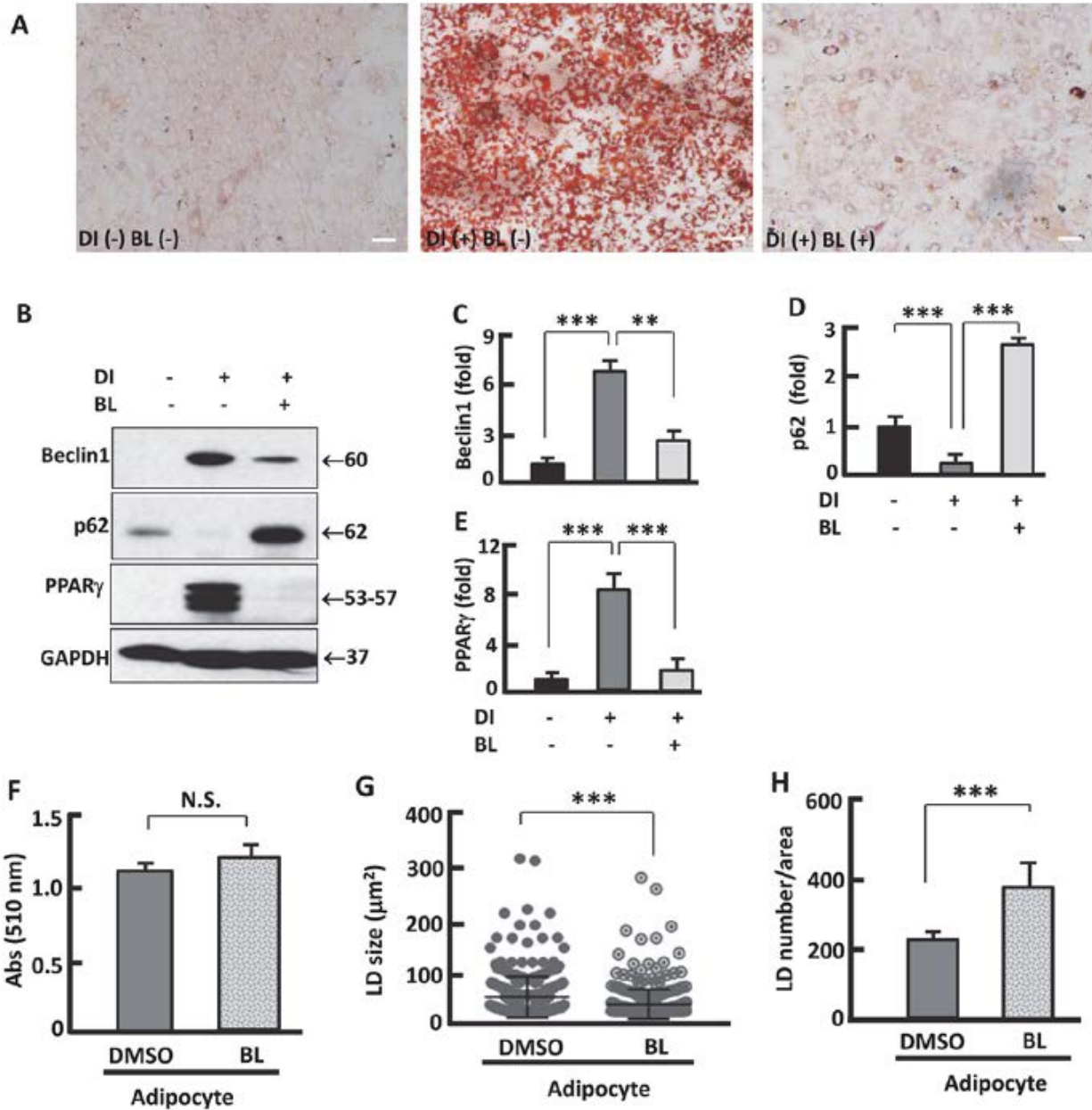


**Figure 3. Effects of autophagosome inhibitors on adipocyte maturation and lipid droplets.**

(A) Supplement of bafilomycin A1 (4 nM) and leupeptin (0.4  $\mu\text{g/ml}$ ) in the media (day 0-10) suppressed 3T3L1 preadipocyte differentiation. The cells were stained with oil red O at day 10. DI, differentiation induction; BL, bafilomycin A1 + leupeptin. Scale bar = 50  $\mu\text{m}$ . (B) Western blot analysis of autophagy (beclin 1 and p62) and adipocyte maturation (PPAR $\gamma$ ). (C-E) Densitometric analysis of western blot images as shown in panel B. (F) Fully differentiated 3T3L1 adipocytes (day 10) were treated with bafilomycin A1 (0.1  $\mu\text{M}$ ) and leupeptin (10  $\mu\text{g/ml}$ ) for 4 days (day 11-14); the cells treated with DMSO served as the controls. Oil red O staining of mature adipocytes at day 14, followed by the measurement of absorbance at 510 nm. (G-H) Measurement of lipid droplet size (G) and number (H) after autophagy was inhibited for 4 days in adipocytes. The measurements were conducted on 8 -10 images (0.04  $\text{mm}^2$ ) for each treatment, and a representative distribution of lipid droplet size was shown in panel G, and the numbers were averaged and shown in panel H. BL, bafilomycin A1 + leupeptin. Results are expressed as means  $\pm$  SD. \*\*,  $p < 0.01$ ; \*\*\*,  $p < 0.0001$ ; NS, not significant;  $n = 3-5$ .

**Figure 4**

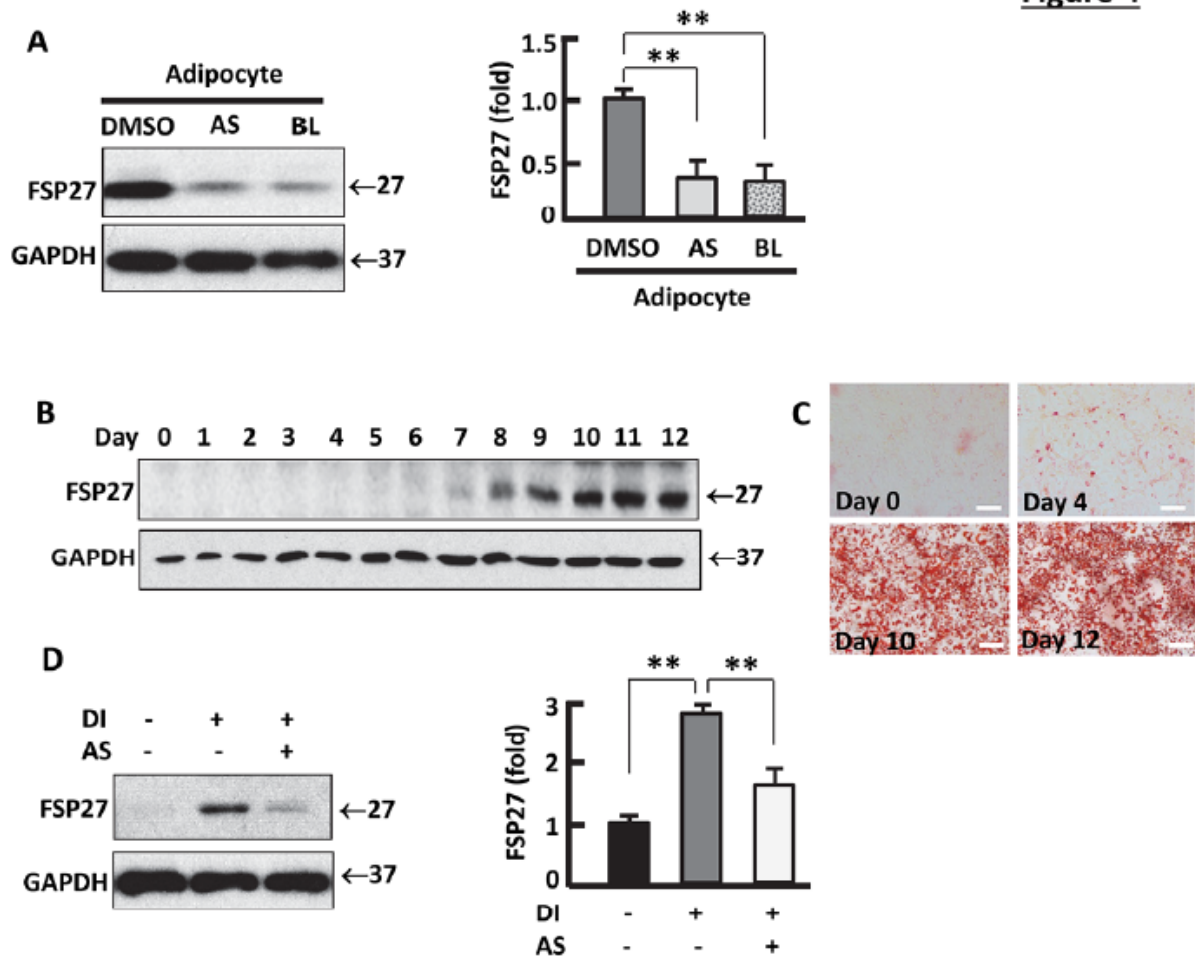


**Figure 4. Suppression of FoxO1-autophagy axis downregulated FSP27 in adipocytes.** (A) Western blotting and densitometric analysis of FSP27 in mature adipocytes. Fully differentiated 3T3L1 adipocytes (day 10) were treated with the inhibitors of FoxO1 (AS1842856, 1  $\mu$ M) and autophagy (0.1  $\mu$ M bafilomycin A1+ 10  $\mu$ g/ml leupeptin) for 4 days (day 11-14), followed by western blot analysis (control cells were treated with DMSO). (B-C) Kinetics of FSP27 expression (B) during 3T3L1 preadipocyte differentiation (C). FSP27 protein level was analyzed by western blotting, with GAPDH probed as the loading control (B). The 3T3L1 preadipocytes

were cultured and differentiated as described in Materials and Methods, and the cells were stained with oil red O on the indicated days (C); scale bar = 100  $\mu\text{m}$ . (D) Inhibition of FoxO1 with AS1842856 (0.1  $\mu\text{M}$ ) downregulated FSP27 during 3T3L1 preadipocyte differentiation, analyzed by western blotting with GAPDH probed as the loading control. AS, AS1842856; BL, bafilomycin A1 + leupeptin. DI, differentiation induction. Results are expressed as means  $\pm$  SD. \*\*,  $p < 0.01$ ,  $n = 3-5$ .

**Figure 5**

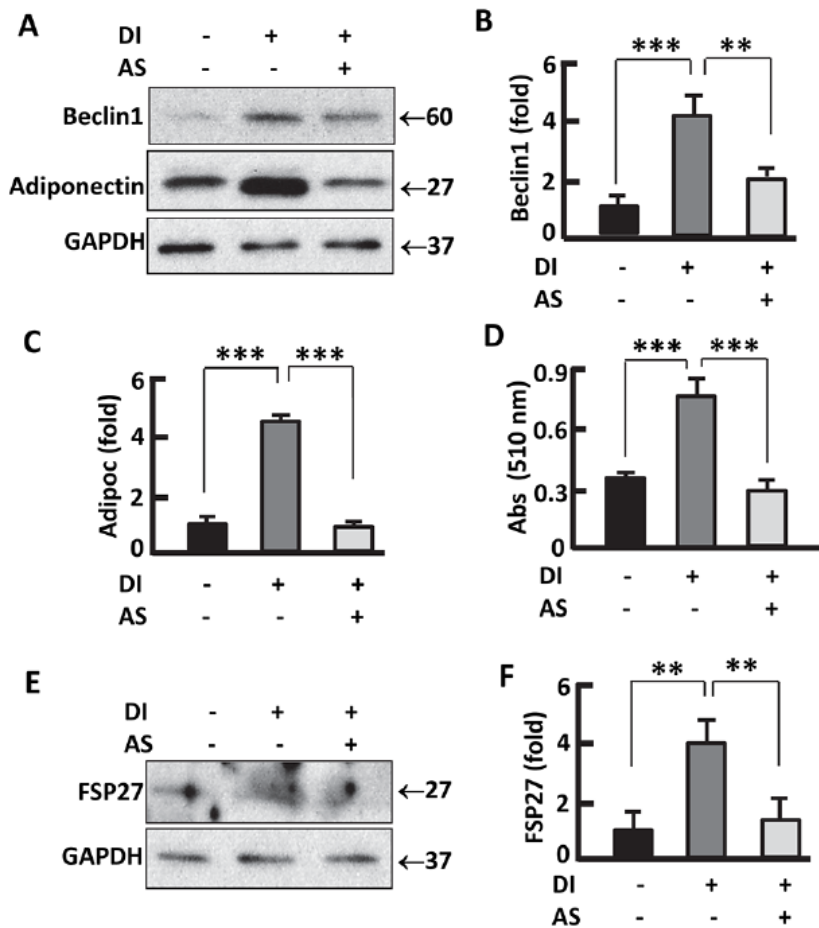


**Figure 5. FoxO1 inhibition suppressed SVF differentiation and autophagy.** (A-D) Treatment of SVF with FoxO1 inhibitor (AS1842856 at 0.1  $\mu$ M) suppressed autophagy (A, B) and preadipocyte differentiation (A, C, D). SVF was isolated and cultured as described in Materials and Methods, and AS1842856 treatment started on day 0 till the end of differentiation procedure. Western blot (A), densitometric analysis (B-C) and oil red O staining (D) were performed to analyze preadipocyte differentiation (A510, adiponectin) and autophagy (beclin 1) markers. (E-F) Western blot and densitometric analysis of FSP27 during SVF differentiation in the presence and absence of AS1842856. DI, differentiation induction; AS, AS1842856. Results are expressed as means  $\pm$  SD. \*\*,  $p < 0.01$ ; \*\*\*,  $p < 0.0001$ ,  $n = 3-5$ .

**Figure 6**

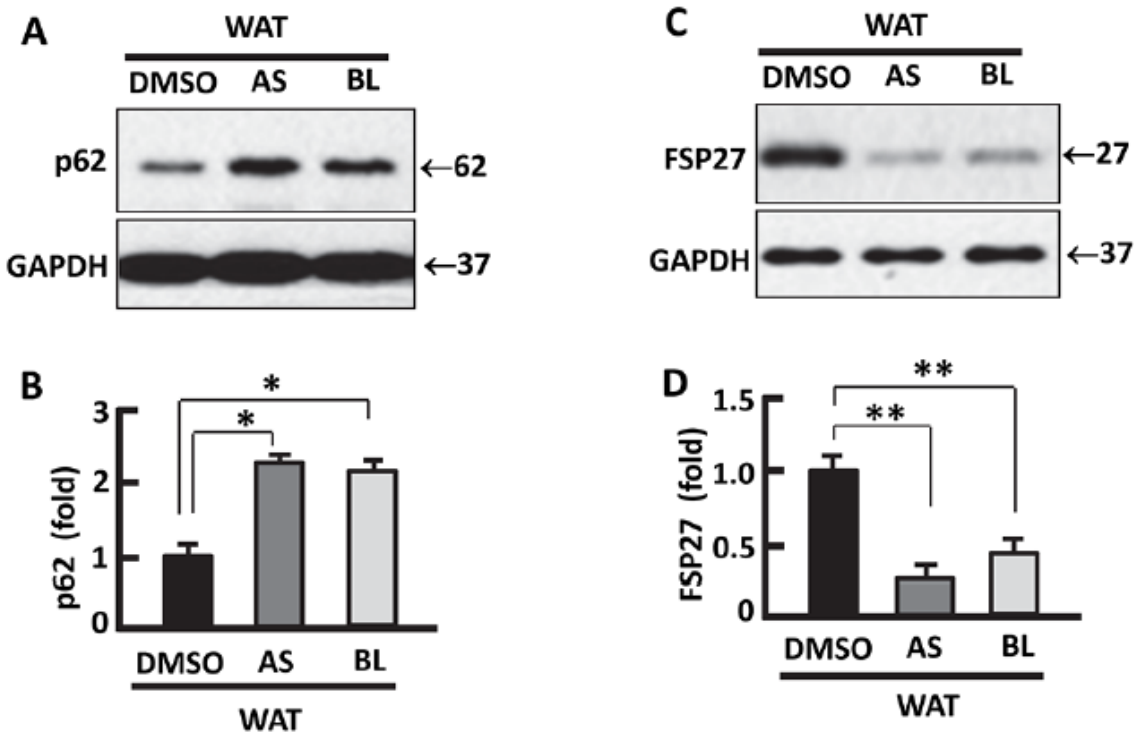


**Figure 6.** *Ex vivo* effects of silencing FoxO1-autophagy axis on FSP27 in white adipose tissue (WAT). (A-B) *Ex vivo* treatment of WAT with FoxO1 antagonist AS1842856 and autophagosome inhibitors BL suppressed autophagy activity (p62 degradation). (C-D) *Ex vivo* treatment of WAT with AS1842856 and BL downregulated FSP27 levels. Fresh WAT explants were processed as described in autophagy flux assay, and the tissue fragments were incubated for an additional 4 h in the presence of DMSO (control), AS1842856 (1  $\mu$ M), and bafilomycin-A1 (0.1  $\mu$ M) plus leupeptin (10  $\mu$ g/ml). Tissue lysates were prepared for p62 and FSP27 analysis by western blotting and densitometry. AS, AS1842856; BL, bafilomycin A1 + leupeptin. Results are expressed as means  $\pm$  SD. \*,  $p < 0.05$ ; \*\*,  $p < 0.001$ ;  $n = 3-5$ .

**Figure 1s**

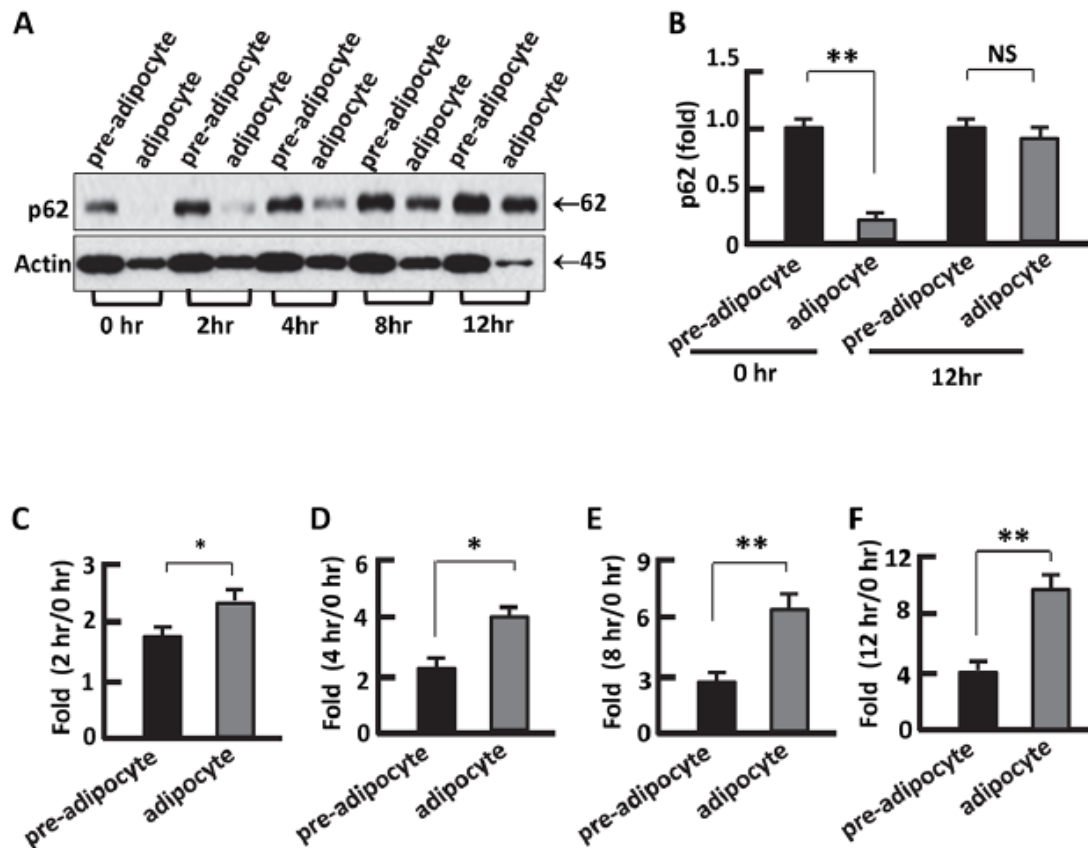


**Figure 1s. Analysis of autophagy flux in 3T3L1 preadipocytes and mature adipocytes. (A)**

Western blot analysis of p62 degradation by autophagy in the absence and presence of bafilomycin A1 (inhibitor of autophagosome acidification, at 0.1  $\mu$ M) and leupeptin (the inhibitor of lysosomal proteases, at 10  $\mu$ g/ml) for 0, 2, 4, 8, and 12 hr. (B) Densitometric analysis of western blot images indicated inhibition of autophagy by bafilomycin A1+ leupeptin at 12 hr prevented p62 decreasing in adipocytes, in comparison with 0-hr time point. (C-F) The rate of p62 accumulation at 2-hr, 4-hr, 8-hr and 12-hr in response to autophagy inhibition. Results are expressed as means  $\pm$  SD. \*,  $p < 0.05$ ; \*\*,  $p < 0.01$ , NS, not significant,  $n = 3-5$ .

## References

1. Ogden CL, Carroll MD, Kit BK, Flegal KM. Prevalence of childhood and adult obesity in the United States, 2011-2012. *JAMA* 2014; 311:806-14.
2. Liu L, Zou P, Zheng L, Linarelli LE, Amarell S, Passaro A, et al. Tamoxifen reduces fat mass by boosting reactive oxygen species. *Cell death & disease* 2015; 6:e1586.
3. Zou P, Liu L, Zheng L, Stoneman RE, Cho A, Emery A, et al. Targeting FoxO1 with AS1842856 suppresses adipogenesis. *Cell Cycle* 2014; 13:3759-67.
4. Cawley J, Meyerhoefer C. The medical care costs of obesity: an instrumental variables approach. *J Health Econ* 2012; 31:219-30.
5. Flegal KM, Kit BK, Orpana H, Graubard BI. Association of all-cause mortality with overweight and obesity using standard body mass index categories: a systematic review and meta-analysis. *JAMA* 2013; 309:71-82.
6. Wang QA, Tao C, Gupta RK, Scherer PE. Tracking adipogenesis during white adipose tissue development, expansion and regeneration. *Nat Med* 2013; 19:1338-44.
7. Cummins TD, Holden CR, Sansbury BE, Gibb AA, Shah J, Zafar N, et al. Metabolic remodeling of white adipose tissue in obesity. *American journal of physiology Endocrinology and metabolism* 2014; 307:E262-77.
8. Jansen HJ, van Essen P, Koenen T, Joosten LA, Netea MG, Tack CJ, et al. Autophagy activity is up-regulated in adipose tissue of obese individuals and modulates proinflammatory cytokine expression. *Endocrinology* 2012; 153:5866-74.
9. Ost A, Svensson K, Ruishalme I, Brannmark C, Franck N, Krook H, et al. Attenuated mTOR signaling and enhanced autophagy in adipocytes from obese patients with type 2 diabetes. *Mol Med* 2010; 16:235-46.
10. Kovsan J, Bluher M, Tarnovscki T, Kloting N, Kirshstein B, Madar L, et al. Altered autophagy in human adipose tissues in obesity. *J Clin Endocrinol Metab* 2011; 96:E268-77.
11. Nunez CE, Rodrigues VS, Gomes FS, Moura RF, Victorio SC, Bombassaro B, et al. Defective regulation of adipose tissue autophagy in obesity. *Int J Obes (Lond)* 2013; 37:1473-80.
12. Kosacka J, Kern M, Kloting N, Paeschke S, Rudich A, Haim Y, et al. Autophagy in adipose tissue of patients with obesity and type 2 diabetes. *Mol Cell Endocrinol* 2015; 409:21-32.
13. Haim Y, Bluher M, Slutsky N, Goldstein N, Kloting N, Harman-Boehm I, et al. Elevated autophagy gene expression in adipose tissue of obese humans: A potential non-cell-cycle-dependent function of E2F1. *Autophagy* 2015; 11:2074-88.
14. Kosacka J, Koch K, Gericke M, Nowicki M, Heiker JT, Kloting I, et al. The polygenetically inherited metabolic syndrome of male WOKW rats is associated with enhanced autophagy in adipose tissue. *Diabetology & metabolic syndrome* 2013; 5:23.
15. Singh R, Xiang Y, Wang Y, Baikati K, Cuervo AM, Luu YK, et al. Autophagy regulates adipose mass and differentiation in mice. *J Clin Invest* 2009; 119:3329-39.
16. Zhang Y, Goldman S, Baerga R, Zhao Y, Komatsu M, Jin S. Adipose-specific deletion of autophagy-related gene 7 (*atg7*) in mice reveals a role in adipogenesis. *Proc Natl Acad Sci U S A* 2009; 106:19860-5.

17. Baerga R, Zhang Y, Chen PH, Goldman S, Jin S. Targeted deletion of autophagy-related 5 (atg5) impairs adipogenesis in a cellular model and in mice. *Autophagy* 2009; 5:1118-30.
18. Zhang C, He Y, Okutsu M, Ong LC, Jin Y, Zheng L, et al. Autophagy is involved in adipogenic differentiation by repressing proteasome-dependent PPAR $\gamma$ 2 degradation. *American journal of physiology Endocrinology and metabolism* 2013; 305:E530-9.
19. Armani A, Cinti F, Marzolla V, Morgan J, Cranston GA, Antelmi A, et al. Mineralocorticoid receptor antagonism induces browning of white adipose tissue through impairment of autophagy and prevents adipocyte dysfunction in high-fat-diet-fed mice. *FASEB J* 2014; 28:3745-57.
20. Cheng Z, White MF. Targeting Forkhead box O1 from the concept to metabolic diseases: lessons from mouse models. *Antioxidants & redox signaling* 2011; 14:649-61.
21. Webb AE, Brunet A. FOXO transcription factors: key regulators of cellular quality control. *Trends Biochem Sci* 2014; 39:159-69.
22. Yamada E, Singh R. Mapping autophagy on to your metabolic radar. *Diabetes* 2012; 61:272-80.
23. Fullgrabe J, Klionsky DJ, Joseph B. The return of the nucleus: transcriptional and epigenetic control of autophagy. *Nature reviews Molecular cell biology* 2014; 15:65-74.
24. Yu X, Long YC, Shen HM. Differential Regulatory Functions of Three Classes of Phosphatidylinositol and Phosphoinositide 3-Kinases in Autophagy. *Autophagy* 2015:0.
25. Nagashima T, Shigematsu N, Maruki R, Urano Y, Tanaka H, Shimaya A, et al. Discovery of novel forkhead box O1 inhibitors for treating type 2 diabetes: improvement of fasting glycemia in diabetic db/db mice. *Mol Pharmacol* 2010; 78:961-70.
26. Kang R, Zeh HJ, Lotze MT, Tang D. The Beclin 1 network regulates autophagy and apoptosis. *Cell Death Differ* 2011; 18:571-80.
27. Klionsky DJ, Abdalla FC, Abeliovich H, Abraham RT, Acevedo-Arozena A, Adeli K, et al. Guidelines for the use and interpretation of assays for monitoring autophagy. *Autophagy* 2012; 8:445-544.
28. Mizushima N, Yoshimori T, Levine B. Methods in mammalian autophagy research. *Cell* 2010; 140:313-26.
29. Konige M, Wang H, Sztalryd C. Role of adipose specific lipid droplet proteins in maintaining whole body energy homeostasis. *Biochim Biophys Acta* 2014; 1842:393-401.
30. Nishino N, Tamori Y, Tateya S, Kawaguchi T, Shibakusa T, Mizunoya W, et al. FSP27 contributes to efficient energy storage in murine white adipocytes by promoting the formation of unilocular lipid droplets. *J Clin Invest* 2008; 118:2808-21.
31. Jambunathan S, Yin J, Khan W, Tamori Y, Puri V. FSP27 promotes lipid droplet clustering and then fusion to regulate triglyceride accumulation. *PloS one* 2011; 6:e28614.
32. Sun Z, Gong J, Wu H, Xu W, Wu L, Xu D, et al. Perilipin1 promotes unilocular lipid droplet formation through the activation of Fsp27 in adipocytes. *Nature communications* 2013; 4:1594.
33. Emont MP, Yu H, Jun H, Hong X, Maganti N, Stegemann JP, et al. Using a 3D Culture System to Differentiate Visceral Adipocytes In Vitro. *Endocrinology* 2015; 156:4761-8.
34. Aune UL, Ruiz L, Kajimura S. Isolation and differentiation of stromal vascular cells to beige/brite cells. *Journal of visualized experiments : JoVE* 2013.

35. Toh SY, Gong J, Du G, Li JZ, Yang S, Ye J, et al. Up-regulation of mitochondrial activity and acquirement of brown adipose tissue-like property in the white adipose tissue of fsp27 deficient mice. *PloS one* 2008; 3:e2890.
36. Zhou L, Park SY, Xu L, Xia X, Ye J, Su L, et al. Insulin resistance and white adipose tissue inflammation are uncoupled in energetically challenged Fsp27-deficient mice. *Nature communications* 2015; 6:5949.
37. Tanaka N, Takahashi S, Matsubara T, Jiang C, Sakamoto W, Chanturiya T, et al. Adipocyte-specific disruption of fat-specific protein 27 causes hepatosteatosis and insulin resistance in high-fat diet-fed mice. *J Biol Chem* 2015; 290:3092-105.
38. O-Sullivan I, Zhang W, Wasserman DH, Liew CW, Liu J, Paik J, et al. FoxO1 integrates direct and indirect effects of insulin on hepatic glucose production and glucose utilization. *Nature communications* 2015; 6:7079.
39. Titchenell PM, Chu Q, Monks BR, Birnbaum MJ. Hepatic insulin signalling is dispensable for suppression of glucose output by insulin in vivo. *Nature communications* 2015; 6:7078.
40. Lu M, Wan M, Leavens KF, Chu Q, Monks BR, Fernandez S, et al. Insulin regulates liver metabolism in vivo in the absence of hepatic Akt and Foxo1. *Nat Med* 2012; 18:388-95.
41. Cheng Z, Guo S, Copps K, Dong X, Kollipara R, Rodgers JT, et al. Foxo1 integrates insulin signaling with mitochondrial function in the liver. *Nat Med* 2009; 15:1307-11.
42. Dong XC, Copps KD, Guo S, Li Y, Kollipara R, DePinho RA, et al. Inactivation of hepatic Foxo1 by insulin signaling is required for adaptive nutrient homeostasis and endocrine growth regulation. *Cell Metab* 2008; 8:65-76.
43. Munekata K, Sakamoto K. Forkhead transcription factor Foxo1 is essential for adipocyte differentiation. *In Vitro Cell Dev Biol Anim* 2009; 45:642-51.
44. Higuchi M, Dusting GJ, Peshavariya H, Jiang F, Hsiao ST, Chan EC, et al. Differentiation of human adipose-derived stem cells into fat involves reactive oxygen species and Forkhead box O1 mediated upregulation of antioxidant enzymes. *Stem cells and development* 2013; 22:878-88.
45. Rutkowski JM, Stern JH, Scherer PE. The cell biology of fat expansion. *J Cell Biol* 2015; 208:501-12.
46. Cheng Z. FoxO1: mute for a tuned metabolism? *Trends in endocrinology and metabolism: TEM* 2015; 26:402-3.
47. Cheng Z, White MF. The AKTion in non-canonical insulin signaling. *Nat Med* 2012; 18:351-3.
48. Deutsch MJ, Schriever SC, Roscher AA, Ensenaer R. Digital image analysis approach for lipid droplet size quantitation of Oil Red O-stained cultured cells. *Anal Biochem* 2014; 445:87-9.

## **Chapter 4 FoxO1 interacts with transcription factor EB and differentially regulates mitochondrial uncoupling proteins via autophagy in adipocytes**

Longhua Liu,<sup>1</sup> Zhipeng Tao,<sup>1</sup> Louise D. Zheng,<sup>1</sup> Joseph Brooke,<sup>1</sup> Cayleen Smith,<sup>1</sup> Dongmin Liu,<sup>1</sup> Yun-Chau Long,<sup>2</sup> Zhiyong Cheng<sup>1\*</sup>

<sup>1</sup> Department of Human Nutrition, Foods and Exercise, Fralin Life Science Institute, College of Agriculture and Life Science, Virginia Tech, Blacksburg, Virginia, USA.

<sup>2</sup> Department of Biochemistry, Yong Loo Lin School of Medicine, National University of Singapore, Singapore.

Correspondence: Dr. Zhiyong Cheng, 1981 Kraft Drive, Blacksburg, VA 24061, USA. Phone: (540) 231 9445; Fax: (540) 231 5522; email: [zcheng@vt.edu](mailto:zcheng@vt.edu).

---

**This chapter has been published in *Cell Death Discovery* (2016) 2, 16066.**

**Abstract:** Mitochondrial uncoupling proteins (UCPs) are inducible and play an important role in metabolic and redox homeostasis. Recent studies have suggested that FoxO1 controls mitochondrial biogenesis and morphology, but it remains largely unknown how FoxO1 may regulate mitochondrial UCPs. Here we show that FoxO1 interacted transcription factor EB (Tfeb), a key regulator of autophagosome and lysosome, and mediated the expression of UCP1, UCP2 and UCP3 differentially via autophagy in adipocytes. UCP1 was downregulated but UCP2 and UCP3 were upregulated during adipocyte differentiation, which was associated with increased Tfeb and autophagy activity. However, inhibition of FoxO1 suppressed Tfeb and autophagy, attenuating UCP2 and UCP3 but increasing UCP1 expression. Pharmacological blockage of autophagy recapitulated the effects of FoxO1 inhibition on UCPs. Chromatin immunoprecipitation assay demonstrated that FoxO1 interacted with Tfeb by directly binding to its promoter, and silencing FoxO1 led to drastic decrease in Tfeb transcript and protein levels. These data provide the first line of evidence that FoxO1 interacts with Tfeb to regulate autophagy and UCP expression in adipocytes. Dysregulation of FoxO1 → autophagy → UCP pathway may account for metabolic changes in obesity.

**Keywords:** FoxO1, autophagy, mitochondrial uncoupling protein, adipocyte, Tfeb

## **Introduction**

Obesity is one of the most pressing health concerns in the US.<sup>1-3</sup> The growing epidemic of obesity has been attributed largely to modern lifestyle characteristic of energy overconsumption and physical inactivity.<sup>3,4</sup> As such, the strategies limiting energy intake or increasing energy expenditure have been proposed for obesity prevention.<sup>3-5</sup> Mitochondria play a central role in cellular energy homeostasis.<sup>3,6-8</sup> In particular, induction of mitochondrial uncoupling protein (UCP) in mice promotes energy dissipation and protects against obesity, while genetic UCP deficiency causes obesity.<sup>5,9,10</sup> In line with these findings, UCP polymorphisms have been increasingly reported in obese humans,<sup>11,12</sup> and adipose UCP gene expression is significantly lower in morbidly obese people than in lean individuals.<sup>13</sup> These studies suggest that dysregulation of UCPs contributes to development of obesity, and understanding the mechanism of regulation of UCPs in adipocytes may lead to new options for obesity prevention and treatment.

UCPs are a family of mitochondrial transporters (or mitochondrial anion carriers) in the inner membrane.<sup>14,15</sup> In adipocytes or adipose tissue, three isoforms of UCP have been identified, UCP1, UCP2, and UCP3, although their expression levels vary.<sup>14-18</sup> UCP1 is primarily expressed in brown adipose tissue, and it uncouples mitochondrial respiration from ATP production/oxidative phosphorylation, dissipating energy in the form of heat.<sup>14,15</sup> Under certain conditions (e.g., cold exposure), UCP1 expression in white adipocytes can be significantly induced, leading to a browning phenotype.<sup>17</sup> UCP2 and UCP3 share amino acid identity with UCP1 (59% and 57%, respectively), and their function in mitochondrial uncoupling is still under

investigation.<sup>14, 15, 18</sup> Although some studies suggested that UCP2 and UCP3 were proton channels like UCP1, others regarded them as ion channels that limit the production of reactive oxygen species, and export toxic fatty acid anions and peroxides from mitochondrial matrix.<sup>14, 15, 18, 19</sup>

FoxO1 is a transcription factor that regulates mitochondrial function and adipocyte differentiation.<sup>2, 20-23</sup> Activation of FoxO1 in the liver alters mitochondrial biogenesis, morphology and function in the insulin resistant mice, while genetic ablation of FoxO1 significantly normalizes mitochondria and metabolism.<sup>21, 24</sup> In adipocytes, silencing FoxO1 with specific antagonist or siRNA potently inhibits cell differentiation and lipid accumulation, accompanied with changes in expression of mitochondrial respiration chain proteins.<sup>2, 22, 23</sup> Recently we found that FoxO1 controlled lipid droplet growth and adipose autophagy, the cellular process that has been implicated in adipocyte differentiation.<sup>25-29</sup> Moreover, genetic and pharmacologic inhibition of autophagy leads to browning of white adipose tissue, characteristic of increased UCP1 expression.<sup>26-29</sup> However, it is unknown how mechanistically FoxO1 regulates autophagy and other UCPs (i.e., UCP2 and UCP3). In the present work, we show that FoxO1-mediated autophagy upregulates UCP2 and UCP3 in adipocytes but downregulates UCP1. Mechanistically, FoxO1 interacted with transcription Factor EB (Tfeb), a key regulator of autophagosome and lysosome,<sup>30</sup> by directly binding to the promoter and regulating its expression.

## Results

### **Expression patterns of UCPs during adipocyte differentiation.**

Following an established protocol, we cultured 3T3-L1 pre-adipocytes and induced cell differentiation.<sup>2, 31</sup> Maturation of adipocytes was paralleled with significant lipid accumulation as measured by oil red O staining and spectrophotometric reading at 510 nm (Figure 1, A-B).<sup>2, 32, 33</sup> Interestingly, the expression of UCP1, UCP2 and UCP3 showed distinctive kinetics during adipocyte differentiation (Figure 1, C-E). In contrast to UCP1 that underwent downregulation (Figure 1, C), UCP2 and UCP3 were upregulated drastically (Figure 1, D-E). These data support the notion that upregulation of UCP1 counteracts lipid accumulation in adipocytes,<sup>34, 35</sup> and add evidence to the hypothesis that UCP2 and UCP3 are required for lipid metabolism.<sup>14, 15, 19, 36</sup>

### **Inhibition of FoxO1 suppressed the coordinated expression of UCPs in adipocytes.**

FoxO1 regulates mitochondrial morphology and biogenesis,<sup>21, 24</sup> but it remains largely unknown how FoxO1 is related to mitochondrial UCPs. Upon inhibiting FoxO1 with a specific antagonist AS1842856,<sup>2, 37</sup> we found that the coordinated expression of UCP1, UCP2 and UCP3 was significantly disturbed in 3T3-L1 cells (Figure 2). A 3-fold increase in UCP1 expression was induced by the treatment with AS1842856 ( $p < 0.001$ ; Figure 2, A). By contrast, inhibition of FoxO1 markedly reduced the expression of UCP2 (by 58%,  $p < 0.0001$ ; Figure 2, B) and UCP3 (by 87%,  $p < 0.0001$ ; Figure 2, C). These changes were associated with a drastic suppression of adipocyte differentiation, leading to about 50% reduction of lipid accumulation in the adipocytes

( $p < 0.001$ ) (Figure 2, D). In addition, AS1842856 resulted in marked inhibition of autophagy (Figure 2, E, F; Figure 1s). Given that UCP1 can be regulated by modulation of autophagy,<sup>26-29</sup> the inhibition of autophagy by AS1842856 may account for the altered UCPs in the adipocytes.

### **Suppression of autophagy recapitulated the effects of silencing FoxO1 on UCPs.**

To examine the role of autophagy in UCP regulation, we measured kinetics of autophagy during adipogenesis (Figure 3, Figure 1s). Adipocyte differentiation was accompanied with a gradual downregulation of p62 (Figure 3 A-C), the protein that was exclusively degraded by autophagy.<sup>25, 38, 39</sup> This change was concurrent with upregulation of Tfeb (Figure 3 A-B), the transcription factor shown to regulate both autophagosome and lysosome,<sup>30</sup> supporting the notion that autophagy is induced during adipogenesis.<sup>25, 28, 40</sup> To test if autophagy contributed to the coordinated expression of UCPs, we blocked autophagy in adipocytes using bafilomycin-A1 and leupeptin, the established inhibitors of autophagosome acidification and lysosomal proteases, respectively.<sup>25, 38, 39</sup> As expected, bafilomycin-A1 and leupeptin potently attenuated autophagy thereby increasing p62 abundance (Figure 1s). Intriguingly, inhibition of autophagy significantly increased UCP1 transcript (by 2.2-fold,  $p < 0.001$ ) but reduced the expression of UCP2 (by 38%,  $p < 0.01$ ) and UCP3 (by 89%,  $p < 0.001$ ) in adipocytes (Figure 3, D-F), concomitant with suppression of adipogenesis (Figure 3, G). These data recapitulated the effects of silencing FoxO1 on UCPs during adipocyte differentiation (Figure 2), thereby underlining the importance of FoxO1-autophagy axis in the coordinated expression of UCP1, UCP2 and UCP3.

### **Distribution and activity of nuclear FoxO1 was upregulated in differentiating**

**adipocytes.** Nuclear distribution and activity of FoxO1 as a transcription factor is regulated by insulin-induced phosphorylation.<sup>8, 41</sup> To examine how insulin present in the differentiation media affects FoxO1 distribution and activity, we measured total FoxO1 protein level and phosphorylated FoxO1 during adipocyte differentiation (Figure 4, A-B). Intriguingly, FoxO1 underwent drastic upregulation during the cell differentiation, which significantly outweighed insulin-induced FoxO1 phosphorylation (Figure 4, A). Indeed, densitometric analysis of western blot images confirmed that un-phosphorylated FoxO1 was increased during adipocyte differentiation, indicative of an increased distribution of nuclear FoxO1 (Figure 4, B). To further validate this, we isolated nuclear fractions from preadipocytes (day 0), differentiating adipocytes (day 6), and differentiated adipocytes (day 12) for activity analysis. As shown in Figure 4 C, FoxO1 activity was upregulated by 1.9-fold ( $p < 0.01$ ) and 1.5-fold ( $p < 0.01$ ) in the nuclear fractions from differentiating adipocytes and differentiated adipocytes, respectively, in comparison with that from preadipocytes. Therefore, nuclear distribution and FoxO1 activity was overtly increased during adipogenesis.

### **FoxO1 regulated Tfeb by directly binding to its promoter.**

Tfeb has been shown to regulate both autophagosome and lysosome.<sup>30</sup> Because Tfeb protein level and FoxO1 activity were coincidentally upregulated during adipocyte differentiation (Figures 3-4), we asked whether Tfeb underwent transcriptional elevation during adipogenesis. By

conducting qPCR analysis we found that Tfeb transcript was upregulated by 3.1-fold ( $p < 0.001$ ) and 2.5-fold ( $p < 0.001$ ) on day 6 and day 12, respectively (Figure 5A). Intriguingly, inhibition of FoxO1 led to significant suppression of Tfeb transcript (Figure 5B-C), accompanied with reduced abundance of Tfeb protein (Figure 5D). These results strongly suggest that FoxO1 is an upstream regulator of Tfeb. To examine whether FoxO1 interacts with Tfeb directly, we analyzed the promoter sequence in mouse Tfeb gene (gene ID 21425) and conducted chromatin immunoprecipitation (ChIP) assay. As shown in Figure 5E, the promoter of Tfeb bears 3 insulin response elements (IRE), the specific binding sites for FoxO1 to interact with target genes.<sup>21, 41</sup> In addition, the abundance of Tfeb promoter bound to FoxO1 was higher in mature adipocytes than in preadipocytes (Figure 5F), in line with the increased distribution and activity of nuclear FoxO1 (Figure 4). However, FoxO1 antagonist AS1842856 significantly reduced the abundance of Tfeb promoter bound to FoxO1 (Figure 5 B,F). Therefore, FoxO1 directly regulates Tfeb gene expression through protein-DNA interaction.

## **Discussion**

FoxO1 and Tfeb have been implicated in autophagy regulation,<sup>25, 30, 42, 43</sup> but the interaction between these two transcription factors has not been reported. In this study we found that Tfeb was upregulated during adipocyte differentiation (Figure 3), concomitant with increased distribution and activity of nuclear FoxO1 (Figure 4). Importantly, FoxO1 directly bound to the promoter of Tfeb to achieve a transcriptional regulation (Figure 5). Inhibition of FoxO1 reduced both Tfeb transcript level and protein abundance, accompanied with downregulation of autophagy (Figure 5). Moreover, blockage of FoxO1-autophagy axis led to dysregulation of

UCPs and suppressed adipocyte differentiation (Figures 1-3), suggesting that FoxO1-mediated autophagy is critical for coordinated expression of UCP1, UCP2, and UCP3 during adipogenesis. To our knowledge, this is the first line of evidence demonstrating the regulation of UCP2 and UCP3 by autophagy and its relation with FoxO1.

The differential UCP expression patterns during adipogenesis support the notion that UCP2 and UCP3 function differently from UCP1.<sup>14, 15, 18, 19</sup> UCP1 was gradually downregulated during adipocyte differentiation (Figure 1), but inhibition of the FoxO1-autophagy axis upregulated UCP1 and significantly reduced lipid accumulation (Figures 2-3). It suggests that FoxO1-autophagy axis acts as a suppressor of UCP1, the physiological role of which may reside in preserving carbon flux and favoring lipid synthesis for adipocyte maturation. Indeed, adipocytes overexpressing UCP1 showed impairment of oxidative phosphorylation but stimulation of glycolysis and lactate production, which directs carbon flux away from lipid synthesis and prevents lipid accumulation and adipocyte maturation.<sup>34, 35</sup> On the other hand, FoxO1-autophagy axis appeared to be an inducer of UCP2 and UCP3 and promote adipogenesis (Figures 2-3). Given that UCP2 and UCP3 regulated reactive oxygen species and lipid peroxide,<sup>18, 19, 44</sup> the FoxO1-autophagy-UCP2/UCP3 axis may serve to maintain redox and lipid homeostasis that is critical for adipocyte differentiation.<sup>23, 45</sup> To this end, silencing of FoxO1 disturbs redox balance and prevents preadipocyte differentiation.<sup>23</sup>

The downstream pathway by which the FoxO1-autophagy axis differentially regulates UCPs remains to be defined. Although we cannot rule out the possibility that FoxO1 might directly regulate transcription of UCP genes, targeting FoxO1 or autophagy led to similar effects on UCP expression (Figures 2-3), corroborating an important role of the FoxO1 → autophagy cascade in

UCP regulation. Previous study suggested that suppression of autophagy by deleting Atg7 in skeletal muscle or liver promoted secretion of fibroblast growth factor 21 (FGF21), which in turn induced UCP1 in adipose tissue.<sup>46</sup> Also, it was shown that suppression of autophagy reduced the stability of peroxisome proliferator-activated receptors  $\gamma$  (PPAR $\gamma$ ),<sup>40</sup> the key regulator of adipogenesis that also mediates UCP2 and UCP3 expression.<sup>2, 18</sup> To this end, we found that targeting the FoxO1-autophagy axis with inhibitors significantly reduced PPAR $\gamma$  level,<sup>25</sup> which may account for the downregulation of UCP2 and UCP3 (Figures 2-3). Thus, future study examining the role of FGF21 and PPAR $\gamma$  in the regulatory network of FoxO1-autophagy axis will be of interest.

Taken together, our study demonstrates for the first time that FoxO1 induces Tfeb by binding to its promoter, and FoxO1-autophagy axis differentially regulates UCP1, UCP2, and UCP3 in adipocytes. Given obesity is linked to dysregulation of FoxO1,<sup>2, 41</sup> autophagy,<sup>38, 47-49</sup> and UCPs,<sup>5, 10-12</sup> further studies to establish the molecular mechanism and physiologic function of the FoxO1-autophagy-UCPs axis will be of critical importance to treat obesity and its related metabolic disorders.

## **Materials and methods**

### **Materials**

3T3-L1 preadipocytes (ATCC<sup>®</sup> CL-173<sup>™</sup>) were purchased from ATCC (Manassas, VA).

Dulbecco's modified Eagle's (DMEM) medium was from Corning Inc (Manassas, VA). Fetal bovine serum (FBS) was from GeneMate (Kaysville, UT). Dexamethasone, 3-isobutyl-1-

methylxanthine (IBMX) and rosiglitazone were purchased from Cayman Chemical (Ann Arbor, MI). Penicillin/streptomycin (P/S) was from GE Healthcare Life Sciences HyClone Laboratories (Logan, UT). Insulin was from Sigma-Aldrich (St. Louis, MO). FoxO1 inhibitor AS1842856 was from EMD Millipore (San Diego, CA). Autophagy inhibitors bafilomycin A1 and leupeptin were from LC Laboratories (Woburn, MA) and DOT Scientific Inc (Burton, MI), respectively.

### **Cell culture and treatment**

3T3-L1 preadipocytes were cultured as previously described.<sup>2,31</sup> Briefly, the cells were cultured in basal media (DMEM media supplemented with 10% FBS, 100 units/ml penicillin and 100 µg/ml streptomycin (1 × P/S)), at 37 °C in a humidified atmosphere of 5% CO<sub>2</sub>. The media were replaced every 2 days. 3T3-L1 preadipocytes were grown to confluence (day 0), and further maintained in fresh basal media for 2 days (days 1–2). At the end of day 2, the medium was changed to differentiation medium I: DMEM supplemented with 10% FBS, P/S (1 ×), IBMX (0.5 mM), dexamethasone (1 µM), insulin (1 µg/ml), and rosiglitazone (2 µM). At the end of day 4, the medium was changed to differentiation medium II: DMEM supplemented with 10% FBS, P/S (1 ×), and insulin (1 µg/ml). At the end of day 6, the medium was changed back to basal media, and the cells were maintained in basal medium (fresh basal medium was supplied every 2 days) until fully differentiated (day 12). Control preadipocytes were maintained in basal media and supplied with fresh medium every other day till day 12. Treatments with inhibitors (e.g., AS1842856 or bafilomycin A1 plus leupeptin) started on day 0 through day 12 (during differentiation) at the indicated concentrations.

## **Measurement of lipid accumulation in adipocytes**

Lipid accumulation in adipocytes was measured by oil red O staining.<sup>2, 25</sup> The oil red O working solution was freshly prepared by mixing 0.35% stock solution with dH<sub>2</sub>O (6:4) and filtered, and the staining was conducted on day 0, day 6, day 12 as described.<sup>2, 25</sup> Briefly, the media were removed and the cells were washed once with phosphate buffered saline (PBS), and fixed in 4% formaldehyde at room temperature for 10 minutes. Subsequently, the cells were washed once with dH<sub>2</sub>O, once with 60% isopropanol, and air dried. Oil red O working solution was added and the staining lasted for 1 hour at room temperature. Afterwards, the stained cells were washed with dH<sub>2</sub>O for 4 times, and oil red O retained in the cells was extracted with isopropanol, and quantified by the absorbance at 500 nm on a Synergy™ H4 Hybrid Multi-Mode Microplate Reader (BioTek Instruments, Inc).

## **RNA extraction and cDNA synthesis**

RNAs were extracted from cells with RNeasy Mini Kits (Qiagen) according to the manufacturer's instruction. The RNA samples were used to synthesize cDNA by reverse transcription PCR using iScript™ cDNA Synthesis Kits (BioRad) according to the manufacturer's instruction.

## Real time PCR

Gene expression was analyzed by quantitative real time PCR on a ViiA™ 7 Real-Time PCR System (Life Technology, Grand Island, NY, USA).<sup>1</sup> The primers used in this study were 5'-CAG CTT GCC TGG CAG ATA TCA-3' (forward) and 5'-TTG GAT CTG AAG GCG GAC TT-3' (reverse) for UCP1; 5'-TCT GCC CAG TCC CAT TCT CT-3' (forward) and 5'-GGG AGG TGA GGT GGG AAG TAA-3' (reverse) for UCP2; 5'-ACC TCC ATA GGC AGC AAA GGA-3' (forward) and CGG AGG GCT GAA GTC CAA (reverse) for UCP3; 5'-CCC TGC CAT TGT TAA GAC C-3' (forward) and 5'-TGC TGC TGT TCC TGT TTT C-3' (reverse) for Ppargc1 $\alpha$ ; 5'-CCA CCC CAG CCA TCA ACA C-3' (forward) and 5'-CAG ACA GAT ACT CCC GAA CCT T-3' (reverse) for Tfeb; and 5'-ACAGTCCATGCCATCACTGCC-3' (forward) and 5'-GCCTGCTTCACCACCTTCTTG-3' (reverse) for GAPDH as a reference gene.

## ChIP assay

ChIP assay was performed with an EZ-Magna ChIP A/G Chromatin Immunoprecipitation Kit (EMD Millipore, cat # 17-10086) as described previously.<sup>21</sup> Briefly, the cell culture was treated with 1% formaldehyde for 10 minutes, and the crosslinking reactions was stopped by adding glycine to a final concentration of 125mM and incubating for 5 minutes at room temperature. Then the cells were rinsed with PBS, harvested in lysis buffer, and incubate for 15 minutes. DNA was sheared and immunoprecipitation was conducted with a ChIP-grade anti-FoxO1 antibody (ab39670) from Abcam as described previously.<sup>21</sup> Primers used to amplify the promoter of Tfeb were 5'-CCCCAAGTGGAAGTTGCTAA-3' (forward) and 5'-

ATGGCCCGTGATATGACTTT-3' (reverse). PCR products were resolved by electrophoresis on 2.5% agarose gel.

### **Measurement of nuclear FoxO1 activity**

Nuclear fractions were isolated from cells using a TransAM<sup>®</sup> Nuclear Extract Kit (Active Motif, cat # 40010), and FoxO1 activities were determined using a TransAM<sup>®</sup> FKHR (FOXO1) Transcription Factor ELISA Kits (Active Motif, cat # 46396) according to the manufacturer's instructions.

### **Western blotting**

To prepare cell lysates, the cells were washed with ice-cold PBS and homogenized using a Bullet Blender (Next Advance, Averill Park, NY, USA) in PLC lysis buffer (30 mM HEPES, pH 7.5, 150 mM NaCl, 10% glycerol, 1% Triton X-100, 1.5 mM MgCl<sub>2</sub>, 1 mM EGTA, 10 mM NaPPi, 100 mM NaF, 1 mM Na<sub>3</sub>VO<sub>4</sub>) supplemented with protease inhibitor cocktail (Roche), 1 mM PMSF.<sup>2, 31</sup> Total protein concentrations of the lysates were determined using the DC protein assay (Bio-Rad). Western blotting and image analysis were conducted as described previously.<sup>2,</sup>

<sup>31</sup> Antibody information: GAPDH (MA5-15738) and  $\beta$ -actin (MA5-15739) antibodies from Pierce (Rockford, IL, USA); antibodies against FoxO1 (9454s), phospho-FoxO1 (Thr24) antibody (9464s), LC3 (2775s) and p62 (SQSTM1, 5114S) from Cell Signaling Technology (Beverly, MA, USA); Tfeb (A303-673A) antibody from Bethyl Laboratories, Inc. (Montgomery, TX, USA).

## **Statistical analyses**

All results were expressed as mean  $\pm$  Standard Deviation (SD), and underwent analysis of variance (ANOVA) to determine p values;  $p < 0.05$  was considered statistically significant.

## **Acknowledgements**

This work was supported, in part, by USDA National Institute of Food and Agriculture Hatch Project 1007334 (ZC) and NIH grant 1R01AT007077 (DL). Work in YCL lab was supported by grants Singapore Ministry of Education Academic Research Fund (T1-2011 Sep-05 and T1-2014 Apr -05).

## **Conflicts of interest**

None disclosed.

## **Abbreviations:**

AS or AS1842856: 5-amino-7-(cyclohexylamino)-1-ethyl-6-fluoro-4-oxo-1,4-dihydroquinoline-3-carboxylic acid;

Atg7: autophagy related 7

ATP: adenosine triphosphate

BL: bafilomycin-A1 and leupeptin

ChIP: chromatin immunoprecipitation

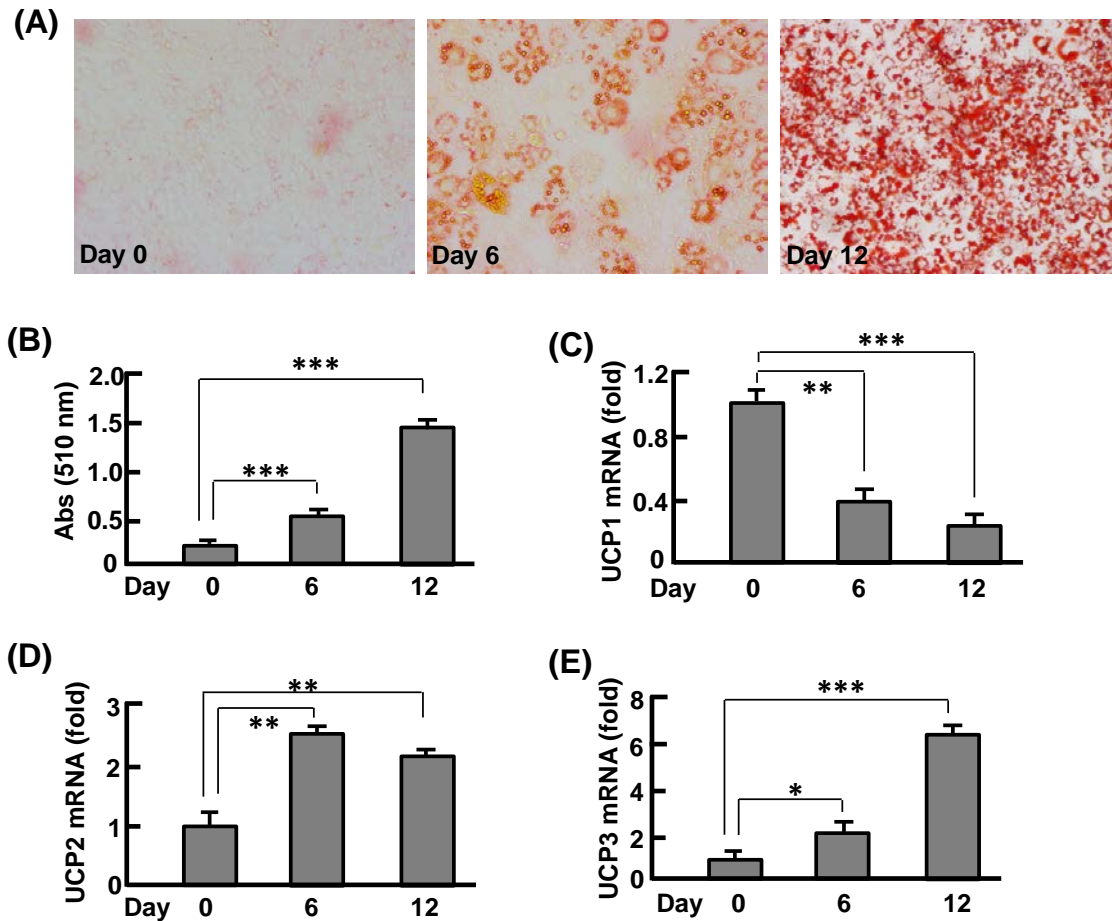
DI: differentiation induction

FBS: fetal bovine serum

FoxO1: forkhead box O1  
FGF21: fibroblast growth factor 21  
GAPDH: glyceraldehyde 3-phosphate dehydrogenase  
LC3: microtubule-associated protein 1A/1B-light chain 3-phosphatidylethanolamine conjugate  
p62: sequestosome 1 (SQSTM1)  
PPAR $\gamma$ : peroxisome proliferator-activated receptor gamma  
qPCR: quantitative polymerase chain reaction  
Tfeb: transcription factor EB  
UCP: uncoupling protein

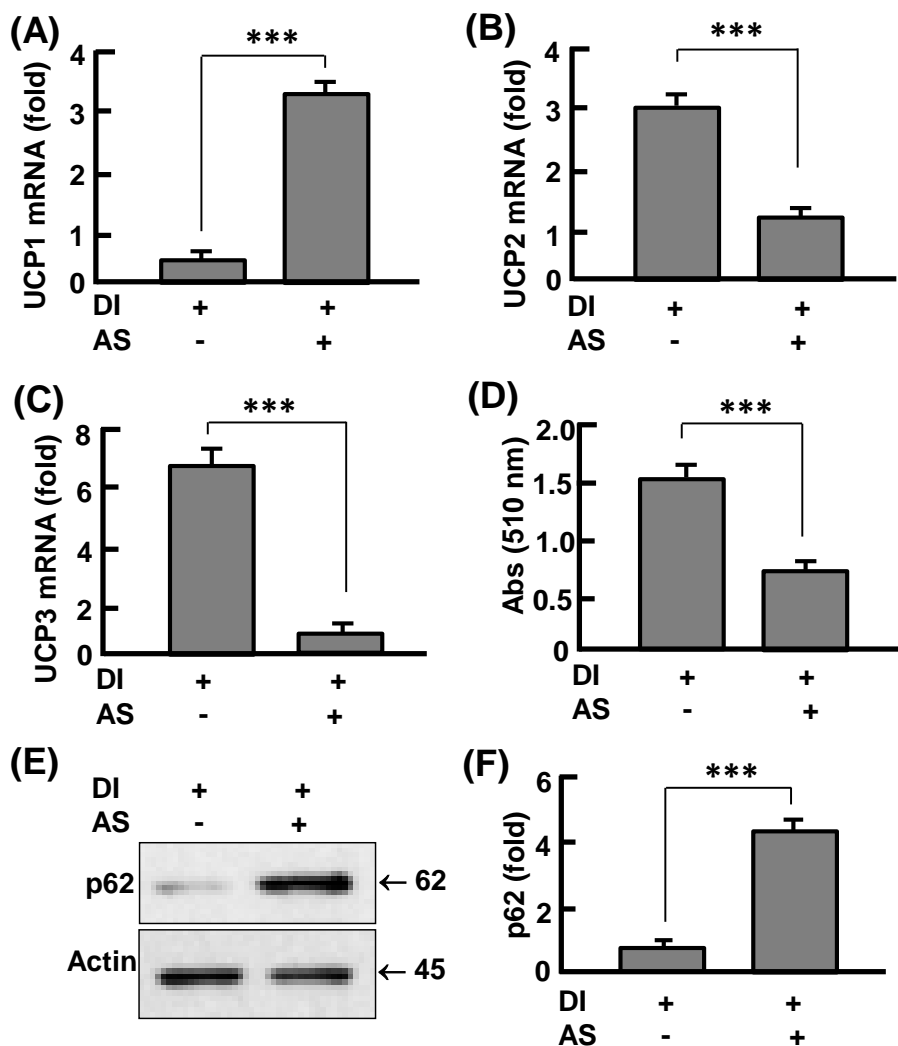
## Figures

**Figure 1**

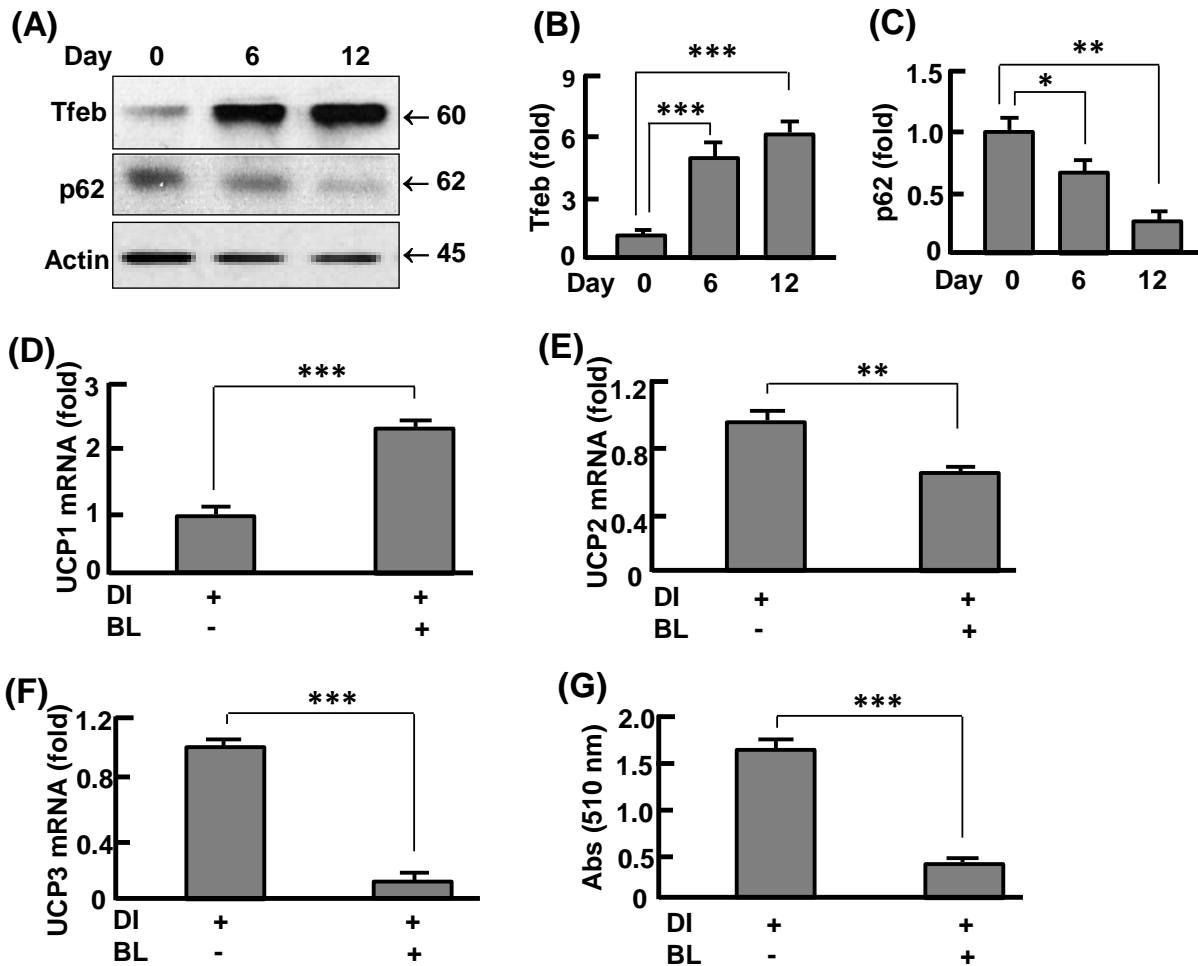


**Figure 1. Expression of UCPs during 3T3-L1 adipocyte differentiation.** (A-B) Measurement of lipid accumulation during adipocyte differentiation. The cells were cultured and differentiated as described in Materials and Methods, and lipid accumulation was measured by oil red O staining (A) and absorbance at 510 nm (B). (C-D) qPCR analysis of UCP1 (C), UCP2 (D), and UCP3 (E) during adipocyte differentiation. Results were presented as mean  $\pm$  SD; n=3-4; \*, p<0.05; \*\*, p<0.01; \*\*\*, p<0.001.

**Figure 2**



**Figure 2. Effects of FoxO1 inhibition on UCPs and autophagy.** (A) Inhibition of FoxO1 upregulated UCP1. (B) Inhibition of FoxO1 down-regulated UCP2. (C) Inhibition of FoxO1 down-regulated UCP3. (D) Inhibition of FoxO1 prevented lipid accumulation in adipocytes. (E-F) Inhibition of FoxO1 attenuated autophagy (p62 degradation). The cells were cultured and treated (days 0-12) as described in Materials and Methods. DI, differentiation induction; AS, AS1842856 (0.1  $\mu$ M). Results were presented as mean  $\pm$  SD; n=3-4; \*\*, p<0.01; \*\*\*, p<0.001.

**Figure 3**

**Figure 3. Autophagy was required for coordinated expression of UCPs in adipocytes.** (A-C) Western blot (A) and densitometric (B-C) analysis of Tfeb and p62 suggested that autophagy was upregulated during adipocyte differentiation. (D) Effects of autophagy inhibitors bafilomycin A1 and leupeptin on UCP1 expression. (E) Effects of bafilomycin A1 and leupeptin on UCP2 expression. (F) Effects of bafilomycin A1 and leupeptin on UCP3 expression. (G) Effects of bafilomycin A1 and leupeptin on lipid accumulation. The cells were cultured and treated as described in Materials and Methods, and the treatment with autophagy inhibitors was conducted on days 0-12. DI, differentiation induction; BL, bafilomycin A1 (4 nM) and leupeptin (0.4  $\mu$ g/ml). Results were presented as mean  $\pm$  SD; n=3-4; \*, p<0.05; \*\*, p<0.01; \*\*\*, p<0.001.

**Figure 4**

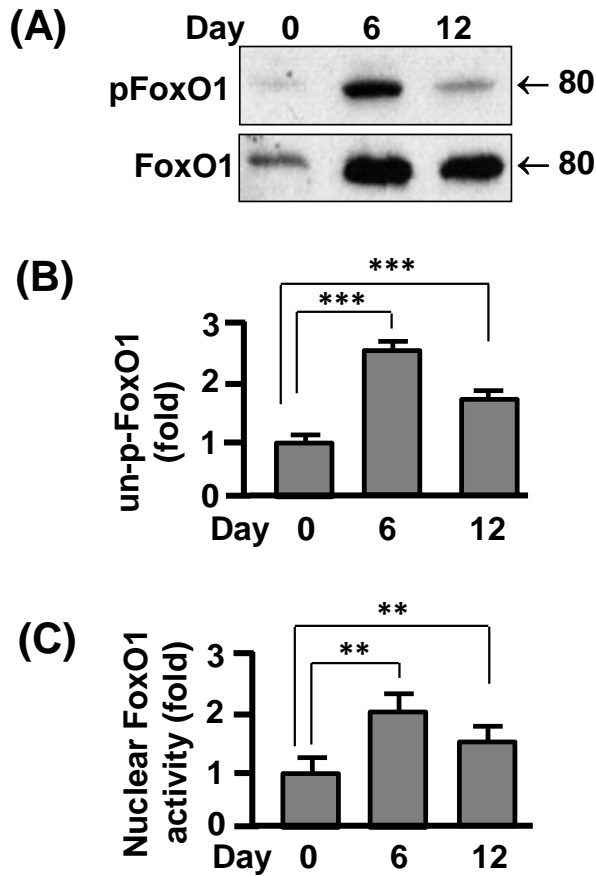


**Figure 4. Distribution and activity of nuclear FoxO1 increased during adipogenesis.** (A) Western blot analysis of total FoxO1 and phosphorylated FoxO1 (pFoxO1) during 3T3-L1 adipocyte differentiation. (B) Measurement of un-phosphorylated (or nuclear) FoxO1 (un-p-FoxO1) by densitometric analysis of western blot images. (C) Measurements of FoxO1 activity in the nuclear fractions isolated from adipocytes on days 0, 6 and 12 during differentiation. Results were presented as mean  $\pm$  SD; n=3-4; \*\*, p<0.01; \*\*\*, p<0.001.

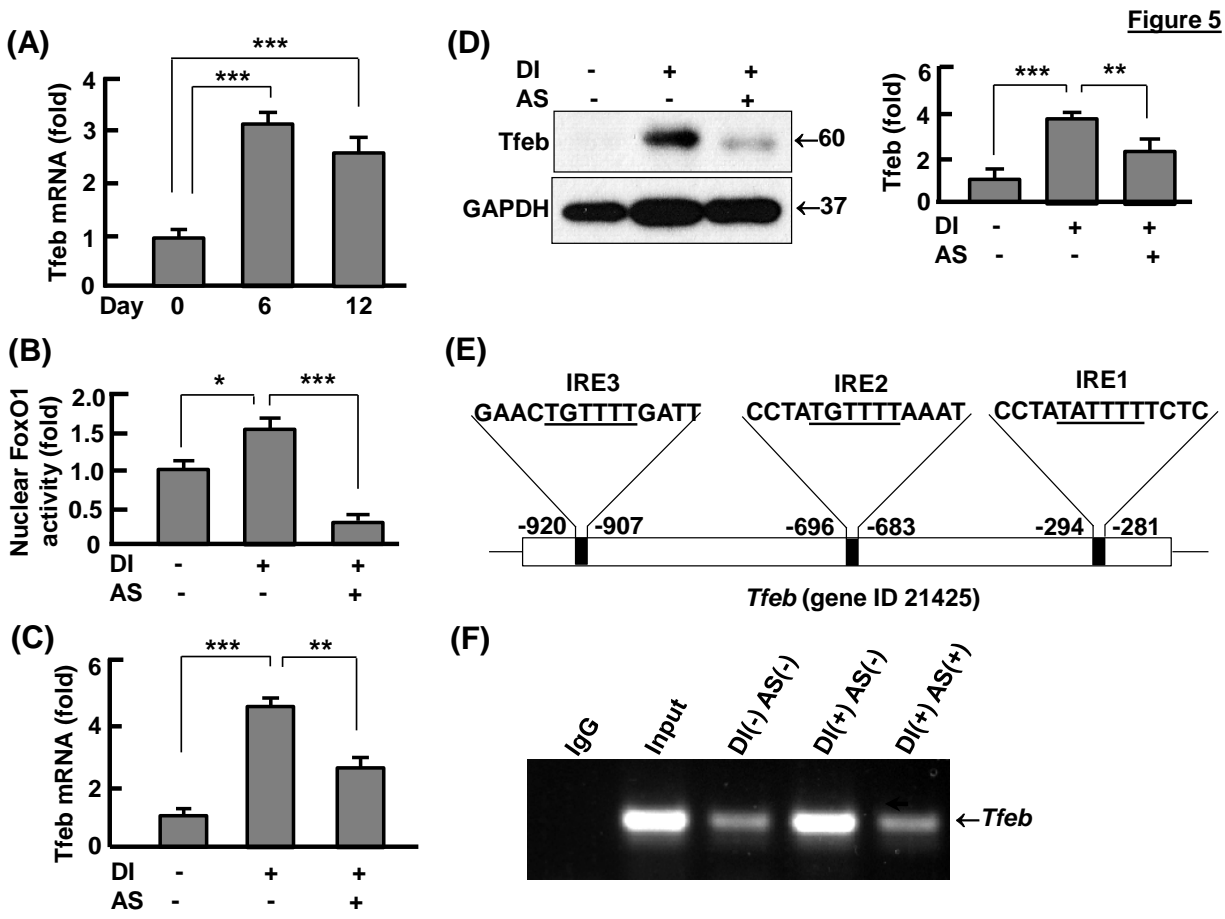


**Figure 5. FoxO1 regulated Tfeb expression.** (A) Tfeb transcript was analyzed on days 0, 6, and 12 during adipocyte differentiation. (B) FoxO1 inhibitor AS1842856 (0.1  $\mu$ M) potently suppressed FoxO1 activity in the nuclear fractions isolated from adipocytes. (C-D) Inhibition of FoxO1 prevented Tfeb upregulation during adipocyte differentiation, both at transcript (C) and protein (D) levels. (E) Tfeb gene bears three FoxO1-binding (i.e., insulin response element, IRE) sites in its promoter region. (F) Chromatin immune-precipitation (ChIP) assay of FoxO1-Tfeb interaction using a FoxO1 specific antibody. DI, differentiation induction; AS, AS1842856. The cells were cultured and treated (day 0-12), and ChIP assay conducted as described in Materials and Methods. Results were presented as mean  $\pm$  SD; n=3-4; \*, p<0.05; \*\*, p<0.01; \*\*\*, p<0.001.

**Figure 1s**

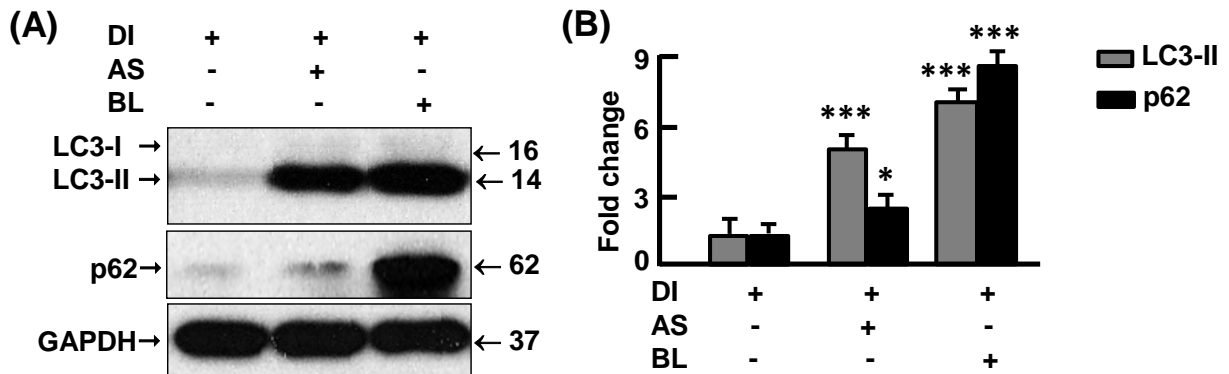


**Figure 1s. Measurement of autophagy flux.** After terminal differentiation (day 12), 3T3-L1 cells were treated with FoxO1 inhibitor AS1842856 (1  $\mu$ M) or autophagy inhibitors bafilomycin A1 (0.1  $\mu$ M) and leupeptin (10  $\mu$ g/ml) for 6 hours; vehicle (DMSO) was used as the treatment control. The cells were washed and lysed for western blot (A) and densitometric (B) analyses to measure p62 and LC3-II. DI, differentiation induction; AS, AS1842856; BL, bafilomycin A1 and leupeptin. Results were presented as mean  $\pm$  SD, and comparison was performed between untreated and treated cells; n=3-4; \*, p<0.05; \*\*\*, p<0.001.

## References

1. Zheng LD, Linarelli LE, Liu L, Wall SS, Greenawald MH, Seidel RW, et al. Insulin resistance is associated with epigenetic and genetic regulation of mitochondrial DNA in obese humans. *Clinical epigenetics* 2015; 7:60.
2. Zou P, Liu L, Zheng L, Stoneman RE, Cho A, Emery A, et al. Targeting FoxO1 with AS1842856 suppresses adipogenesis. *Cell Cycle* 2014; 13:3759-67.
3. Cheng Z, Almeida FA. Mitochondrial alteration in type 2 diabetes and obesity: an epigenetic link. *Cell Cycle* 2014; 13:890-7.
4. Hill JO, Wyatt HR, Peters JC. Energy balance and obesity. *Circulation* 2012; 126:126-32.
5. Feldmann HM, Golozoubova V, Cannon B, Nedergaard J. UCP1 ablation induces obesity and abolishes diet-induced thermogenesis in mice exempt from thermal stress by living at thermoneutrality. *Cell Metab* 2009; 9:203-9.
6. Cheng Z, Schmelz EM, Liu D, Hulver MW. Targeting mitochondrial alterations to prevent type 2 diabetes-Evidence from studies of dietary redox-active compounds. *Molecular nutrition & food research* 2014; 58:1739-49.
7. Cheng Z, Ristow M. Mitochondria and metabolic homeostasis. *Antioxidants & redox signaling* 2013; 19:240-2.
8. Cheng Z, Tseng Y, White MF. Insulin signaling meets mitochondria in metabolism. *Trends in endocrinology and metabolism: TEM* 2010; 21:589-98.
9. Kopecky J, Clarke G, Enerback S, Spiegelman B, Kozak LP. Expression of the mitochondrial uncoupling protein gene from the aP2 gene promoter prevents genetic obesity. *J Clin Invest* 1995; 96:2914-23.
10. Kopecky J, Rossmeisl M, Hodny Z, Syrový I, Horáková M, Kolarová P. Reduction of dietary obesity in aP2-Ucp transgenic mice: mechanism and adipose tissue morphology. *Am J Physiol* 1996; 270:E776-86.
11. Acosta A, Camilleri M, Shin A, Vazquez-Roque MI, Iturrino J, Lanza IR, et al. Association of UCP-3 rs1626521 with obesity and stomach functions in humans. *Obesity (Silver Spring)* 2015; 23:898-906.
12. Brondani Lde A, de Souza BM, Assmann TS, Boucas AP, Bauer AC, Canani LH, et al. Association of the UCP polymorphisms with susceptibility to obesity: case-control study and meta-analysis. *Mol Biol Rep* 2014; 41:5053-67.
13. Oberkofler H, Dallinger G, Liu YM, Hell E, Krempler F, Patsch W. Uncoupling protein gene: quantification of expression levels in adipose tissues of obese and non-obese humans. *J Lipid Res* 1997; 38:2125-33.
14. Brand MD, Esteves TC. Physiological functions of the mitochondrial uncoupling proteins UCP2 and UCP3. *Cell Metab* 2005; 2:85-93.
15. Rousset S, Alves-Guerra MC, Mozo J, Miroux B, Cassard-Doulcier AM, Bouillaud F, et al. The biology of mitochondrial uncoupling proteins. *Diabetes* 2004; 53 Suppl 1:S130-5.
16. Pedersen SB, Bruun JM, Kristensen K, Richelsen B. Regulation of UCP1, UCP2, and UCP3 mRNA expression in brown adipose tissue, white adipose tissue, and skeletal muscle in rats by estrogen. *Biochem Biophys Res Commun* 2001; 288:191-7.

17. Ye L, Wu J, Cohen P, Kazak L, Khandekar MJ, Jedrychowski MP, et al. Fat cells directly sense temperature to activate thermogenesis. *Proc Natl Acad Sci U S A* 2013; 110:12480-5.
18. Bugge A, Siersbaek M, Madsen MS, Gondor A, Rougier C, Mandrup S. A novel intronic peroxisome proliferator-activated receptor gamma enhancer in the uncoupling protein (UCP) 3 gene as a regulator of both UCP2 and -3 expression in adipocytes. *J Biol Chem* 2010; 285:17310-7.
19. Cioffi F, Senese R, de Lange P, Goglia F, Lanni A, Lombardi A. Uncoupling proteins: a complex journey to function discovery. *Biofactors* 2009; 35:417-28.
20. Cheng Z. FoxO1: mute for a tuned metabolism? *Trends in endocrinology and metabolism: TEM* 2015; 26:402-3.
21. Cheng Z, Guo S, Copps K, Dong X, Kollipara R, Rodgers JT, et al. Foxo1 integrates insulin signaling with mitochondrial function in the liver. *Nat Med* 2009; 15:1307-11.
22. Munekata K, Sakamoto K. Forkhead transcription factor Foxo1 is essential for adipocyte differentiation. *In Vitro Cell Dev Biol Anim* 2009; 45:642-51.
23. Higuchi M, Dusting GJ, Peshavariya H, Jiang F, Hsiao ST, Chan EC, et al. Differentiation of human adipose-derived stem cells into fat involves reactive oxygen species and Forkhead box O1 mediated upregulation of antioxidant enzymes. *Stem cells and development* 2013; 22:878-88.
24. O-Sullivan I, Zhang W, Wasserman DH, Liew CW, Liu J, Paik J, et al. FoxO1 integrates direct and indirect effects of insulin on hepatic glucose production and glucose utilization. *Nature communications* 2015; 6:7079.
25. Liu L, Zheng L, Zou P, Brooke J, Smith C, Long YC, et al. FoxO1 antagonist suppresses autophagy and lipid droplet growth in adipocytes. *Cell Cycle* 2016; 15.
26. Singh R, Xiang Y, Wang Y, Baikati K, Cuervo AM, Luu YK, et al. Autophagy regulates adipose mass and differentiation in mice. *J Clin Invest* 2009; 119:3329-39.
27. Zhang Y, Goldman S, Baerga R, Zhao Y, Komatsu M, Jin S. Adipose-specific deletion of autophagy-related gene 7 (atg7) in mice reveals a role in adipogenesis. *Proc Natl Acad Sci U S A* 2009; 106:19860-5.
28. Baerga R, Zhang Y, Chen PH, Goldman S, Jin S. Targeted deletion of autophagy-related 5 (atg5) impairs adipogenesis in a cellular model and in mice. *Autophagy* 2009; 5:1118-30.
29. Armani A, Cinti F, Marzolla V, Morgan J, Cranston GA, Antelmi A, et al. Mineralocorticoid receptor antagonism induces browning of white adipose tissue through impairment of autophagy and prevents adipocyte dysfunction in high-fat-diet-fed mice. *FASEB J* 2014; 28:3745-57.
30. Settembre C, Di Malta C, Polito VA, Garcia Arencibia M, Vetrini F, Erdin S, et al. TFEB links autophagy to lysosomal biogenesis. *Science* 2011; 332:1429-33.
31. Liu L, Zou P, Zheng L, Linarelli LE, Amarell S, Passaro A, et al. Tamoxifen reduces fat mass by boosting reactive oxygen species. *Cell death & disease* 2015; 6:e1586.
32. Zebisch K, Voigt V, Wabitsch M, Brandsch M. Protocol for effective differentiation of 3T3-L1 cells to adipocytes. *Anal Biochem* 2012; 425:88-90.
33. Ramirez-Zacarias JL, Castro-Munozledo F, Kuri-Harcuch W. Quantitation of adipose conversion and triglycerides by staining intracytoplasmic lipids with Oil red O. *Histochemistry* 1992; 97:493-7.

34. Si Y, Palani S, Jayaraman A, Lee K. Effects of forced uncoupling protein 1 expression in 3T3-L1 cells on mitochondrial function and lipid metabolism. *J Lipid Res* 2007; 48:826-36.
35. Si Y, Shi H, Lee K. Metabolic flux analysis of mitochondrial uncoupling in 3T3-L1 adipocytes. *PloS one* 2009; 4:e7000.
36. Thompson MP, Kim D. Links between fatty acids and expression of UCP2 and UCP3 mRNAs. *FEBS Lett* 2004; 568:4-9.
37. Nagashima T, Shigematsu N, Maruki R, Urano Y, Tanaka H, Shimaya A, et al. Discovery of novel forkhead box O1 inhibitors for treating type 2 diabetes: improvement of fasting glycemia in diabetic db/db mice. *Mol Pharmacol* 2010; 78:961-70.
38. Kovsan J, Bluher M, Tarnovscki T, Kloting N, Kirshtein B, Madar L, et al. Altered autophagy in human adipose tissues in obesity. *J Clin Endocrinol Metab* 2011; 96:E268-77.
39. Yamada E, Singh R. Mapping autophagy on to your metabolic radar. *Diabetes* 2012; 61:272-80.
40. Zhang C, He Y, Okutsu M, Ong LC, Jin Y, Zheng L, et al. Autophagy is involved in adipogenic differentiation by repressing proteasome-dependent PPAR $\gamma$ 2 degradation. *American journal of physiology Endocrinology and metabolism* 2013; 305:E530-9.
41. Cheng Z, White MF. Targeting Forkhead box O1 from the concept to metabolic diseases: lessons from mouse models. *Antioxid Redox Signal* 2011; 14:649-61.
42. Fullgrabe J, Klionsky DJ, Joseph B. The return of the nucleus: transcriptional and epigenetic control of autophagy. *Nature reviews Molecular cell biology* 2014; 15:65-74.
43. Martini-Stoica H, Xu Y, Ballabio A, Zheng H. The Autophagy-Lysosomal Pathway in Neurodegeneration: A TFEB Perspective. *Trends Neurosci* 2016; 39:221-34.
44. Storz P. Forkhead homeobox type O transcription factors in the responses to oxidative stress. *Antioxidants & redox signaling* 2011; 14:593-605.
45. Tormos KV, Anso E, Hamanaka RB, Eisenbart J, Joseph J, Kalyanaraman B, et al. Mitochondrial complex III ROS regulate adipocyte differentiation. *Cell Metab* 2011; 14:537-44.
46. Kim KH, Jeong YT, Oh H, Kim SH, Cho JM, Kim YN, et al. Autophagy deficiency leads to protection from obesity and insulin resistance by inducing Fgf21 as a mitokine. *Nat Med* 2013; 19:83-92.
47. Lavallard VJ, Meijer AJ, Codogno P, Gual P. Autophagy, signaling and obesity. *Pharmacol Res* 2012; 66:513-25.
48. Nunez CE, Rodrigues VS, Gomes FS, Moura RF, Victorio SC, Bombassaro B, et al. Defective regulation of adipose tissue autophagy in obesity. *Int J Obes (Lond)* 2013; 37:1473-80.
49. Kosacka J, Kern M, Kloting N, Paeschke S, Rudich A, Haim Y, et al. Autophagy in adipose tissue of patients with obesity and type 2 diabetes. *Mol Cell Endocrinol* 2015; 409:21-32.

## **Chapter 5 Tamoxifen Reduces Fat Mass by Boosting Reactive Oxygen Species**

Longhua Liu, Peng Zou, Louise Zheng, Leah E. Linarelli, Sarah Amarell, Austin Passaro,

Dongmin Liu, Zhiyong Cheng\*

Department of Human Nutrition, Foods and Exercise, Fralin Life Science Institute, College of Agriculture and Life Science, Virginia Tech, Blacksburg, Virginia, USA.

Correspondence: Dr. Zhiyong Cheng, 1981 Kraft Drive, Blacksburg, VA 24061, USA. Phone: (540) 231 9445; Fax: (540) 231 5522; email: [zcheng@vt.edu](mailto:zcheng@vt.edu).

---

**This chapter has been published in *Cell Death and Disease* (2015) 6, e1586.**

**Abstract:** As the pandemic of obesity is growing, a variety of animal models have been generated to study the mechanisms underlying adiposity development and metabolic disorders. Tamoxifen (Tam) is widely used to activate Cre recombinase that spatiotemporally controls target gene expression and regulates adiposity in laboratory animals. However, a critical question remains as to whether Tam itself affects adiposity and possibly confounds the functional study of target genes in adipose tissue. Here we administrated Tam to Cre-absent forkhead box O1 (FoxO1) floxed mice (f-FoxO1) and insulin receptor substrate Irs1/Irs2 double floxed mice (df-Irs), and found Tam induced approximately 30% reduction ( $p < 0.05$ ) in the fat mass with insignificant change in body weight. Mechanistically, Tam promoted reactive oxygen species (ROS) production, apoptosis and autophagy, which was associated with down-regulation of adipogenic regulator peroxisome proliferator-activated receptor gamma ( $PPAR\gamma$ ) and de-differentiation of mature adipocytes. However, normalization of ROS potently suppressed Tam-induced apoptosis, autophagy and adipocyte de-differentiation, suggesting ROS may account, at least in part, for the changes. Importantly, Tam-induced ROS production and fat mass reduction lasted for 4-5 weeks in the f-FoxO1 and df-Irs mice. Our data suggest that Tam reduces fat mass via boosting ROS, thus making a recovery period crucial for post-treatment study.

**Keywords:** Tamoxifen, adipose tissue, ROS, apoptosis, autophagy, de-differentiation

## Introduction

Excess fat mass or adiposity is the hallmark of obesity, the rapid growing epidemic in the globe.<sup>1</sup> <sup>2</sup> In the United States, over two-thirds of adults are overweight or obese according to the statistics of years 2011-2012.<sup>3</sup> For children, the overweight or obese population accounts for about 25% in the 2-5 year olds and 33% in school students (including adolescents).<sup>3</sup> It is estimated that obesity care accounts for 21% of national health expenditures in the U.S., equal to 190.2 billion U.S. dollars per year.<sup>4</sup> Because adipose tissue is an important endocrine organ, which secretes adipokines or cytokines that regulate inflammatory responses and metabolic homeostasis, aberrant adiposity dysregulates adipokine levels and leads to a variety of metabolic disorders and complications, such as diabetes and cardiovascular diseases.<sup>5</sup> As such, the healthcare burden that obesity imposes on the society is far greater.

To understand the molecular mechanism of obesity development, various laboratory rodent models have been generated to study the gain or loss of functions of different genes.<sup>6,7</sup> To this end, the Cre/lox site-specific recombination system has been versatile to generate conditional mouse mutants, controlling gene expression and activity in target tissues.<sup>8,9</sup> In particular, Tamoxifen (Tam) is used to activate Cre recombinases spatiotemporally *in vivo* through intra-peritoneal (IP) or subcutaneous administration.<sup>10-12</sup> Injection of Tam at a dose of 1-8 mg/kg body weight for 5 consecutive days deletes target genes, thus establishing a versatile system to study functional genes in obesity.<sup>8-12</sup>

The use of Tam in clinical treatments has led to the argument about its potential effect on body fat or weight gain in human patients.<sup>13, 14</sup> This raises the question as to whether and how Tam influences adipocytes and fat mass in the experimental animal models after administration. Exclusion of direct regulation of adiposity by Tam as a confounding factor in animal models is critical to better understand target genes in adipogenesis and metabolic homeostasis. In the present work, we present the evidence that 5-day administration of Tam significantly reduces mouse fat mass, which persists till weeks 4-5 after the treatment. At cellular level, Tam promotes the production of reactive oxygen species (ROS), which is accompanied with enhanced apoptosis, autophagy and adipocyte dedifferentiation. However, treatment of adipocytes with antioxidant n-acetyl cysteine (NAC) dramatically counteracted Tam-induced ROS and suppressed apoptotic and autophagic markers, concomitant with reversal of adipocyte dedifferentiation. *In vivo*, fat mass was restored upon the normalization of ROS, which is associated with suppressed adipocyte dedifferentiation and downregulated apoptotic and autophagic markers. Our data reveals a ROS-mediated mechanism by which Tam induces fat mass reduction. Since it may confound the post-treatment study, deliberate determination of the recovery period after Tam administration is essential to understand the functions of target genes using Tam-induced knockout mice.

## **Results**

**Tam induced fat mass reduction in mice.** To test the effect of Tam on fat mass, we conducted 5-day I.P. administration of Tam (1 mg/20 g body weight) on FoxO1 floxed mice (f-FoxO1),<sup>15-17</sup> by following a standard protocol established previously.<sup>12</sup> Two weeks after Tam

administration, the body fat was reduced by 34% ( $p < 0.05$ ) in f-FoxO1 mice (Figure 1, A). To validate the findings, we treated Irs1 and Irs2 double floxed mice without Cre recombinase (df-Irs) in a similar way,<sup>15, 16</sup> and found the fat mass was also significantly reduced (26%,  $p < 0.05$ ) (Figure 1s, A). However, the changes in body weight were insignificant (Figure 1, B; Figure 1s, B). Monitoring of fat mass suggested that the reduction was persistent till week 5 (week 4 in df-Irs mice), after which the fat percentage was comparable to the pre-treatments (Figure 1, A; Figure 1s, A). In line with this, the weight of epididymal white adipose tissue (eWAT) was significantly reduced in Tam treated f-FoxO1 mice at week 2, while there was no significant difference at week 6 (Figure 1, C-D). By contrast, injection of the vehicle (sunflower oil) caused indiscernible change in the body fat mass (Figure 1, A; Figure 1s, A). Therefore, the reduction of fat mass in mice arose primarily from Tam treatment. Given both two mouse models shared the phenotype, we used f-FoxO1 mice for the following mechanistic study.

**Tam promoted apoptosis and autophagy in adipose tissue.** The regulators of apoptosis and autophagy were implicated in the regulation fat mass.<sup>18-23</sup> To examine whether Tam had effects on apoptosis and autophagy, we used eWAT at week 2 and week 6 after Tam administration, and analyzed the mediators of apoptosis and autophagy — the activated or cleaved caspase 3 (Cas3(c)) and microtubule-associated protein 1A/1B-light chain 3-phosphatidylethanolamine conjugate (LC3b), respectively.<sup>24, 25</sup> As shown in Figure 2 A-B, Tam treatment increased the level of Cas3(c) by 6.8 folds ( $p < 0.0001$ ), and LC3b by 1.9 folds ( $p < 0.05$ ) at week 2. However, these changes were largely reversed at week 6 and showed no statistical significance (Figure 2 C-D).

**Tam promoted the production of reactive oxygen species (ROS).** ROS and resultant oxidative stress play an important role in apoptosis and autophagy.<sup>26-28</sup> To examine whether ROS and oxidative stress was involved in Tam-induced effects, we analyzed heme oxygenase 1 (HO1), the sensitive indicator of cellular oxidative stress.<sup>29</sup> Tam treatment upregulated HO1 protein level by 6 folds ( $p < 0.0001$ ) in the mice at week 2 (Figure 3A); however, at week 6, the HO1 abundance in the treated mice was comparable to that in untreated mice, showing no statistical significance (Figures 3a and b). Interestingly, the HO1 levels in untreated mice were higher at week 6 than at week 2, supporting the notion that HO1 expression increases with age<sup>30, 31</sup>. Consistently, ROS level in the adipose tissue was 2.3-fold higher in Tam-treated mice than in vehicle-treated mice at week 2 (Figure 3C), but it became statistically insignificant at week 6 (Figure 3D). Interestingly, the up- and down-regulation of ROS and HO1 levels seems to coincide well with the changes in cas3(c), LC3b, and fat mass (Figures 1-3).

**Antioxidant abolished Tam-induced ROS, apoptosis and autophagy.** To map the interaction between ROS and other Tam-induced cellular events, we treated 3T3L1 adipocytes with Tam combined with a potent ROS-scavenger n-acetyl cysteine (NAC).<sup>32, 33</sup> As observed in adipose tissue, Tam induced significant upregulation of HO1 in 3T3L1 adipocytes, and the effect was dose-dependent in the tested range of 0-128  $\mu$ M (Figure 2s). Tam also promoted ROS production by 2.5 folds ( $p < 0.01$ ) in 3T3L1 adipocytes (Figure 4A), and significantly upregulated the apoptosis and autophagy regulators cas3(c) and LC3b (Figure 4B-C). However, inclusion of

NAC in the treatments significantly prevented Tam-induced ROS and HO1 elevation, and normalized the protein levels of cas3(c) and LC3b (Figure 4 A-C).

### **Antioxidant reversed Tam-induced reduction in cell density and adipocyte**

**population.** Because alteration in adipocyte number affects adiposity,<sup>2</sup> we asked whether Tam treatment influenced cell density. Compared with the vehicle treated adipocytes, Tam-treated cells showed a significant decrease in cell density (24%,  $p < 0.05$ ), consistent with the upregulation of apoptotic marker (Figure 5A-B, Figure 4 B-C). Interestingly, the population of lipid-droplet-containing cells (i.e., mature adipocytes) also declined (36%,  $p < 0.05$ ), implying a process of “de-differentiation” might be induced by Tam (Figure 5A, C).<sup>34-36</sup> Regardless, addition of the ROS scavenger NAC largely restored the cell density and population of mature adipocytes (Figure 5 A-C).

### **Antioxidant reversed Tam-induced downregulation of Peroxisome**

**proliferator-activated receptor gamma (PPAR $\gamma$ ).** PPAR $\gamma$  is a key regulator of adipogenesis (*de novo* generation of mature adipocytes) and adipocyte de-differentiation.<sup>34, 35, 37</sup> The observation of reduced population of mature adipocytes after Tam treatment prompted us to analyze the effect of Tam on PPAR $\gamma$ . As shown in Figure 6 A, PPAR $\gamma$  protein level was reduced by 74% ( $p < 0.01$ ) in Tam treated adipocytes. However, co-treatment of the adipocytes with Tam and NAC significantly restored PPAR $\gamma$  level. These data suggest that Tam may regulate adipogenesis or population of mature adipocytes through PPAR $\gamma$ , and ROS plays a central role in the regulation. Consistent with this hypothesis, we found the PPAR $\gamma$  level was dramatically

decreased (69%,  $p < 0.01$ ) in the adipose tissue of Tam-treated mice at week 2 (Figure 6 C), which is accompanied with increased ROS production and oxidative stress indicator HO1 (Figure 3A-C). At week 6 when ROS production and HO1 level backed to normal (Figure 3D), however, the abundance of PPAR $\gamma$  returned comparable to that in the control mice (Figure 6D). In addition, the reversal of ROS overproduction and PPAR $\gamma$  suppression was accompanied with normalization of fat mass at week 6 (Figure 1, Figure 1s, Figure 3, Figure 6).

## Discussion

Tam has been widely used to activate inducible Cre recombinase and knock out target genes in mechanistic studies adipose development and metabolic homeostasis<sup>8, 11, 12, 38-41</sup> However, the effect of Tam administration on adipocytes and adipose tissue has not been investigated to the best of our knowledge. In this study, we chose to use f-FoxO1 bearing no Cre recombinase for Tam treatment, aiming to rule out the effect of Cre activation (or gene deletion) on fat mass. We found that 5-day administration of Tam led to significant reduction of fat mass in mice, which lasted for 4-5 weeks after the last injection. The findings were validated in Cre-absent df-Irs mice. The Tam-induced fat mass reduction could confound the effects of gene knockout, making it critical to allow for 6 weeks as a recovery period before further study is conducted. Note that the recovery period may vary with different animal models, thus warranting a deliberate determination for a specific laboratory model to establish a reliable experimental system.

The mechanism by which Tam reduces fat mass includes several cellular events. Tam treatment increased apoptosis and autophagy, the processes that reduce adipocyte number and have been implicated in adipose regulation.<sup>2, 18-23</sup> Indeed, the cell density and population of mature adipocytes decreased after Tam treatment. Tam also promoted adipocyte de-differentiation and ROS production, whereas normalization of ROS level markedly prevented Tam-induced adipocyte de-differentiation, apoptosis and autophagy, concomitant with restoration of mature adipocyte population and fat mass. Together, our data strongly suggest that the short-term (5-day) treatment with Tam reduces fat mass via boosting ROS production.

Tam was shown to induce ROS and oxidative stress in breast cancer cells, hepatoblastoma cells, retinal cells and platelets through activation of NAD(P)H oxidase.<sup>32, 42-45</sup> The ROS-boosting effect of Tam was extended and further validated by our study in adipocytes and adipose tissues. Importantly, we found that ROS elevation resulted in PPAR  $\gamma$  down-regulation and adipocyte de-differentiation, which support the notion that mature adipocytes undergo de-differentiation under stress conditions.<sup>34, 35</sup> It was shown that proinflammatory adipocytokines (e.g., TNF $\alpha$ ) could promote adipocyte de-differentiation through down-regulation of PPAR $\gamma$ .<sup>34, 35</sup> Given that ROS elevation or oxidative stress increases TNF $\alpha$  production,<sup>46</sup> Tam may promote adipocyte de-differentiation by activating a ROS-TNF $\alpha$ -PPAR $\gamma$  axis.

The effect of Tam on fat mass in humans, e.g., breast cancer patients, remains controversial. While Tam was reported to increase fat mass through its anti-oestrogenic effect,<sup>13</sup> recent studies loosened the conclusion by showing Tam has no effect on the fat mass in breast cancer patients.<sup>14</sup> It should be noted that the Tam dosage and treatment duration for mice in this study significantly differs from that for the long-term Tam treatment of breast cancer patients. To

activate Cre recombinase to knock out target genes, animal models are typically treated for 5 consecutive days (administration of 1-8 mg/20g body weight or 50-400 mg/kg body weight, once a day<sup>8-12</sup>). However, Tam therapy for breast cancer patients in the United States generally lasts 5 years, with a dose of 20 mg (either one 20 mg tablet or two 10 mg tablets) taken by mouth once a day.<sup>47-49</sup> Assuming the body weight of breast cancer patients ranges from 50 kg to 80 kg, the average daily use of Tam would be 0.25-0.4 mg/kg, a dosage being 0.06%-0.8% of that used in animal models. Owing to different dosage and treatment duration, the effect of Tam on mouse fat mass observed in this study might not be phenocopied in breast cancer patients with Tam therapy.

## **Materials and methods**

**Materials** Dulbecco's modified Eagle's (DMEM) medium was from Corning Inc (Manassas, VA). Fetal bovine serum (FBS) was from GeneMate (Kaysville, UT). Dexamethasone, 3-isobutyl-1-methylxanthine (IBMX), rosiglitazone and tamoxifen (Tam) were purchased from Cayman chemical (Ann Arbor, MI). Penicillin/streptomycin (P/S) was from GE Healthcare Life Sciences HyClone Laboratories (Logan, UT). Insulin and n-acetyl cysteine (NAC) were from Sigma-Aldrich (St. Louis, MO). Phosphate buffered saline (PBS) was from Caisson Laboratories, Inc (North Logan, UT).

**Mice** The FoxO1 floxed and mice (f-FoxO1) and Irs1/Irs2 double floxed mice (df-Irs) were bred and housed as previously described.<sup>15, 16, 50</sup> Briefly, the mice were housed in plastic cages on a 12 h light-dark photocycle, with free access to water and regular chow diet. Before Tam treatment experiments, male mice (14-16 week old) were weighed and fat mass was measured with a Bruker Minispec LF90 NMR Analyzer ((Bruker Optics, Inc). Then the mice were transferred to a biosafety level 2 (BSL2) room, and administrated with Tam (1 mg/20 g body weight) or the vehicle (sunflower oil) by I.P. injection (, once a way for 5 consecutive days). After Tam administration, the cages were changed every 2 days until week 2, when the mice were transferred into BSL1 room and the measurement of body fat mass was resumed. Depending on the experimental design, the mice were weighed and sacrificed to harvest tissue for snap freezing in liquid nitrogen, at week 2 or week 6 after Tam treatment. All the procedures of experiment and waste disposal followed NIH guideline and were approved by the Virginia Tech Institutional Animal Care and Use Committee.

**Cell culture and Treatment** 3T3-L1 preadipocytes (ATCC<sup>®</sup> CL-173<sup>™</sup>, Manassas, VA) were cultured in basal media (i.e., DMEM media supplemented with 10% FBS, 100 units/ml penicillin and 100 µg/ml streptomycin (1 × P/S)), at 37 °C in a humidified atmosphere of 5% CO<sub>2</sub>. The media were replaced every two days. Differentiation of 3T3-L1 cells was induced as described previously with minor modifications.<sup>51</sup> Briefly, 3T3-L1 cells were grown to confluence (day 0), and maintained in fresh basal media (BMI) for two days (days 1-2). At the end of day 2, BMI medium was changed to differentiation medium I (DMI): DMEM supplemented with 10% FBS, P/S (1 ×), IBMX (0.5 mM), dexamethasone (1 µM), insulin (1 µg/ml) and rosiglitazone (2 µM). At the end of day 4, DMI medium was changed to

differentiation medium II (DMII): DMEM supplemented with 10% FBS, P/S (1 ×), and insulin (1 µg/ml). At the end of day 6, DMII medium was changed to basal media (BMII), and the cells were maintained in BMII (replaced with fresh basal medium every two days) until fully differentiated (day 12). As a control, preadipocytes were maintained in BMI till day 12, and the medium was replaced fresh one every two days. Upon full differentiation, 3T3-L1 adipocytes were treated with Tam for 48 hours at concentrations of 0, 8, 16, 32, 64, and 128 µM, and the vehicle 0.1% sunflower as a treatment control.<sup>12</sup> When applicable, NAC was added at a concentration of 1 mM with Tam for a 48-hour treatment to study the role of ROS.<sup>32</sup> Images of the cells were captured on day 12 with a Nikon ECLIPSE TS100 microscope, and cell counting and population analysis was performed with NIH ImageJ software.

**ROS measurement** ROS in adipocytes and adipose tissue was measured as previously described,<sup>52, 53</sup> with a cell-permeable dye 5,6-carboxy-2',7'-dichlorofluorescein diacetate (Carboxy-DCFDA, Molecular Probes). Snap frozen adipose tissues were weighed and transferred into buffered medium (5 mmol/l HEPES in PBS) for quick thawing to improve the probe diffusion. After rapid thawing, medium was discarded. Samples were exposed to 8 µM Carboxy-DCFDA in fresh medium and were incubated at 37°C for 45 min under agitation. Medium was then removed, and samples were further incubated in a lysis buffer (0.1% SDS, Tris-HCl, pH 7.4) for 15 min at 4°C. After homogenization, samples were centrifuged at 16,000g for 20 min at 4°C. Supernatants were collected and subjected to fluorescence analysis at 530 nm under excitation at 485 nm using a Synergy H4 Hybrid Multi-Mode Microplate Reader (BioTek Instruments, Inc.).

To measure ROS in 3T3L1 adipocytes, 1- 5 x 10<sup>6</sup> cells were harvested with trypsin and washed 3 times with cold PBS, followed by incubation with 8 μM Carboxy-DCFDA in fresh medium (5 mmol/l HEPES in PBS) and were incubated at 37°C for 45 min under agitation. Medium was then removed, and samples were further incubated in PLC lysis buffer:<sup>15, 50</sup> (30 mM Hepes, pH 7.5, 150 mM NaCl, 10% glycerol, 1% Triton X-100, 1.5 mM MgCl<sub>2</sub>, 1 mM EGTA, 10 mM NaPPi, 100 mM NaF, 1 mM Na<sub>3</sub>VO<sub>4</sub>) supplemented with protease inhibitor cocktail (Roche) and 1 mM PMSF for 15 min at 4°C. After homogenization, samples were centrifuged at 16,000g for 20 min at 4°C. Supernatants were collected and subjected to fluorescence analysis at 530 nm under excitation at 485 nm, and total protein was determined with DC protein assay (Bio-Rad) on a Synergy H4 Hybrid Multi-Mode Microplate Reader (BioTek Instruments, Inc.). The ROS levels were normalized to the total protein for each cell dish.

**Western Blot** To prepare tissue lysates, snap frozen adipose tissues were weighed and homogenized with a Bullet Blender<sup>®</sup> (Next Advance, Inc.), in PLC lysis buffer supplemented with protease inhibitor cocktail (Roche), 1 mM PMSF, 10 μM TSA (Trichostatin A, Selleckchem) and 5 mM Nicotinamide (Alfa Aesar).<sup>15, 50</sup> For cell lysates, the 3T3L1 adipocytes were washed with ice-cold PBS and homogenized with a Bullet Blender. Total protein concentrations of the lysates were determined using the DC protein assay (Bio-Rad). Western blot and image analysis were conducted as described previously.<sup>15</sup> Antibody catalog numbers and vendors are as follows: cleaved caspase-3 Rabbit mAb (9664) and LC3B antibody (2775) from Cell Signaling Technology; PPAR-gamma antibody (MA5-14889), LC3 Antibody (PA1-16930) and GAPDH antibody (MA5-15738) from Pierce or Thermo Fisher Scientific Inc; heme oxygenase-1 antibody (3391-100) from BioVision, Inc.

**Statistical analyses** All results are expressed as means  $\pm$  s.d. and are analyzed by analysis of variance to determine p values;  $p < 0.05$  was considered statistically significant.

## **Acknowledgement**

We thank Dr. Ronald Depinho (University of Texas MD Anderson Cancer Center) and Dr. Morris F. White (Children's Hospital Boston, Harvard Medical School) for providing the f-FoxO1 and df-Irs mice, respectively. Funding for this work was provided, in part, by the Virginia Agricultural Experiment Station and the Hatch Program of the National Institute of Food and Agriculture, US Department of Agriculture (to ZC), and by grant 1R01AT007077 from the National Center for Complementary and Alternative Medicine in the National Institute of Health (to DL). Publication of this article was supported by Virginia Tech's Open Access Subvention Fund.

## **Conflict of interest**

The authors declare no conflict of interest.

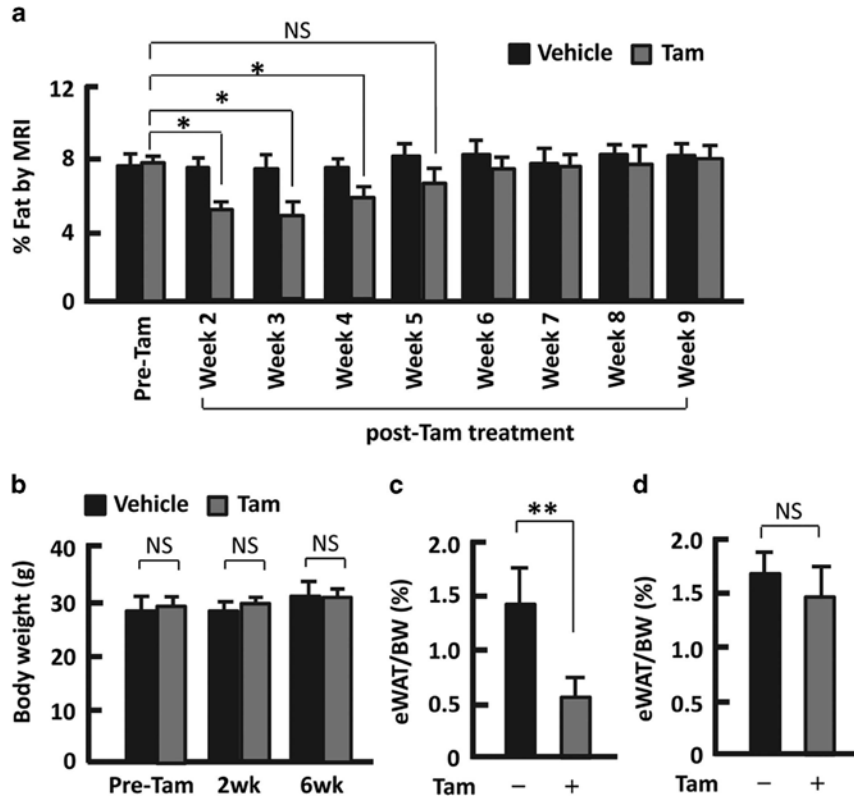
## **Abbreviations:**

Carboxy-DCFDA: 5, 6-carboxy-2', 7'-dichlorofluorescein diacetate  
Cas3(c): cleaved caspase 3  
df-Irs: Irs1/Irs2 double floxed mice  
eWAT: epididymal white adipose tissue

FoxO1: forkhead box O1  
f-FoxO1: FoxO1 floxed mice  
HO1: heme oxygenase 1  
Irs: insulin receptor substrate  
I.P.: intra-peritoneal  
LC3: microtubule- associated protein 1A/1B-light chain 3-phosphatidylethanolamine conjugate  
NAC: N-acetyl cysteine  
PPAR $\gamma$ : peroxisome proliferator-activated receptor gamma  
ROS: reactive oxygen species  
Tam: Tamoxifen

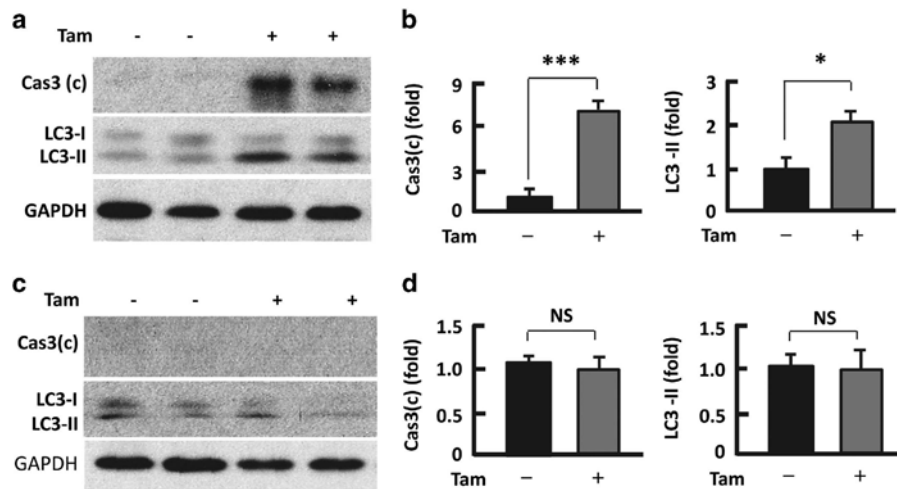
## Figures

Figure 1



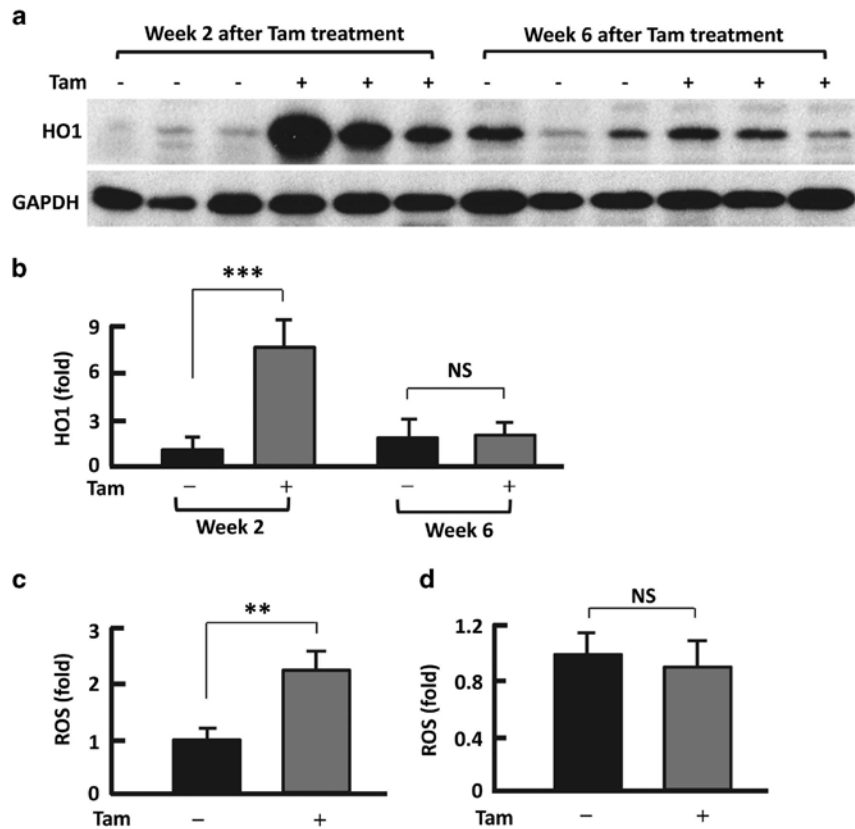
**Figure 1 Tam reduced fat mass in f-FoxO1 mice.** (a) The kinetics of fat mass regulation after 5-day administration of Tam. (b) Measurement of body weight before Tam treatment (pre-Tam), 2 weeks (2wk) and 6 weeks (6wk) after Tam injection. (c) The weight of epididymal adipose tissue (eWAT) at week 2 in mice treated with Tam. (d) The weight of eWAT at week 6 in mice treated with Tam. n = 4–6; \*P<0.05; \*\*P<0.01; NS, not significant

**Figure 2**



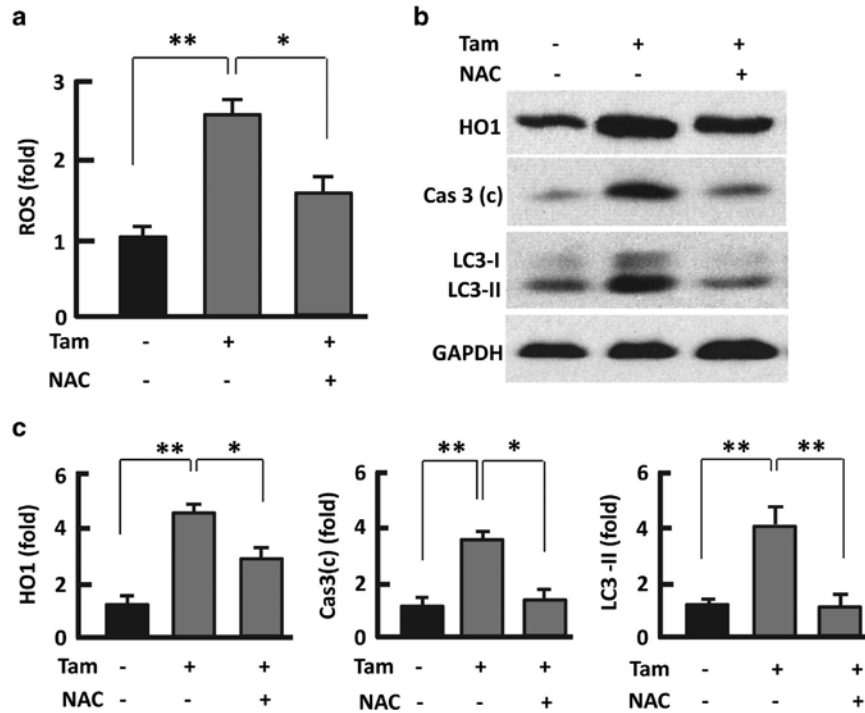
**Figure 2 Tam increased apoptotic and autophagic regulators in adipose tissue.** (a and b) At week 2 after Tam administration, western blotting (a) was performed to analyze Cas3(c) and LC3 with densitometric analysis (b) of western blotting images using the NIH ImageJ software; n = 5–7. (c and d) At week 6 after Tam administration, western blotting (c) was performed to analyze Cas3(c) and LC3, and densitometric analysis (d) of western blotting images with the NIH ImageJ software; n = 5–7. GAPDH (glyceraldehyde 3-phosphate dehydrogenase) was probed as a loading control. \*P<0.05; \*\*\*P<0.0001; NS, not significant

**Figure 3**



**Figure 3 Tam promoted ROS and oxidative stress.** (a) Western blotting analysis of HO1 in mouse adipose tissues at weeks 2 and 6, respectively, after Tam administration, with GAPDH (glyceraldehyde 3-phosphate dehydrogenase) probed as a loading control. (b) Densitometric analysis of western blotting images using the NIH ImageJ software;  $n = 6-8$ . (c) Measurement of ROS in adipose tissue at week 2 after Tam administration ( $n = 3-4$ ). (d) Measurement of ROS in adipose tissue at week 6 after Tam administration ( $n = 3-4$ ). \*\* $P < 0.01$ ; \*\*\* $P < 0.0001$ ; NS, not significant

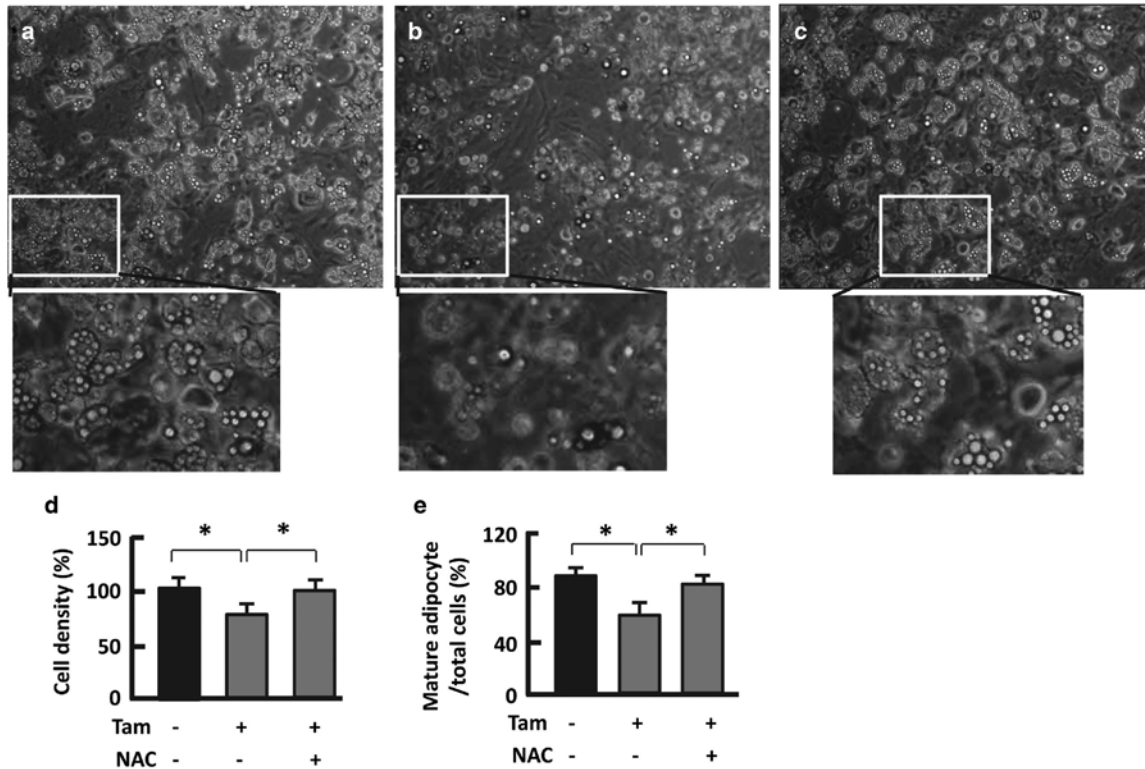
**Figure 4**



**Figure 4 Antioxidant NAC attenuated ROS level and reversed Tam effects. (a)**

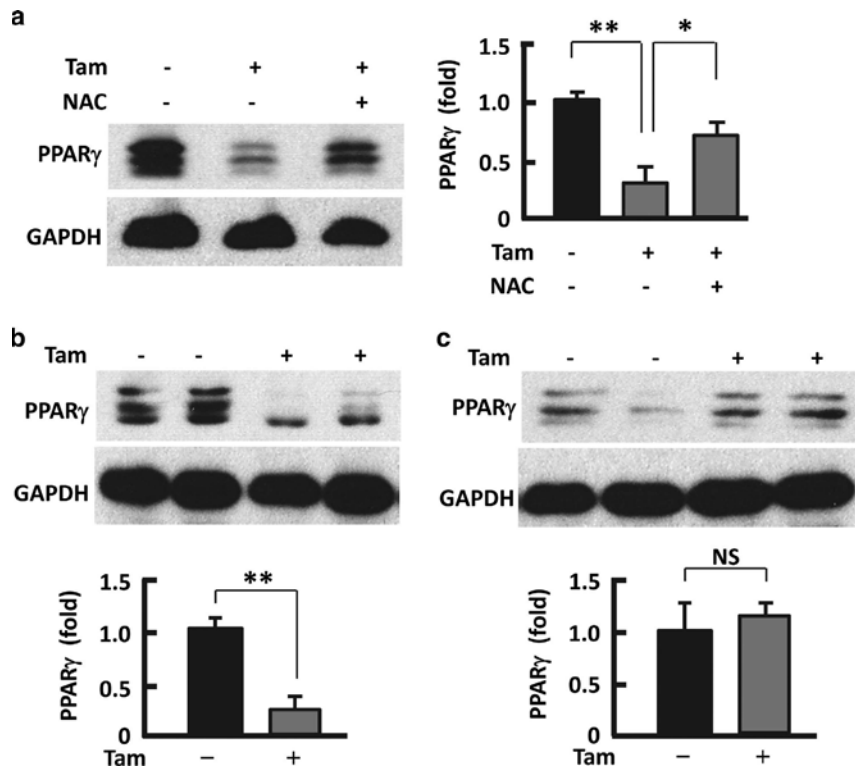
Measurement of ROS in 3T3L1 adipocytes. (b and c) Western blotting analysis (b) of HO, Cas3 (c) and LC3 in 3T3L1 adipocytes after 48-h treatment with Tam (128  $\mu$ M) or Tam (128  $\mu$ M) plus NAC (1 mM), with densitometric analysis (c) of western blotting images using the NIH ImageJ software; GAPDH (glyceraldehyde 3-phosphate dehydrogenase) was probed as a loading control. n = 3–5; \*P<0.05; \*\*P<0.01

Figure 5



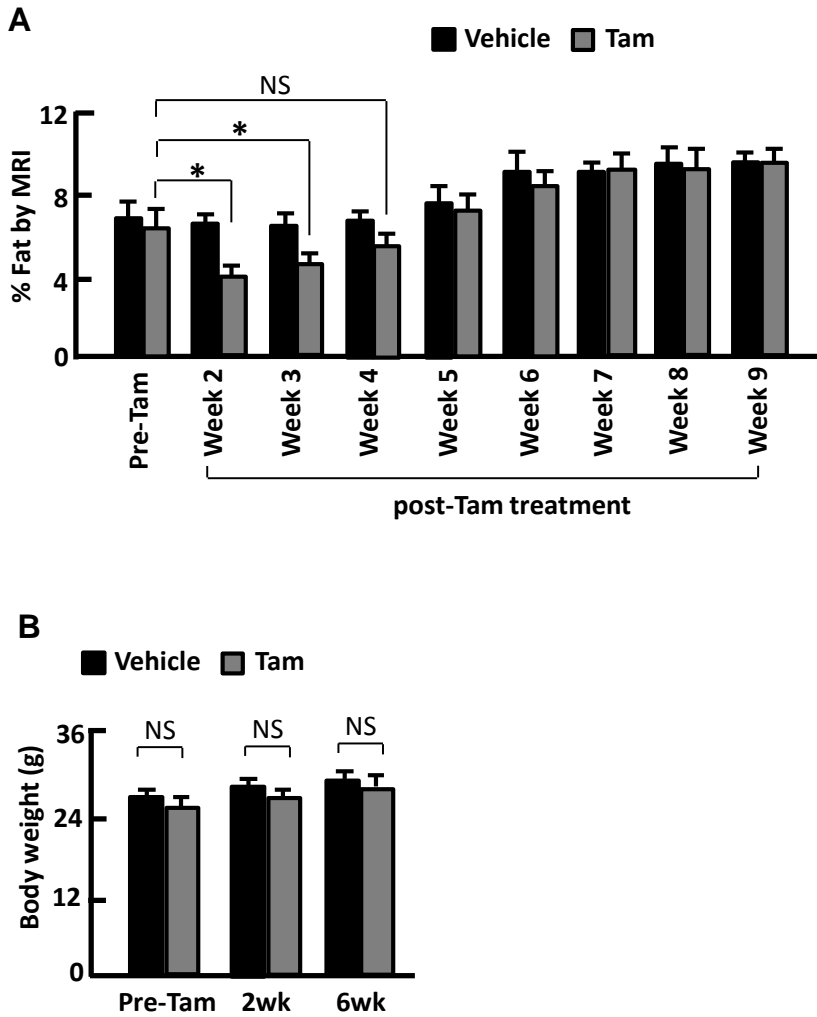
**Figure 5 Antioxidant NAC mitigates Tam effect on cell density and mature adipocyte population.** (a–c) Microscopy imaging of 3T3L1 adipocytes treated with vehicle (a), 128 μM Tam (b) and Tam (128 μM) plus NAC (1 mM) (c). The microscope was set at × 100. (d and e) Measurement of cell density and population of mature adipocytes using the NIH ImageJ software; n = 6–8. \*P<0.05

Figure 6



**Figure 6 Counteracting or normalizing ROS reduced Tam effect on PPAR $\gamma$ .** (a) Western blotting analysis (left panel) of PPAR $\gamma$  in 3T3L1 adipocytes after 48-h treatment with Tam (128  $\mu$ M) or Tam (128  $\mu$ M) plus NAC (1 mM), with densitometric analysis (right panel) of western blotting images using the NIH ImageJ software; n = 3–5. (b) At week 2 after Tam administration, western blotting (upper panel) was performed to analyze PPAR $\gamma$ , with densitometric analysis (lower panel) of western blotting images using the NIH ImageJ software; n = 3–5. (c) At week 6 after Tam administration, western blotting (upper panel) was performed to analyze PPAR $\gamma$ , with densitometric analysis (lower panel) of western blotting images using the NIH ImageJ software; n = 3–5. GAPDH (glyceraldehyde 3-phosphate dehydrogenase) was probed as a loading control. \*P<0.05; \*\*P<0.01

**Figure 1s**



**Figure 1s. Tam reduced fat mass in df-Irs mice.** (A) The kinetics of fat mass regulation after 5-day administration of Tam. (B) Measurement of body weight before Tam treatment (pre-Tam), 2 weeks (2 wk) and 6 weeks (6 wk) after Tam injection. \*,  $p < 0.05$ ; NS, not significant.

**Figure 2s**

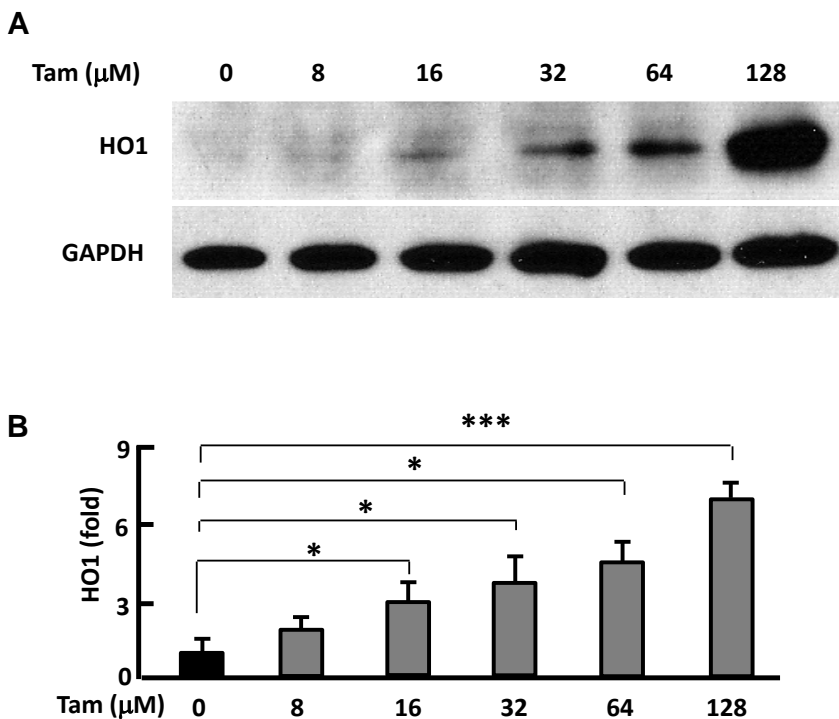


**Figure 2s. Tam induced oxidative stress in 3T3L1 adipocytes.** Cells were lysed after 48-hour treatment with Tam at various concentrations, and the cell lysates underwent western blot (panel A) for HO1 measurement, with densitometric analysis (panel B) of western blot images using NIH ImageJ software; n=3-5. GAPDH was probed as a loading control. \*,  $p < 0.05$ ; \*\*\*,  $p < 0.0001$ .

## References

1. Cheng Z, Almeida FA. Mitochondrial alteration in type 2 diabetes and obesity: an epigenetic link. *Cell Cycle* 2014; 13:890-7.
2. Wang QA, Tao C, Gupta RK, Scherer PE. Tracking adipogenesis during white adipose tissue development, expansion and regeneration. *Nat Med* 2013; 19:1338-44.
3. Ogden CL, Carroll MD, Kit BK, Flegal KM. Prevalence of childhood and adult obesity in the United States, 2011-2012. *JAMA* 2014; 311:806-14.
4. Cawley J, Meyerhoefer C. The medical care costs of obesity: an instrumental variables approach. *Journal of health economics* 2012; 31:219-30.
5. Niswender K. Diabetes and obesity: therapeutic targeting and risk reduction - a complex interplay. *Diabetes Obes Metab* 2010; 12:267-87.
6. Kanasaki K, Koya D. Biology of obesity: lessons from animal models of obesity. *Journal of biomedicine & biotechnology* 2011; 2011:197636.
7. Nilsson C, Raun K, Yan FF, Larsen MO, Tang-Christensen M. Laboratory animals as surrogate models of human obesity. *Acta pharmacologica Sinica* 2012; 33:173-81.
8. Feil S, Valtcheva N, Feil R. Inducible Cre mice. *Methods Mol Biol* 2009; 530:343-63.
9. Li M, Indra AK, Warot X, Brocard J, Messaddeq N, Kato S, et al. Skin abnormalities generated by temporally controlled RXRalpha mutations in mouse epidermis. *Nature* 2000; 407:633-6.
10. Reinert RB, Kantz J, Misfeldt AA, Poffenberger G, Gannon M, Brissova M, et al. Tamoxifen-Induced Cre-loxP Recombination Is Prolonged in Pancreatic Islets of Adult Mice. *PloS one* 2012; 7:e33529.
11. Sassmann A, Offermanns S, Wettschureck N. Tamoxifen-inducible Cre-mediated recombination in adipocytes. *Genesis* 2010; 48:618-25.
12. Imai T, Jiang M, Chambon P, Metzger D. Impaired adipogenesis and lipolysis in the mouse upon selective ablation of the retinoid X receptor alpha mediated by a tamoxifen-inducible chimeric Cre recombinase (Cre-ERT2) in adipocytes. *Proceedings of the National Academy of Sciences of the United States of America* 2001; 98:224-8.
13. Nguyen MC, Stewart RB, Banerji MA, Gordon DH, Kral JG. Relationships between tamoxifen use, liver fat and body fat distribution in women with breast cancer. *International journal of obesity and related metabolic disorders : journal of the International Association for the Study of Obesity* 2001; 25:296-8.
14. Francini G, Petrioli R, Montagnani A, Cadirni A, Campagna S, Francini E, et al. Exemestane after tamoxifen as adjuvant hormonal therapy in postmenopausal women with breast cancer: effects on body composition and lipids. *British journal of cancer* 2006; 95:153-8.
15. Cheng Z, Guo S, Copps K, Dong X, Kollipara R, Rodgers JT, et al. Foxo1 integrates insulin signaling with mitochondrial function in the liver. *Nature medicine* 2009; 15:1307-11.

16. Dong XC, Copps KD, Guo S, Li Y, Kollipara R, DePinho RA, et al. Inactivation of hepatic Foxo1 by insulin signaling is required for adaptive nutrient homeostasis and endocrine growth regulation. *Cell metabolism* 2008; 8:65-76.
17. Paik JH, Kollipara R, Chu G, Ji H, Xiao Y, Ding Z, et al. FoxOs are lineage-restricted redundant tumor suppressors and regulate endothelial cell homeostasis. *Cell* 2007; 128:309-23.
18. Yeh WC, Bierer BE, McKnight SL. Rapamycin inhibits clonal expansion and adipogenic differentiation of 3T3-L1 cells. *Proceedings of the National Academy of Sciences of the United States of America* 1995; 92:11086-90.
19. Bell A, Grunder L, Sorisky A. Rapamycin inhibits human adipocyte differentiation in primary culture. *Obesity research* 2000; 8:249-54.
20. Polak P, Cybulski N, Feige JN, Auwerx J, Ruegg MA, Hall MN. Adipose-specific knockout of raptor results in lean mice with enhanced mitochondrial respiration. *Cell metabolism* 2008; 8:399-410.
21. Pattingre S, Bauvy C, Levade T, Levine B, Codogno P. Ceramide-induced autophagy: to junk or to protect cells? *Autophagy* 2009; 5:558-60.
22. Gullicksen PS, Hausman DB, Dean RG, Hartzell DL, Baile CA. Adipose tissue cellularity and apoptosis after intracerebroventricular injections of leptin and 21 days of recovery in rats. *International journal of obesity and related metabolic disorders : journal of the International Association for the Study of Obesity* 2003; 27:302-12.
23. Della-Fera MA, Qian H, Baile CA. Adipocyte apoptosis in the regulation of body fat mass by leptin. *Diabetes, obesity & metabolism* 2001; 3:299-310.
24. Tanida I, Ueno T, Kominami E. LC3 and Autophagy. *Methods Mol Biol* 2008; 445:77-88.
25. Porter AG, Janicke RU. Emerging roles of caspase-3 in apoptosis. *Cell death and differentiation* 1999; 6:99-104.
26. Yuan L, Wei S, Wang J, Liu X. Isoorientin induces apoptosis and autophagy simultaneously by reactive oxygen species (ROS)-related p53, PI3K/Akt, JNK, and p38 signaling pathways in HepG2 cancer cells. *Journal of agricultural and food chemistry* 2014; 62:5390-400.
27. Liu SY, Chen CL, Yang TT, Huang WC, Hsieh CY, Shen WJ, et al. Albumin prevents reactive oxygen species-induced mitochondrial damage, autophagy, and apoptosis during serum starvation. *Apoptosis : an international journal on programmed cell death* 2012; 17:1156-69.
28. Ghavami S, Eshragi M, Ande SR, Chazin WJ, Klonisch T, Halayko AJ, et al. S100A8/A9 induces autophagy and apoptosis via ROS-mediated cross-talk between mitochondria and lysosomes that involves BNIP3. *Cell research* 2010; 20:314-31.
29. Poss KD, Tonegawa S. Reduced stress defense in heme oxygenase 1-deficient cells. *Proceedings of the National Academy of Sciences of the United States of America* 1997; 94:10925-30.
30. Hirose W, Ikematsu K, Tsuda R. Age-associated increases in heme oxygenase-1 and ferritin immunoreactivity in the autopsied brain. *Leg Med (Tokyo)* 2003; 5 Suppl 1:S360-6.
31. Lavrovsky Y, Song CS, Chatterjee B, Roy AK. Age-dependent increase of heme oxygenase-1 gene expression in the liver mediated by NFkappaB. *Mechanisms of ageing and development* 2000; 114:49-60.

32. Cho KS, Yoon YH, Choi JA, Lee SJ, Koh JY. Induction of autophagy and cell death by tamoxifen in cultured retinal pigment epithelial and photoreceptor cells. *Investigative ophthalmology & visual science* 2012; 53:5344-53.
33. Suzuki YJ, Tsuchiya M, Packer L. Thioctic acid and dihydrolipoic acid are novel antioxidants which interact with reactive oxygen species. *Free radical research communications* 1991; 15:255-63.
34. Zhang B, Berger J, Hu E, Szalkowski D, White-Carrington S, Spiegelman BM, et al. Negative regulation of peroxisome proliferator-activated receptor-gamma gene expression contributes to the antiadipogenic effects of tumor necrosis factor-alpha. *Mol Endocrinol* 1996; 10:1457-66.
35. Xing H, Northrop JP, Grove JR, Kilpatrick KE, Su JL, Ringold GM. TNF alpha-mediated inhibition and reversal of adipocyte differentiation is accompanied by suppressed expression of PPARgamma without effects on Pref-1 expression. *Endocrinology* 1997; 138:2776-83.
36. De Pauw A, Tejerina S, Raes M, Keijer J, Arnould T. Mitochondrial (dys)function in adipocyte (de)differentiation and systemic metabolic alterations. *The American journal of pathology* 2009; 175:927-39.
37. Spiegelman BM. PPAR-gamma: adipogenic regulator and thiazolidinedione receptor. *Diabetes* 1998; 47:507-14.
38. Terrand J, Bruban V, Zhou L, Gong W, El Asmar Z, May P, et al. LRP1 controls intracellular cholesterol storage and fatty acid synthesis through modulation of Wnt signaling. *The Journal of biological chemistry* 2009; 284:381-8.
39. Imai T, Takakuwa R, Marchand S, Dentz E, Bornert JM, Messaddeq N, et al. Peroxisome proliferator-activated receptor gamma is required in mature white and brown adipocytes for their survival in the mouse. *Proceedings of the National Academy of Sciences of the United States of America* 2004; 101:4543-7.
40. Dali-Youcef N, Matakis C, Coste A, Messaddeq N, Giroud S, Blanc S, et al. Adipose tissue-specific inactivation of the retinoblastoma protein protects against diabetes because of increased energy expenditure. *Proceedings of the National Academy of Sciences of the United States of America* 2007; 104:10703-8.
41. Konishi M, Nakamura H, Miwa H, Chambon P, Ornitz DM, Itoh N. Role of Fgf receptor 2c in adipocyte hypertrophy in mesenteric white adipose tissue. *Molecular and cellular endocrinology* 2008; 287:13-9.
42. Shah VP, Chegini HA, Vishneski SR, Weatherman RV, Blackmore PF, Dobrydneva Y. Tamoxifen promotes superoxide production in platelets by activation of PI3-kinase and NADPH oxidase pathways. *Thrombosis research* 2012; 129:36-42.
43. Kallio A, Zheng A, Dahllund J, Heiskanen KM, Harkonen P. Role of mitochondria in tamoxifen-induced rapid death of MCF-7 breast cancer cells. *Apoptosis : an international journal on programmed cell death* 2005; 10:1395-410.
44. Bursch W, Ellinger A, Kienzl H, Torok L, Pandey S, Sikorska M, et al. Active cell death induced by the anti-estrogens tamoxifen and ICI 164 384 in human mammary carcinoma cells (MCF-7) in culture: the role of autophagy. *Carcinogenesis* 1996; 17:1595-607.
45. Lee YS, Kang YS, Lee SH, Kim JA. Role of NAD(P)H oxidase in the tamoxifen-induced generation of reactive oxygen species and apoptosis in HepG2 human hepatoblastoma cells. *Cell death and differentiation* 2000; 7:925-32.

46. Esposito K, Nappo F, Marfella R, Giugliano G, Giugliano F, Ciotola M, et al. Inflammatory cytokine concentrations are acutely increased by hyperglycemia in humans: role of oxidative stress. *Circulation* 2002; 106:2067-72.
47. Fisher B, Costantino J, Redmond C, Poisson R, Bowman D, Couture J, et al. A randomized clinical trial evaluating tamoxifen in the treatment of patients with node-negative breast cancer who have estrogen-receptor-positive tumors. *The New England journal of medicine* 1989; 320:479-84.
48. Gail MH, Costantino JP, Bryant J, Croyle R, Freedman L, Helzlsouer K, et al. Weighing the risks and benefits of tamoxifen treatment for preventing breast cancer. *Journal of the National Cancer Institute* 1999; 91:1829-46.
49. Reis SE, Costantino JP, Wickerham DL, Tan-Chiu E, Wang J, Kavanah M. Cardiovascular effects of tamoxifen in women with and without heart disease: breast cancer prevention trial. National Surgical Adjuvant Breast and Bowel Project Breast Cancer Prevention Trial Investigators. *Journal of the National Cancer Institute* 2001; 93:16-21.
50. Guo S, Copps KD, Dong X, Park S, Cheng Z, Poci A, et al. The Irs1 branch of the insulin signaling cascade plays a dominant role in hepatic nutrient homeostasis. *Molecular and cellular biology* 2009; 29:5070-83.
51. Zebisch K, Voigt V, Wabitsch M, Brandsch M. Protocol for effective differentiation of 3T3-L1 cells to adipocytes. *Analytical biochemistry* 2012; 425:88-90.
52. Sadagurski M, Cheng Z, Rozzo A, Palazzolo I, Kelley GR, Dong X, et al. IRS2 increases mitochondrial dysfunction and oxidative stress in a mouse model of Huntington disease. *The Journal of clinical investigation* 2011; 121:4070-81.
53. Benani A, Troy S, Carmona MC, Fioramonti X, Lorsignol A, Leloup C, et al. Role for mitochondrial reactive oxygen species in brain lipid sensing: redox regulation of food intake. *Diabetes* 2007; 56:152-60.

## Chapter 6 Conclusions and future direction

### Conclusions

This project has led to the key findings as summarized below:

- (1) The kinetics of FoxO1 activation follows a series of sigmoid curves that show multiple activation-inactivation transitions during adipogenesis<sup>1</sup>. Inhibition of FoxO1 leads to stage-dependent suppression of adipocyte differentiation. Our findings explain well the controversial reports in the literature that either persistent inhibition or activation of FoxO1 prevents the adipocyte differentiation.
- (2) FoxO1 may induce adipocyte autophagy through Tfeb<sup>2</sup>. FoxO1 expression and activity is elevated during adipogenesis, which is paralleled with upregulation of Tfeb, the key regulator of autophagosome and lysosome. Indeed, autophagy activity is enhanced during adipocyte differentiation. ChIP assays confirm that FoxO1 can directly bind to the promoter of Tfeb. Consistently, inhibitor of FoxO1 blocks the interaction between FoxO1 and Tfeb promoter, resulting to reduced Tfeb transcript and protein expression.
- (3) The FoxO1-autophagy axis plays a critical role in adipocyte biology<sup>2, 3</sup>. First, it regulates adipogenesis and lipid droplet through FSP27. Pharmacological inhibition of FoxO1 or autophagy similarly suppressed FSP27, which prevents adipocyte differentiation. In mature (or terminally differentiated) adipocytes, blockage of the FoxO1-autophagy axis leads to smaller but more numerous lipid droplets, a phenotype frequently observed in browning of adipose tissue. Secondly, inhibition of the FoxO1-autophagy axis differentially regulates UCP1, UCP2 and UCP3 in adipocytes. In particular, UCP1 is

induced by the inhibition of FoxO1-autophagy axis, serving as a second line of evidence of browning of white adipocyte. Given that positive energy balance contributes to obesity, targeting the FoxO1-autophagy axis may have the potential to treat or prevent obesity.

(4) Generation of tamoxifen-induced knockout mice should consider a recovery period to exclude the direct effects of tamoxifen on fat mass (or adiposity) <sup>4</sup>. To develop inducible adipose FoxO1 knockout mice, we examined the effects of tamoxifen treatment on adiposity in Cre-null mice. We found that tamoxifen administration following a standard protocol led to pronounced decrease in fat mass, likely through inducing ROS and apoptosis. The fat-reducing effects last 4-5 weeks for the test mice. To exclude the confounding effects of Tamoxifen, it is important to consider the recovery time before phenotyping inducible knockout mice.

## **Future direction**

1. Investigate the role of FoxO1 regulating adipose autophagy *in vivo* and examine its potential to prevent obesity. Autophagy *in vivo* may be subject to regulation by various molecules. For instance, mTOR and AMPK have been shown to regulate autophagy<sup>5,6</sup>. It is of interest to examine whether FoxO1 plays a dominant role in adipose autophagy, and how it may affect the interactions of mTOR and AMPK with autophagy. Generation of adipose tissue-specific FoxO1 knockout mice (aFoxO1KO) is under way. The effects of aFoxO1KO on adipose autophagy, adiposity, and metabolism will be examined.

2. Study the interactions between FoxO1 and other FoxO transcription factors in the regulation of adipose autophagy and adiposity. FoxO1 is the primary FoxO isoform, and FoxO3 and FoxO4 are also expressed in adipocytes<sup>7, 8</sup>. Whether and how FoxO1 interacts with FoxO3 and FoxO4 is unknown. Previous studies show that FoxOs (Foxo1, 3, 4) have marked redundant role in liver, muscle and heart<sup>9-11</sup>. It is plausible that, when FoxO1 is deleted from adipose tissue, FoxO3 and/or FoxO4 compensate for FoxO1 deficiency in the regulation of autophagy and adiposity. To test this, the same loxp-Cre system will be used to generate adipose specific double or triple knockout mice for the study.

## References

1. Zou P, Liu L, Zheng L, Stoneman RE, Cho A, Emery A, et al. Targeting FoxO1 with AS1842856 suppresses adipogenesis. *Cell Cycle* 2014; 13:3759-67.
2. Longhua Liu ZT, Louise D Zheng, Joseph P Brooke, Cayleen M Smith, Dongmin Liu, Yun Chau Long and Zhiyong Cheng. FoxO1 interacts with transcription factor EB and differentially regulates mitochondrial uncoupling proteins via autophagy in adipocytes. *Cell Death Discovery* 2016; 2.
3. Liu L, Zheng LD, Zou P, Brooke J, Smith C, Long YC, et al. FoxO1 antagonist suppresses autophagy and lipid droplet growth in adipocytes. *Cell Cycle* 2016; 15:2033-41.
4. Liu L, Zou P, Zheng L, Linarelli LE, Amarell S, Passaro A, et al. Tamoxifen reduces fat mass by boosting reactive oxygen species. *Cell death & disease* 2015; 6:e1586.
5. Kim J, Kundu M, Viollet B, Guan KL. AMPK and mTOR regulate autophagy through direct phosphorylation of Ulk1. *Nature cell biology* 2011; 13:132-41.
6. Egan DF, Shackelford DB, Mihaylova MM, Gelino S, Kohnz RA, Mair W, et al. Phosphorylation of ULK1 (hATG1) by AMP-activated protein kinase connects energy sensing to mitophagy. *Science* 2011; 331:456-61.
7. Higuchi M, Disting GJ, Peshavariya H, Jiang F, Hsiao ST, Chan EC, et al. Differentiation of human adipose-derived stem cells into fat involves reactive oxygen species and Forkhead box O1 mediated upregulation of antioxidant enzymes. *Stem cells and development* 2013; 22:878-88.
8. Nakae J, Kitamura T, Kitamura Y, Biggs WH, 3rd, Arden KC, Accili D. The forkhead transcription factor Foxo1 regulates adipocyte differentiation. *Dev Cell* 2003; 4:119-29.
9. Xiong X, Tao R, DePinho RA, Dong XC. The autophagy-related gene 14 (Atg14) is regulated by forkhead box O transcription factors and circadian rhythms and plays a critical role in hepatic autophagy and lipid metabolism. *J Biol Chem* 2012; 287:39107-14.
10. Milan G, Romanello V, Pescatore F, Armani A, Paik JH, Frasson L, et al. Regulation of autophagy and the ubiquitin-proteasome system by the FoxO transcriptional network during muscle atrophy. *Nature communications* 2015; 6:6670.
11. Sengupta A, Molkentin JD, Yutzey KE. FoxO transcription factors promote autophagy in cardiomyocytes. *J Biol Chem* 2009; 284:28319-31.